The Dissertation Committee for Xiaosa Xu Certifies that this is the approved version of the following dissertation:

Conserved Modulation of the CONSTITUTIVE PHOTOMORPHOGENIC1 E3 Ubiquitin Ligase Activity by the bHLH Transcription Factors, PHYTOCHROME INTERACTING FACTORs

Committee:

Enamul Huq, Supervisor

Stanley J Roux

Steven A Vokes

Alan M Lloyd

Craig R Linder

Conserved Modulation of the CONSTITUTIVE PHOTOMORPHOGENIC1 E3 Ubiquitin Ligase Activity by the bHLH Transcription Factors, PHYTOCHROME INTERACTING FACTORs

by

Xiaosa Xu, B.S.

Dissertation

Presented to the Faculty of the Graduate School of

The University of Texas at Austin

in Partial Fulfillment

of the Requirements

for the Degree of

Doctor of Philosophy

The University of Texas at Austin

May 2016

Dedication

I dedicate this dissertation to my great family especially to my parents for their upbringing of me to be a sincere and strong man. I also dedicate this work to my loving wife and newborn little son who lights up my life like sunshine.

Acknowledgements

First of all, I would like to thank my supervisor Dr. Enamul Huq for his inspiration, support and encouragement through the graduate school life. Without his patient guidance, I won't be able to complete my PhD successfully. I would remember his sincere advice to me that, “Life is full of trouble, your job is to find a solution”.

I would like to thank all my Ph.D. committee members, Dr. Stanley J Roux, Dr. Steven A Vokes, Dr. Craig R Linder, and Dr. Alan M Lloyd for their valuable suggestions on my projects and constant encouragement to overcome difficulties.

I would also like to thank all the members of Dr. Huq and Dr. Roux labs for their great friendships and valuable help. Special thanks to the postdoc collaborators: Drs. Inyup Paik, Ling Zhu and Qingyun Bu for teaching me the experimental techniques and encouragement for conducting my research. Special thanks to my undergraduate assistant Andrew Nguyen for his hard work.

Ph.D. life is a journey of renewal. I thank to all the people that supported me for successfully completing it.

Conserved Modulation of the CONSTITUTIVE PHOTOMORPHOGENIC1 E3 Ubiquitin Ligase Activity by the bHLH Transcription Factors, PHYTOCHROME INTERACTING FACTORs

Xiaosa Xu, Ph. D.

The University of Texas at Austin, 2016

Supervisor: Enamul Huq

As sessile organism, plants are informed of the time of the day and their place of growth by a collection of photoreceptors that detect changing intensity, quality, and direction of light in the environment. Among these photoreceptors, phytochromes (A, B, C, D, E) are the major ones to drive a developmental switch for initial emergence of seedlings from subterranean darkness into sunlight, called plant photomorphogenesis. Previous studies have identified many regulators in the phytochorme-mediated photomorphogenesis pathway. Among them, CONSTITUTIVELY PHOTOMORPHOGENIC 1/ SUPPRESSOR OF PHYTOCHROME A (COP1/SPA) complex and PHYTOCHROME INTERACTING FACTORs (PIF1, 3, 4, 5, 7, 8) are key negative regulators that can suppress photomorphogenesis individually. However, the functional relationships between the COP1-SPA and the PIFs are still unknown. Here in my dissertation project, I showed that PIFs have nontranscriptional roles by acting as cofactors of the COP1 E3 Ubiquitin ligase to enhance the trans-ubiquitination and subsequent degradation of the substrates of COP1, including LONG HYPOCOTYL 5 (HY5), LONG HYPOCOTYL IN FAR-RED 1 (HFR1) and a newly identified substrate

HECATE 2 (HEC2), to suppress photomorphogenesis. HFR1 also promotes the degradation of PIF1 in the dark via direct heterodimerization to trigger rapid seed germination upon light exposure. The reciprocal co-degradation between PIF1 and HFR1 is dependent on the ubi/26S-proteasome pathway *in vivo*. In addition, the *cop1* and *pif1, 3, 4, 5* mutant combinations showed overproliferation of stigmatic tissues phenotype similar to *HEC* overexpression plants. Biochemical and genetic evidence showed that HECs are highly abundant in the *cop1 pifs* mutant flowers. Moreover, HECs negatively regulate the PIFs' binding activity to the G-box regions of promoters of flower pattern genes, *SEP1* and *SEP3*. Taken together, these data revealed the conserved modulation of the COP1 Ubiquitin E3 ligase activity by PIFs, uncovered a suicidal co-degradation mechanism between the HFR1 and PIF1 to fine tune seed germination and seedling development, and demonstrated a novel function of COP1 and PIFs in regulating flower pattern development.

Table of Contents

List of Tables

List of Figures

Chapter I: Introduction

THE ROLE OF LIGHT IN PLANT GROWTH AND DEVELOPMENT

As sessile organisms, plants use light as an important resource to regulate their growth and development through their life cycle. These regulations start from the activation of seed germination when they were buried under soil to the seedling etiolation (plant skotomorphognesis) during their rapid growth toward the surface of the soil (Chory et al., 1996). Upon light exposure and trigger of deetiolation (plant photomorphogenesis), light is playing critical roles on further growth and developmental processes including phototropic growth, shade avoidance response, chloroplast movement, stomatal opening, flowering time and circadian clock (Sullivan et al., 2003). Among all these processes, the early stage regulation of seed germination and plant skotomorphognesis and photomorphogenesis by light were most well studied in recent decades.

Seed germination

Seed germination is the first and most crucial step of plant life cycle especially for annual plants, which secures the survival of the future generation. As sessile organisms, plants have evolved different mechanisms that integrate internal and external signals in order to suppress or activate seed germination under stress or favorable conditions, respectively. Phytohormones including abscisic acid, gibberellic acid and ethylene are three of the key endogenous signals regulating seed germination (Finkelstein et al., 2002; Schwechheimer et al., 2008; KeÇpczyński et al., 1997). Light activation and cold treatment are two of the most important external signals that induce germination of dormant seeds in *Arabidopsis* (Oh et al., 2004; Penfield et al., 2005). Studies in decades have demonstrated that both internal and external signals can function either independently or by cross-talking

with each other to regulate seed germination (Brady et al., 2003; Chory 1996l; Weitbrecht et al., 2011; Lin et al., 2009; Lee et al., 2012).

Light dependent regulation of seed germination is mainly triggered by phytochromes, which are the photoreceptors for red/far-red light (Casal and Sánchez, 1998). phyA and phyB are the two major phytochromes that mediate red/far-red light germination (Shinomura et al., 1994, 1996; Casal and Sánchez, 1998). The red/far-red reversible low fluence responses (LFR) germination is mainly mediated by phyB (Shinomura et al., 1994, 1996; Furuya and Eberhard, 1996). phyA, in contrast, mainly control very low fluence responses (VLFR) and the far-red light high irradiance response (far-red HIR) (Casal and Sánchez, 1998). phyE was also shown to play a role in the germination of *Arabidopsis* seeds under continuous far-red light (Hennig et al., 2002).

Plant skotomorphognesis and photomorphogenesis

After seed germination, plants employ two contrasting developmental programs to succeed in ambient light conditions: skotomorphogenesis and photomorphogenesis (Figure 1.1). Skotomorphogenesis is characterized by elongated hypocotyl, closed cotyledon and an apical hook to allow young seedlings to grow rapidly in darkness using the reserve energy present in the seed. By contrast, photomorphogenesis is the process where light signals inhibit the rapid elongation of hypocotyl, expand the cotyledons and promote greening to allow seedling body plan for optimal light harvesting capacity and autotrophic growth.

To promote photomorphogenesis and actively suppress skotomorphogenic development, plants have evolved multiple photoreceptors to track a wide spectrum of light wavelengths in a local environment. These include the UVB-RESISTANCE 8 (UVR8 for UV-B light), cryptochromes (cry), phototropins (phots) and ZEITLUPE/FLAVIN-

BINDING, KELCH REPEAT, F BOX 1/LOV KELCH PROTEIN 2 family of photoreceptors (ZTL/FKF1/LKP2) (for UV-A/blue light) and phytochromes (phy) (for red/far-red light) (Kami et al., 2010).

PHOTORECEPTORS OF LIGHT SIGNALING PATHWAYS

UVR8

Light is not only an important resource for photosynthesis and signals for growth and development, but also can be a threat to the integrity of plants. UV-B is the major harmful light for plants. Upon exposure to UV-B light, the hypocotyl elongation of *Arabidopsis* seedlings was inhibited and large number of genes expressions were also suppressed (Kim et al., 1998; Boccalandro et al., 2001; Suesslin et al., 2003; Ulm et al., 2004). UVR8 was identified as the photoreceptor for UV-B light (Rizzini et al., 2011). UVR8 could perceive UV-B light and trigger the change of downstream gene expression leading to the biosynthesis of flavonols and morphological changes through the interaction with CONSTITUTIVELY PHOTOMORPHOGENIC1 (COP1) to protect plants from the burning by sun light (Favory et al., 2009; Rizzini et al., 2011; Jenkins et al., 2014).

Cryptochromes

Cryptochromes are UV-A/blue light photoreceptors that play critical roles during the deetiolation process and photoperiodic control of flowering (Lin et al., 2003; Liscum et al., 2003; Chaves et al., 2011; Kami et al., 2010). In *Arabidopsis*, there are three cryptochrome photoreceptors, named as cry1, cry2 and cry3. Though their carboxy terminal domains are significantly different, they share partially overlapping functions (Guo et al., 1998; Yang et al., 2000). cry1 and cry2 were shown to directly interact with CONSTITUTIVELY PHOTOMORPHOGENIC1/ SUPPRESSOR OF PHYA (COP1/SPA) complex to inhibit the E3 ligase activity of COP1 to promote plant

photomorphongenesis and flowering (Wang et al., 2001; Yang et al., 2001; Zuo et al., 2011; Lian et al., 2011; Liu et al., 2011). Additionally, upon light activation, cry2 promotes flowering by directly interacting with transcription factors CRY2-INTERACTING bHLH (CIB1, 2, 4, 5) and triggering the gene expression of FLOWERING LOCUS T (FT) (Liu et al., 2013).

Phototropins

Phototropins were discovered as the blue light receptors that play a major role for the phototropic responses. In *Arabidopsis*, there are two phototropins, phot1 and phot2 (Briggs, et al., 2001; Liscum et al., 1995). In addition to the phototropism, phot1 and phot2 were also shown to regulate the chloroplast movements and stomatal opening (Briggs and Christie, 2002; Wada et al., 2003). The phototropins are mainly composed of two LOV (Light, Oxygen, Voltage) photosensory domains and a carboxy-terminal Ser/Thr protein kinase domain (Briggs and Christie, 2002). Upon perceiving light, the phot1 and phot2 autophosphorylations are activated as the initial events in the transmission of the light signal (Inoue et al., 2008). The subsequent signal transduction involves the phosphorylation of downstream signaling components but diversify among phototropism, stomatal opening and chloroplast movements (Takemiya et al., 2013; Christie et al., 2011; Demarsy et al., 2012; Kong et al., 2013).

ZTL/FKF1/LKP2 family

There is an additional family of photoreceptors including ZEITLUPE/FLAVIN-BINDING, KELCH REPEAT, F BOX 1/LOV KELCH PROTEIN 2 (ZTL/FKF1/LKP2) that uses the UV-A/blue light spectrum in plants to control the photoperiodic floral transition (Ito et al., 2012; Sawa et al., 2007; Fornara et al., 2009; Song et al., 2012; Suetsugu et al., 2013). Different from phototropins, there is only one LOV domain in these

proteins and six Kelch repeats are conserved among them (Suetsugu et al., 2013). In addition, these proteins contain F-box, which can form SCF E3 Ubiquitin ligase complex with Skp1 and Cullin1 (CUL1) protein to trigger the ubiquitination and subsequent degradation of target proteins, including TIMING OF CAB EXPRESSION 1 (TOC1), PSEUDO RESPONSE REGULATOR5 (PRR5) and CONSTANS (CO) etc (Ito et al., 2012; Kim et al., 2007; Sawa et al., 2007; Song et al., 2012).

Phytochromes

Light signals especially the red and far-red regions of the light spectrum perceived by the phytochrome family of photoreceptors regulate a plethora of plant responses throughout their life cycle. These include seed germination, seedling deetiolation, shade avoidance response, stomatal development and flowering (Kami et al., 2010; Chen et al., 2014; Leivar et al., 2014). In *Arabidopsis*, the phytochrome family of photoreceptors is encoded by five members (*PHYA-PHYE*) (Mathews et al., 1997). phyA was classified as type I phytochrome, which is stable in the dark. In contrast, phyB to phyE, which belong to the type II phytochrome, are stable in the light (Mathews et al., 1997).

In the early stage of plant growth and development, except the regulation of seed germinations, which were reviewed above, phytochromes also perceive the ambient red (R) and far-red (FR) light signals in the environment and promote gradual progression to photomorphogenic development by orchestrating elaborate signaling mechanisms (Jiao et al., 2007; Leivar and Quail, 2011). These include allosteric conformation change of phys to a biologically active Pfr form from an inactive Pr form followed by nuclear translocation to inhibit two classes of repressors of plant photomorphogenesis called PHYTOCHROME INTERACTING FACTORs (PIFs) and CONSTITUTIVELY PHOTOMORPHOGENIC/DEETIOLATED/FUSCA (COP/DET/FUS) complex (Figure

1.1) (Leivar and Quail, 2011; Lau and Deng, 2012). In darkness, these dual repressors are actively promoting skotomorphogenic development by suppressing photomorphogenesis and therefore, inhibition of these repressors allows gradual progression to photomorphogenic development.

PHYTOCHROME INTERACTING FACTORS (PIFS)

PIFs belong to the basic helix-loop-helix (bHLH) family of transcription factors (Toledo-Ortiz et al., 2003; Duek et al., 2005). There are seven PIFs in *Arabidopsis* that function in a both partially differential and largely overlapping manner to regulate gene expression and ultimately photomorphogenesis (Leivar and Quail, 2011; Zhang et al., 2013; Shin et al., 2009; Leivar et al., 2008). All PIFs interact with the Pfr forms of phytochromes with differential affinities (Leivar and Quail, 2011; Castillon et al., 2007). Phytochromes interact with PIFs through the APB (Active Phytochrome B Binding) or APA (Active Phytochrome A binding) domains present at the amino (N)-terminus of PIFs. Conversely, PIFs displayed higher affinity for the N-terminus of phytochromes (Shen et al., 2008; Zhu et al., 2000). Direct physical interaction of PIFs with phys leads to the light-induced phosphorylation followed by ubiquitylation and subsequent degradation of PIFs by the ubiquitin/26S proteasome system (UPS). In addition, light-induced phosphorylation is necessary for degradation of PIF3 (Ni et al., 2013). The degradation kinetics of PIFs under various light quality and quantity, and early posttranslational modifications have been extensively investigated **(**Leivar and Quail, 2011**).** A putative polyubiquitin binding factor called HEMERA is also necessary for degradation of PIF1 and PIF3 under prolonged light (Chen et al., 2010; Galvão et al., 2012). However, the kinases that phosphorylate PIFs and the E3 ligases that ubiquitylate PIFs in response to light are under intense investigation.

Light-induced phosphorylation of PIFs is one of the first posttranslational modifications in PIFs before their degradation (Leivar and Quail, 2011). It is a prerequisite for degradation of PIFs through the 26S proteasome system. Therefore, an intense search is underway for identifying the kinases that phosphorylate PIFs in response to light. The first candidate considered for a PIF kinase was phytochrome itself as phytochrome has been shown to function as a serine/threonine kinase with a histidine kinase ancestry (Yeh et al., 1998). Direct physical interaction with phytochrome is necessary for the light-induced phosphorylation and degradation of PIFs. Plant phytochrome has been shown to phosphorylate other substrates including PKS1, FHY1, and IAA proteins (Shen et al., 2009; Fankhauser et al., 1999; Colón-Carmona et al., 2000). In addition, bacterial phytochromes function as histidine kinase (Vierstra and Davis, 2000; Bhoo et al., 2001). However, the drawback of all the above studies is that both the Pr and Pfr forms of phytochromes phosphorylated most of the substrates, despite the fact that only Pfr is the biologically active form of phytochrome. In addition, convincing *in vivo* evidence supporting the role of phytochrome as a kinase is still lacking, as no kinase inactive mutant form of phytochrome has been described that did not rescue the *phy* mutant phenotypes. Moreover, constitutively nuclear localized phytochromes do not induce photomorphogenesis in the absence of light, suggesting a Pfr-specific signaling mechanism (Huq et al., 2003; Matsushita et al., 2003; Genoud et al., 2008). In addition, a C-terminal single nucleotide deletion mutant of phyB (*phyB-28*) expressing a truncated form without the histidine kinase related domain is still partially functional *in vivo*, suggesting that the putative kinase domain is not essential for phyB function (Krall et al., 2000). However, several recent studies alleviate the concerns raised above. For example, the majority of the biological functions of phytochromes are located within the nucleus (Huq et al., 2003; Matsushita et al., 2003), although phyA displays roles in the cytosol (Paik et al., 2012;

Rösler et al., 2007). The Pfr forms of all phytochromes translocate into the nucleus in response to light, while the Pr form is mostly in the cytosol (Fankhauser and Chen, 2008), suggesting a physical separation of the substrates from the kinase. Moreover, phyB has been shown to sequester PIFs in response to light by direct physical interaction and this sequestration contributes to the biological function of phyB (Park et al., 2012). Many targeted mutations in the putative kinase domain have been described previously that rescued the *phyA* mutant phenotypes (Boylan and Quail 1996). However, these mutants might have rescued *phyA* mutant phenotypes due to phyA-mediated sequestration of PIFs similar to phyB, although sequestration of PIFs by phyA has not been demonstrated yet. Therefore, the rate-limiting steps might be at two levels: one at the nuclear translocation step of phytochromes to promote physical proximity to the substrates, and the other at the Pfr-specific interaction and phosphorylation of the substrates. The Pr-induced phosphorylation described previously might simply be forced phosphorylation due to the use of non-physiological amount of the kinase and substrates in the *in vitro* experiments (Yeh et al., 1998; Fankhauser et al., 1999; Colón-Carmona et al., 2000). Thus, the kinase hypothesis as one of the major biochemical functions of phytochromes might be worth revisiting.

COP1/SPA COMPLEX

As discussed above, photomorphogenesis is repressed by two distinct classes of proteins: one encodes bHLH transcription factors (PIFs) and the other (COP/DET/FUS) complex involves ubiquitin-mediated degradation of the positively acting factors (Figure 1.1). The *cop*/*det*/*fus* mutant seedlings exhibit constitutive deetiolation phenotype in dark, which have short hypocotyls, open and expanded cotyledons, and high levels of

anthocyanin as light grown seedlings (Deng et al., 1992; Wei and Deng 1996; Schwechheimer and Deng, 2000).

COP/DET/FUS proteins are defined into three different protein complexes based on their biochemical and genetic characterizations: the COP1/SPA complex, the COP9 signalsome (CSN) and the COP10–DET1–DDB1 (CDD) complex (Lau and Deng, 2012). COP1 is one of the major repressors among these factors. It is a RING-type E3 ubiquitin ligase that is conserved from plants to vertebrates (Osterlund et al., 2000; Deng et al., 1992; Dornan et al., 2004; Bianchi et al., 2003; Yi and Deng, 2005). COP1 contains a ring-finger zinc binding domain at amino-terminal, a coiled-coiled domain and several WD-40 repeats domain at the carboxyl-terminus (Deng et al., 1992). It forms multiple complexes with SUPPRESSOR OF PHYTOCHROME A-105 (SPA1-4) family members to function as a hub for repressing photomorphogenesis in the dark in a tissue-and developmental stage-specific manner (Hoecker et al., 1999; Deng et al., 1992; Laubinger et al., 2004; Osterlund et al., 2000; Zhu et al., 2008; Lau and Deng, 2012). The COP1/SPAs complexes ubiquitylate and degrade positive regulators of plant photomorphogenesis including LONG HYPOCOTYL 5 (HY5), LONG AFTER FAR-RED LIGHT 1 (LAF1), and LONG HYPOCOTYL IN FAR-RED 1 (HFR1) through ubiquitin/26S proteasome-mediated pathway to suppress photomorphogenesis in the dark (Hoecker et al., 1999; Seo et al., 2003; Saijo et al., 2003; Yang et al., 2005; Jang et al., 2005; Zhu et al., 2008).

One of the long standing questions in light signaling pathways is how COP1 is inactivated by light to promote photomorphogenesis. Photobiological experiments demonstrated that both phytochromes and cryptochromes inactivate COP1 in response to red/far-red and blue light, respectively (Osterlund and Deng, 1998). These photoreceptors employ dual mechanisms for this purpose. Under prolonged light as well as relatively shorter light exposure, COP1 is excluded from the nucleus (Subramanian et al., 2004; Pacín

et al., 2014). However, COP1 is also rapidly inactivated by these photoreceptors to trigger light induced gene expression and photomorphogenesis. Cry 1 and Cry 2 have been shown to directly interact with SPA1 to dissociate the COP1-SPA complex in response to blue light as mentioned above (Liu et al., 2011; Lian et al., 2011; Zuo et al., 2011). Yet, how phytochromes inactivate COP1 was still unknown until recently. Instead, COP1-SPA complexes have been shown to regulate functions of phytochromes in the light by triggering the degradation of both type I phytochrome (phyA) and type II phytochrome, (phyB-phyE) (Seo et al., 2004; Jang et al., 2010).

SUMMARY, QUESTIONS AND HYPOTHESIS

Overall, light is an essential commodity for photosynthetic energy production as well as an environmental cue for increasing awareness and fitness to the surrounding conditions. Multiple photoreceptors have been identified to sense different spectrum of light to regulate various stages of plant growth and development. Among these photoreceptors, phytochromes are playing important roles in the seed germination and plant photomorphogeneis. PIFs and COP-SPA complex are two key groups of negative regulators in the phytochrome mediated signaling pathway to suppress plant photomorphogenesis in the dark. However, the relationship between these two groups of repressors was not clear until recently. In other words, why have plants evolved with two classes of repressors? Do they function additively or synergistically?

Therefore, in my dissertation, I proposed the hypothesis that PIFs and COP1-SPA complex can function not only independently but also synergistically to regulate plant growth and development. The specific objectives are:

1. Identification of the function of PIF1 for enhancing the E3 ligase activity of COP1 to synergistically repress photomorphogenesis in Arabidopsis.

2. Illustration the suicidal co-degradation mechanism of PIF1 and HFR1 by COP1 during photomorphogenesis.
3. Identification the regulatory mechanism of PIF1 on promoting HECATE2 degradation via COP1 to regulate photomorphogensis and flower development.

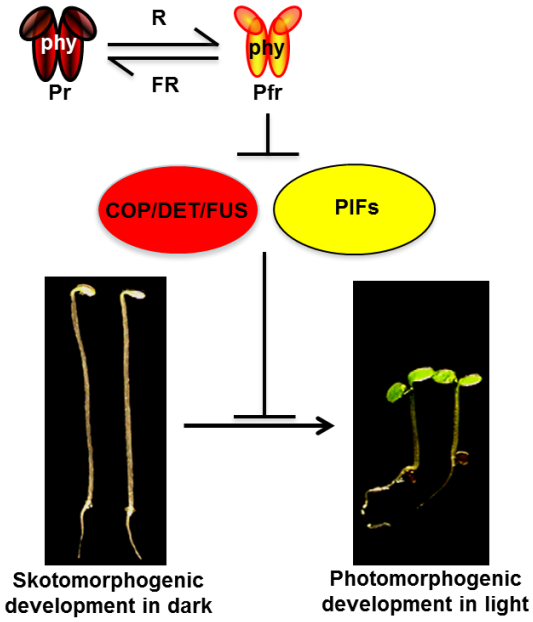

Figure 1.1: A simplified view of the phytochrome-mediated light signaling pathways.

In the dark, phytochromes exist as biologically inactive Pr form. The COP/DET/FUS complexes and PIFs are functioning in the dark to reppress photomorphogenic development. Seedlings grown in the dark show long hypocotyl and closed cotyledons. Under light, phytochrome perceives red/far-red light signals and photoconverts from an inactive Pr form to an active Pfr form. Active Pfr form suppresses the functions of COP1/DET/FUS complexes and PIFs. As a result, seedlings progress toward photomorphogenic development. Seedlings grown in light display short hypocotyl, open and expanded green cotyledons for optimal photosynthesis and autotrophic growth.

Chapter II: PIF1 enhances the E3 ligase activity of COP1 to synergistically repress photomorphogenesis in Arabidopsis

ABSTRACT

CONSTITUTIVE PHOTOMORPHOGENIC1 (COP1) is a RING/WD40 repeat containing ubiquitin E3 ligase that is conserved from plants to humans. COP1 forms complexes with SUPPRESSOR OF PHYA (SPA) proteins, and these complexes degrade positively acting transcription factors in the dark to repress photomorphogenesis. Phytochrome interacting basic helix-loop-helix (bHLH) transcription factors (PIFs) also repress photomorphogenesis in the dark. In response to light, the phytochrome (phy) family of sensory photoreceptors simultaneously inactivates COP1-SPA complexes and induces the rapid degradation of PIFs to promote photomorphogenesis. However, the functional relationship between PIFs and COP1-SPA complexes is still unknown. Here, we present genetic evidence that the *pif* and *cop1/spa Arabidopsis* mutants synergistically promote photomorphogenesis in the dark. LONG HYPOCOTYL 5 (HY5) is stabilized in the *cop1 pif1, spa123 pif1* and the *pif* double, triple and quadruple mutants in the dark. Moreover, the *hy5* mutant suppresses the constitutive photomorphogenic phenotypes of the *pifq* mutant in the dark. PIF1 forms complexes with COP1, HY5 and SPA1, and enhances the substrate recruitment, auto- and trans-ubiquitylation activities of COP1. These data uncover a novel function of PIFs as the potential cofactors of COP1, and provide a genetic and biochemical model of how PIFs and COP1/SPA complexes synergistically repress photomorphogenesis in the dark.

KEYWORDS

COP1-SPA complexes/ photomorphogenesis/ Phytochrome Interacting Factors/ ubiquitin-26S proteasome.

INTRODUCTION

Plants are sessile and photoautotrophic organisms, and therefore have evolved a variety of mechanisms to optimize their growth and development to the ambient light environment. Several classes of photoreceptors enable plants to sense and respond to light. Among these, phytochromes (phys) sense red (R) and far-red (FR) light, cryptochromes (crys) and phototropins (phots) sense UV-A/blue light, and UVR8 senses UV-B light. Light-induced activation of these photoreceptors promotes photomorphogenic development throughout the life cycle of plants, including seed germination, seedling deetiolation, the shade avoidance response, phototropism and flowering (Schaefer and Nagy, 2006; Bae and Choi, 2008; Franklin and Quail, 2010; Chen and Chory, 2011).

Phytochromes are chromoproteins encoded by a small gene family (*PHYA* - *PHYE* in Arabidopsis) that exist as the R light absorbing inactive Pr form in the dark (Mathews and Sharrock, 1997). Upon light absorption, a conformation shift to the FR light absorbing biologically active Pfr form triggers their nuclear translocation and photobody (speckle) formation (Nagatani, 2004; Chen and Chory, 2011). Within the nucleus, the activated Pfr forms of phys physically interact with multiple proteins including a small group of basic helix-loop-helix (bHLH) transcription factors called Phytochrome Interacting Factors (PIFs; PIF1, PIF3-8) (Quail, 2000; Huq and Quail, 2002; Huq et al., 2004; Duek and Fankhauser, 2005; Huq and Quail, 2005; Chen et al., 2010b; Galvao et al., 2012; Paik et al., 2012). PIFs constitutively accumulate in the nucleus in the dark and inhibit photomorphogenesis (Castillon et al., 2007; Henriques et al., 2009; Leivar and Quail, 2011). Upon light exposure, the physical interaction between Pfr and PIFs triggers a cascade of events, including light-induced phosphorylation, ubiquitylation and 26S proteasome-mediated degradation of PIFs (Bauer et al., 2004; Shen et al., 2005; Al-Sady et al., 2006; Shen et al., 2007; Bu et al., 2011). The removal of PIFs after light exposure

results in large-scale changes in gene expression that promote photomorphogenic development (Leivar et al., 2009; Shin et al., 2009; Leivar and Quail, 2011; Zhang et al., 2013; Leivar and Monte, 2014). Consistently, the reduction in PIF level in the *pifq* (*pif1 pif3 pif4 pif5*) quadruple mutant or the overexpression of a truncated form of PIF1 results in photomorphogenic development in the dark (Leivar et al., 2008b; Shen et al., 2008; Shin et al., 2009).

In addition to PIFs, previous genetic studies have identified 11 CONSTITUTIVE PHOTOMORPHOGENIC/DEETIOLATED/FUSCA (COP/DET/FUS) genes that act as negative regulators of photomorphogenesis (Deng et al., 1992; Hoecker, 2005; Henriques et al., 2009; Lau and Deng, 2012). Among these COP/DET/FUS proteins, COP1 is a RING-type E3 ligase that is evolutionarily conserved from plants to vertebrates (Deng et al., 1992; Osterlund et al., 2000; Bianchi et al., 2003; Dornan et al., 2004; Yi and Deng, 2005; Lau and Deng, 2012). COP1 plays a central role in repressing photomorphogenesis in the dark by forming multiple complexes with SUPPRESSOR OF PHYTOCHROME A-105 (SPA1-4) family members in a tissue-and developmental stage-specific manner (Deng et al., 1992; Hoecker et al., 1999; Osterlund et al., 2000; Laubinger et al., 2004; Zhu et al., 2008; Lau and Deng, 2012). These complexes ubiquitylate and degrade positively acting transcription factors such as LONG HYPOCOTYL 5 (HY5)/ LONG AFTER FAR-RED LIGHT 1 (LAF1)/LONG HYPOCOTYL IN FAR-RED 1 (HFR1) to repress photomorphogenesis in the dark (Hoecker et al., 1999; Saijo et al., 2003; Seo et al., 2003; Jang et al., 2005; Yang et al., 2005; Zhu et al., 2008). COP1-SPA complexes also associate with Cullin 4, COP9 signalosome (CSN) and the CDD (for COP10, DDB1a and DET1) complexes, and all three sub complexes synergistically repress photomorphogenesis in the dark (Chen et al., 2010a). Under prolonged light conditions, COP1 is depleted from the nucleus using a nuclear exclusion mechanism that allows these target proteins to accumulate and promote

photomorphogenesis (Osterlund and Deng, 1998; Subramanian et al., 2004; Pacín et al., 2013).

The COP1-SPA complexes also regulate the photoreceptor levels in light. phyA, a type I light-labile phytochrome, is degraded in light in a COP1-dependent manner (Seo et al., 2004). COP1 also degrades type II light stable phytochromes (phyB-phyE) under light. Strikingly, PIFs interact with both COP1 and phyB, and enhance the poly-ubiquitylation of phyB by COP1 *in vitro* (Jang et al., 2010). These data are consistent with an increased abundance of phyB in *pif* mutants resulting in their hypersensitive phenotypes under continuous R light (Leivar et al., 2008a; Leivar and Quail, 2011). Therefore, COP1 desensitizes the signaling pathway by regulating the abundance of the photoreceptors.

The above studies show that PIFs and COP1-SPA complexes act as key regulators of photomorphogenesis in the dark. However, the functional relationship between PIFs and COP1-SPA complexes is still unknown. Previously, it was shown that PIF3 is unstable in *cop1* and *spa* mutants (Bauer et al., 2004; Leivar et al., 2008b), suggesting that PIFs might act downstream of COP1-SPA complexes to repress photomorphogenesis. Here we provide genetic and biochemical evidence that these factors function synergistically as well as additively to repress photomorphogenesis in the dark. Our results have uncovered a novel biochemical function of this group of bHLH transcription factors in optimizing photomorphogenic development of plants.

RESULTS

PIFs and COP1/SPA proteins synergistically repress photomorphogenesis in the dark

To examine the genetic relationship between PIFs and COP1/SPA proteins, we generated various combinations of *pif*s, *cop1* and *spa Arabidopsis thaliana* mutants. Because both PIFs and COP1/SPA proteins repress photomorphogenesis in the dark, we

examined deetiolation phenotypes including hypocotyl length, cotyledon angle, cotyledon area, anthocyanin level and gene expression phenotypes for the wild type (Col-0) and mutant seedlings grown in darkness. As observed previously, wild type and *pif1* displayed etiolated phenotypes, while *cop1-4*, *cop1-6* and *spa123* (*spa1 spa2 spa3*) displayed deetiolated phenotypes under these conditions (Figure 2.1A-D). Strikingly, the *cop1-6 pif1* double and *spa123 pif1* quadruple mutants displayed synergistic deetiolation phenotypes including shorter hypocotyls, higher cotyledon angles, more expanded cotyledon areas and higher anthocyanin levels compared to *cop1-6* and *spa123*, respectively (Figure 2.1A-D). *cop1-4 pif1* also displayed enhanced deetiolation phenotypes compared to *cop1-4* (Figure 2.1A-D); however, because *cop1-4* is a strong allele lacking the WD40 region of COP1, the synergistic effect was not observed for all these phenotypes. Chlorophyll and carotenoid levels were also higher in the *cop1-4pif1*, *cop1-6pif1*, *spa123 pif1* compared to the *cop1-4*, *cop1-6* and *spa123* mutant backgrounds, respectively (Figure. 2.2AB). Among all PIFs, only PIF1 was shown to repress seed germination by directly regulating genes in the GA and ABA pathways in the dark (Oh et al., 2004; Oh et al., 2009). Examination of the seed germination phenotypes for *cop1-4*, *cop1-6*, *spa123* and their combinations with *pif1* revealed that the germination rates of *cop1-4 pif1*, *cop1-6 pif1*, and *spa123 pif1* did not differ from those of *pif1* (Figure. 2.2C). Taken together, these data show that PIF1 and COP1/SPA synergistically repress photomorphogenesis in the dark.

To examine if other PIFs can repress photomorphogenesis synergistically with COP1, we generated a series of higher order mutants among *cop1-4*, *cop1-6* and three additional *pif* (*pif3*, *pif4* and *pif5*) mutants. Phenotypic analyses showed that a combination of *cop1-6* and either *pif1*, *pif3* or *pif4* displays equal synergistic enhancement of photomorphogenesis compared to *cop1-6* in the dark (Figures. 2.3B-2.5B). Moreover, the various mutant combinations of *pif*s with *cop1-6* (*cop1-6 pif13*, *cop1-6 pif14*, *cop1-6 pif15*,

cop1-6 pif134, *cop1-6 pif135*, *cop1-6 pif145* and *cop1-6 pifq*) displayed increasing levels of photomorphogenesis compared to *cop1-6 pif* double mutants (*cop1-6 pif1*, *cop1-6 pif3* and *cop1-6 pif4*) in the dark (Figures. 2.3B-2.5B). The higher order mutant combinations with *cop1-4* also displayed increased photomorphogenesis in the dark (Figures. 2.3A-2.5A); however, because *cop1-4* is a strong allele, the synergistic deetiolation phenotype of *cop1-4* and *pif* combinations was not observed. Taken together, these data suggest that all four PIFs synergistically repress photomorphogenesis with COP1/SPA proteins individually. However, additional PIFs incrementally repress photomorphogenesis in the dark in an additive manner.

pif1 and *cop1/spa123* mutants display synergistic promotion of light-regulated gene expression in the dark

To determine if the above mutant combinations also display synergistic phenotypes at the molecular level, we examined the expression levels of a selected group of genes that are usually expressed in the light-grown seedlings. As expected, *cop1-4*, *cop1-6* and *spa123* displayed higher expression of these genes compared to the wild type under these conditions (Figure 2.6A-D). Consistent with the above results, the expression of these genes was much higher in the *cop1-4 pif1*, *cop1-6 pif1* and *spa123 pif1* compared to that in the *cop1-4*, *cop1-6* and *spa123* backgrounds, respectively (Figure 2.6A-D). These data suggest that PIFs and COP1/SPA proteins synergistically repress both the morphological and molecular phenotypes in darkness.

PIFs promote COP1/SPA-mediated degradation of HY5 posttranslationally in the dark

Previous studies have shown that COP1-SPA complexes interact with the positively acting transcription factors (e.g., HY5, HFR1, LAF1 and others) and induce their degradation through the ubiquitin (ub)/26S proteasome pathway in the dark (Osterlund et

al., 2000; Saijo et al., 2003; Seo et al., 2003; Jang et al., 2005; Yang et al., 2005; Lau and Deng, 2012). HY5 is a bZIP transcription factor whose abundance directly correlates with the level of photomorphogenesis (Osterlund et al., 2000). To determine if the synergistic promotion of photomorphogenesis observed in the various *cop1 pif*s and *spa123 pif1* mutants is due to an increased abundance of HY5 in the dark, we examined HY5 protein and mRNA levels in the *cop1*, *spa123*, *pif1* and the corresponding higher order mutants. Results show that the HY5 protein, but not the *HY5* mRNA, is synergistically stabilized in the *cop1-4 pif1*, *cop1-6 pif1* and *spa123 pif1* compared to that in the *cop1-4*, *cop1-6* and *spa123* backgrounds, respectively (Figure 2.7A-B; Figure 2.8A). Because *pifq* displays constitutive photomorphogenesis similar to *cop1*, we examined the HY5 level in *pifq*, *cop1-6* and *cop1-6 pifq* mutants. Strikingly, HY5 is much more abundant in the *pifq* background compared to the wild type. In addition, HY5 level is much higher in the *cop1-6 pifq* compared to that in the *cop1-6* or *pifq* backgrounds, respectively (Figure 2.7C). However, *HY5* mRNA level is reduced in the *pifq* background compared to the wild type (Figure 2.8B) (Zhang et al., 2013), suggesting that PIFs regulate HY5 level posttranslationally in an additive manner in darkness. Because HY5 is more abundant in the *pifq* background, we examined HY5 level in the various *pif* single, double, triple and quadruple mutant backgrounds. Results show that HY5 is progressively more abundant in the higher order *pif* mutants compared to the wild type and *pif* single mutants, respectively (Figure 2.9A, bottom). Strikingly, the hypocotyl lengths of these mutants inversely correlated with the HY5 level in various *pif* mutant combinations compared to wt (Figure 2.9A-B). These data also suggest that the constitutive photomorphogenic phenotype of *pifq* might be partly due to an increased abundance of HY5 in the dark.

hy5-215 partially suppresses the synergistic promotion of photomorphogenesis in the *cop1-6 pif1* background

To provide genetic evidence that the increased abundance of HY5 in the dark contributes to the synergistic repression of photomorphogenesis by PIFs and COP1, we generated a *cop1-6 pif1 hy5-215* triple mutant. Phenotypic analyses showed that all three deetiolation phenotypes (shorter hypocotyl, expanded cotyledon angle and area) are partially suppressed in the *cop1-6 pif1 hy5-215* triple mutant compared to those in the *cop1-6 pif1* double background (Figure 2.10A-C). These data suggest that the increased amount of HY5 in the dark indeed contributes to the synergistic promotion of photomorphogenesis in the *cop1-6 pif1* double mutant in the dark.

hy5-215 partially suppresses the constitutive photomorphogenic phenotypes of *pifq*

The suppression of *cop1-6 pif1* phenotypes by *hy5-215* as shown above could still be due to the suppression of only the *cop1-6* phenotypes by *hy5-215* as previously shown (Ang et al., 1998). To provide direct genetic evidence that the increased abundance of HY5 in *pifq* in the dark contributes to the constitutive photomorphogenic phenotypes of *pifq*, we generated *pifq hy5-215* quintuple mutant. Phenotypic analyses showed that both the de-etiolation and gene expression phenotypes are partially suppressed in the *pifq hy5-215* quintuple mutant compared to those in the *pifq* background (Figure 2.11A-D). These data strongly suggest that the increased amount of HY5 in *pifq* in the dark contributes to the constitutive photomorphogenic phenotypes of *pifq* in darkness.

PIF1 interacts with COP1, HY5 and SPA1

Because HY5 is more abundant in *cop1 pif1* as well as in *pifq*, we examined if PIF1 could interact with COP1, SPA1 and HY5. Yeast-two-hybrid assays show that PIF1 robustly interacts with COP1 (Figure 2.12A-B). Domain mapping analyses show that the WD40 repeat domain of COP1 is both necessary and sufficient for the interaction with full-

length PIF1 (Figure 2.12A). Conversely, the amino-terminal 55 amino acids containing the active phytochrome binding (APB) domian of PIF1 is both necessary and sufficient for the interaction with full-length COP1 (Figure 2.12B; Figure 2.13). Recently, the bHLH domain of PIF1 was shown to interact with the bZIP domain of HY5 *in vitro* and *in vivo* (Chen et al., 2013). We also examined the interaction between PIF1 and HY5 using yeast two-hybrid assays. Results show that PIF1 interacts with the bZIP domain of HY5 confirming the previous report (Figure 2.14).

To examine the physical interactions between PIF1 and COP1/SPA1 *in vivo*, we expressed fusion proteins in transgenic plants. *In vivo* co-immunoprecipitation (co-IP) assays show that COP1-HA robustly interacts with TAP-PIF1 (Figure 2.12C, left). In addition, PIF1-HA robustly co-immunoprecipitates TAP-SPA1, suggesting that PIF1-HA interacts with TAP-SPA1 *in vivo* (Figure 2.12C, right). Taken together, the yeast two-hybrid and the *in vivo* co-IP assays provide strong evidence that PIF1 can associate with COP1, HY5 and SPA1.

PIF1 enhances the substrate recruitment of COP1

Because PIF1 interacts with both COP1 and HY5, and HY5 is more abundant in the *cop1-6 pif1* background compared to the *cop1-6* and *pif1* backgrounds in the dark, respectively (Figure 2.7), we investigated the biochemical mechanisms by which PIF1 promotes COP1-mediated degradation of HY5. To examine if PIF1 increases the substrate availability of COP1, we performed *in vitro* co-IP assays between COP1 and HY5 in the absence and in the presence of increasing concentrations of PIF1. Results show that PIF1 enhances the interaction between COP1 and HY5 more than two-fold *in vitro* (Figure 2.15A-B). These data suggest that the enhanced interaction between COP1 and HY5 in the

presence of PIFs might contribute to the enhanced degradation of HY5 by COP1 in the dark.

PIF1 enhances the auto- and trans-ubiquitylation activities of COP1

Previously, COP1 displayed the ubiquitin ligase activity in vitro (Saijo et al., 2003; Seo et al., 2003). COP1 showed both autoubiquitylation and transubiquitylation to HY5, HFR1, LAF1 and others in vitro (Saijo et al., 2003; Seo et al., 2003; Yang et al., 2005; Lau and Deng, 2012). To examine the autoubiquitylation of COP1, we performed in vitro ubiquitylation assays in the absence and in the presence of increasing concentrations of PIF1. Results show that PIF1 enhances the autoubiquitylation activity of COP1 in a concentration-dependent manner (Figure 2.16A). HY5 and a control protein (maltose binding protein, MBP) did not display any enhancement as previously observed (Saijo et al., 2003), suggesting that PIF1 specifically enhances the autoubiquitylation activity of COP1.

To investigate the transubiquitylation activity of COP1 to HY5, we performed the *in vitro* transubiquitylation assays as described previously (Saijo et al., 2003; Seo et al., 2003). Immunoblotting with anti-FLAG antibody detecting ubiquitylated proteins showed that PIF1 enhances the transubiquitylation of COP1 to HY5 in a concentration-dependent manner (Figure 2.16B, top panel). Immunoblotting with anti-GST antibody also displayed the ubiquitylated GST-HY5 (Figure 2.16B, middle panel), where only the monoubiquitylation of GST-HY5 was observed under these conditions. This is consistent with the previous *in vitro* results showing only the monoubiquitylation of GST-HY5 by COP1 (Saijo et al., 2003). Quantitation of the transubiquitylated bands in the absence and presence of PIF1 shows that PIF1 enhances the transubiquitylation of HY5 by COP1 ~2-4-fold in a concentration-dependent manner (Figure 2.16C). Overall, PIF1 promotes

COP1-mediated degradation of HY5 by increasing the affinity of COP1 to HY5, the autoubiquitylation of COP1 and the transubiquitylation activity of COP1 to HY5.

DISCUSSION

The genetic and biochemical data presented here provide strong evidence that PIFs and COP1/SPA proteins, two unrelated groups of negative regulators of photomorphogenesis, function independently as well as synergistically to repress photomorphogenesis in the dark (Figure 2.17). Genetic analyses show that *cop1-6* in combination with any of the three *pif* single mutants (*pif1, pif3* and *pif4*) displayed synergistic photomorphogenic phenotypes including the visible morphological (hypocotyl lengths, cotyledon angles and cotyledon areas) and molecular (gene expression) phenotypes in the dark compared to *cop1-6, pif1, pif3* and *pif4* mutants, respectively (Figures 2.1-2.6). Similarly, *spa123 pif1* displayed strong synergistic morphological and molecular phenotypes compared to *spa123* and *pif1* (Figures 2.1-2.6). HY5, a positively acting transcription factor, is synergistically stabilized posttranscriptionally in the *cop1-6 pif1*, *cop1-4 pif1*, and *spa123 pif1* mutants compared to their genetic parents (Figure 2.7). PIF1 forms complexes with COP1, SPA1 and HY5 in yeast and *in vivo* (Figures 2.12-2.14). In addition, *hy5-215* suppresses the synergistic promotion of photomorphogenesis in the *cop1-6 pif1* double mutants (Figure 2.10). Although the above data provide strong evidence that PIFs and COP1/SPA proteins function synergistically in repressing photomorphogenesis in the dark, the results with the *cop1-4* allele were not as conclusive. The *cop1-4* allele is predicted to encode a truncated protein lacking the WD40 region (PIF and HY5 interaction domain), raising the possibility that the observed synergistic phenotypes might be PIF-independent. However, the truncated COP1-4 protein still has the interaction domain for SPA proteins and the E2 enzyme that binds to the RING domain of

COP1 (McNellis et al., 1994). Because PIF1 interacts with SPA1 (Figure 2.12C), one possibility is that this partial protein is still able to recruit HY5 through SPA and PIFs to promote degradation of HY5. The HY5 level in the *cop1-4 pif1* vs *cop1-4* as shown in Figure 2.7A supports this conclusion. Taken together, the comprehensive data presented here strongly suggest that PIFs and COP1/SPA proteins synergistically repress photomorphogenesis in the dark.

PIFs have been shown to regulate a large number of genes directly and indirectly in the dark (Leivar et al., 2009; Shin et al., 2009; Zhang et al., 2013). The majority of these genes promotes photomorphogenic development and are repressed in the dark. Light-induced degradation of PIFs results in derepression of these genes and thereby promotes photomorphogenesis (Leivar and Quail, 2011). Therefore, the *cop* like phenotype of *pifq* was thought to be mainly due to the release of PIFs' transcriptional repression activity (Leivar et al., 2009; Shin et al., 2009; Leivar and Quail, 2011; Leivar and Monte, 2014). Strikingly, the genetic and biochemical data presented here show that the PIF-mediated repression of photomorphogenesis is also due to a posttranslational destabilization of HY5 by PIFs in the dark (Figure 2.7-2.9). HY5 is progressively more stabilized in the double, triple and quadruple *pif* mutants compared to the wild type and *pif* single mutants in the dark, paralleling the increasing photomorphogenic phenotypes of the double, triple and quadruple *pif* mutants (Figures 2.3-2.5; Figure 2.9) (Leivar et al., 2008b; Chen et al., 2013). Moreover, *hy5* suppresses both the morphological and molecular phenotypes of *pifq* in the dark (Figure 2.10). These data are consistent with a previous observation that HY5 level directly correlates with the degree of photomorphogenesis (Figure 2.7-2.9) (Osterlund et al., 2000). Therefore, the *cop*-like phenotype of *pifq* is largely due to an increased abundance of HY5 in the dark. An additional level of complexity is that both PIFs and HY5 bind to the G-box (CACGTG) DNA sequence element in their target genes (Martinez-

Garcia et al., 2000; Jiao et al., 2007; Leivar et al., 2009; Shin et al., 2009; Zhang et al., 2011; Hornitschek et al., 2012; Chen et al., 2013; Zhang et al., 2013), potentially regulating an overlapping set of target genes. Further studies are necessary to distinguish whether the large number PIF target genes is directly regulated by PIFs and/or indirectly by destabilization of HY5, which can bind to the same target genes.

The biochemical mechanisms by which PIFs destabilize HY5 appear to operate at at least three levels. First, PIF1 increases the affinity of COP1 for HY5, thereby increasing the substrate availability of COP1 for ubiquitylation (Figure 2.15A-B). Second, PIF1 promotes autoubiquitylation of COP1 (Figure 2.16A). Finally, PIF1 also promotes transubiquitylation of HY5 by COP1 (Figure 2.16B-C). These data suggest that PIFs function as integral cofactors for COP1 in regulating substrate degradation through the 26S proteasome pathway (Figure 2.18). A variety of mechanisms have been shown to regulate E3 ligase activity in eukaryotic cells. These include enhancement of substrate recruitment and stimulation of auto- and trans-ubiquitylation activity of an E3 ligase. For example, Yin Yang (YY1) enhances the affinity between p53 and its E3 ligase human double minute 2 (Hdm2), thereby increasing the degradation of p53 (Sui et al., 2004). Breast cancer 1 (BRCA1)-associated RING domain protein 1 (BARD1), a ring finger protein, interacts with BRCA1, another ring finger E3 ligase, and this interaction enhances the autoubiquitylation of BRCA1 (Xia et al., 2003). Casitas B-lineage Lymphoma c (Cbl-c), a ring Ub E3 ligase interacts with a Linl-1/Isl-1/Mec-3 (LIM) domain containing protein Hydrogen peroxide-inducible clone-5 (Hic-5). Interaction between these proteins enhances the auto- and trans-ubiquitylation of Cbl-c (Ryan et al., 2012). In Arabidopsis, PIFs have been shown to promote the ubiquitylation of type II photoreceptors by COP1 *in vitro*, and thereby destabilize phyB and other type II phys under prolonged light conditions in a redundant manner (Leivar et al., 2008a; Jang et al., 2010). In addition, SPA proteins also

promote the E3 ligase activity of COP1 (Saijo et al., 2003; Seo et al., 2003). However, these studies only showed PIF- and SPA-mediated enhancement of substrate ubiquitylation by COP1 possibly by increasing substrate recruitment. Our data suggest that PIFs utilize all three mechanisms to regulate the E3 ligase activity of COP1. The demonstration that PIF1 enhances substrate recruitment and stimulates the auto- and trans-ubiquitylation activity of COP1 suggests that PIF1 has multiple layers of regulation that potentially increase the diversity of COP1 substrates as well as the strength of their regulation by COP1 to fine tune photomorphogenesis in plants. Because COP1 is conserved in plants and vertebrates (Yi and Deng, 2005), similar mechanisms might also function to fine tune COP1-regulated processes in vertebrates. In addition, COP1 has been shown to target a plethora of substrates involved in various biological processes in plants (Lau and Deng, 2012). If PIFs interact with any of those substrates, PIFs might modulate the COP1 activity toward those substrates to optimize plant growth and development in response to light. Further studies are necessary to determine if PIFs have a much broader role in regulating plant growth and development than previously described.

MATERIALS AND METHODS

Plant materials, growth conditions and measurements

Seeds of wild type (Col-0) *Arabidopsis thaliana* and various mutants (*pif1, pif3, pif4, pif13, pif34, pif45, pif134, pif135, pif145, pif345, pifq, cop1-4, cop1-6, spa123, hy5-215*) in the Col-0 background were used (McNellis et al., 1994; Oyama et al., 1997; Laubinger et al., 2004; Leivar et al., 2008b). For generation of different *cop1*, *spa123*, *pifs* and *hy5-215* mutant combinations, *cop1 and spa123* were first crossed with *pif1*, *pif3* and *pif4* to generate *cop1-4 pif1*, *cop1-6 pif1*, *cop1-6 pif3*, *cop1-6 pif4* and *spa123 pif1*. The *cop1-4 pif1* and *cop1-6 pif1* double mutants were crossed with *pifq* and *hy5-215* to obtain

the F1 generation. Through genotyping and phenotypic characterization of the F2 population, we identified different mutant combinations (*cop1-4 pif13, cop1-4 pif15, cop1-4 pif135, cop1-4 pifq, cop1-6 pif13, cop1-6 pif14, cop1-6 pif15, cop1-6 pif134, cop1-6 pif135, cop1-6 pif145, cop1-6 pifq,* and *cop1-6 pif1hy5-215*). To generate *pifq hy5*, *pifq* was crossed to *hy5-215*. *pifq hy5* was selected by genotyping a large F2 population and further confirmed by genotyping and phenotypic analyses.

Plants were grown in Metro-Mix 200 soil (Sun Gro Horticulture, Bellevue, WA) under 24-h light at 24 ± 0.5°C. Seeds were surface-sterilized and plated on Murashige and Skoog (MS) growth medium containing 0.9% agar without sucrose as described (Shen et al., 2005). After 3 to 4 d of moist chilling at 4°C in the dark to stratify, seeds were exposed to 3 h of white light at room temperature before being placed in the dark.

To measure hypocotyl lengths, cotyledon areas, and cotyledon angles, digital photographs of 5-day-old dark-grown seedlings were taken and at least 30 seedlings were measured using the publicly available software ImageJ (http://rsb.info.nih.gov/ij/), and the experiments were repeated at least three times.

To measure anthocyanin content, fifty seeds per genotype were plated in triplicate on growth medium supplemented with 2% sucrose and induced to germinate as described above. Subsequently, plates were kept in darkness for 3 days. Anthocyanins were extracted under dim green safelight, and anthocyanin content was determined spectroscopically as described (Schmidt and Mohr, 1981).

To measure chlorophyll and carotenoid contents, the same amounts of seeds were surface-sterilized and plated on MS growth medium without sucrose on filter paper. Plates were kept in darkness for 2.5 days before being exposed to white light for 5 h. To extract chlorophyll and carotenoid, 50-100 mg of fresh tissue was homogenized in liquid nitrogen and then 400 μL methanol was added to the powdered tissue and re-suspended well. The

samples were wrapped in aluminum foil to protect them from light and vortexed for 10 min. Then, 400 µl of 50 mM Tris-HCl, pH 7.5, 1 M NaCl were added and the samples were vortexed again for 10 min. Finally, 400 µL of chloroform was added before vortexing again for 5 min. The samples were left on ice for an additional 5 min before centrifuging at 16,000 g for 5 min. The organic bottom phase was collected and dried in a speed vac at room temperature. The samples were re-suspended in 50-150 µL ethyl acetate, and then 750 µL acetone was added before measuring absorbance at λ=470, 644.8 and 661.8 nm to calculate the chlorophyll and carotenoid content as described (Toledo-Ortíz et al., 2010).

The seed germination assay was performed as described (Oh et al., 2004). Briefly, triplicates of 60 seeds for each genotype were surface sterilized and plated on MS medium within 1 h. The plates were then treated with far red light (34 $\mu mol \cdot m^{-2} \cdot s^{-1}$) for 5 min before being placed in the dark at 21°C. Germination was scored after 6 days of growth.

RNA extraction and quantitative RT-PCR

The qRT-PCR analysis was performed as described with minor variations (Toledo-Ortíz et al., 2010). Total RNA was isolated from 4-d-old dark-grown seedlings using the Spectrum plant total RNA Kit (Sigma-Aldrich Co., St. Louis, MO). One microgram of total RNA was treated with DNase I to eliminate genomic DNA and then reverse transcribed using SuperScript III (Life Technologies Co**.,** Carlsbad, CA) as per the manufacturer's protocol. Real-time PCR was performed using the Power SYBR Green RT-PCR Reagents Kit (Applied Biosystems Inc., Foster City, CA) in a 7900HT Fast Real-Time PCR machine (Applied Biosystems Inc., Foster City, CA). *PP2A* was used as a control to normalize the expression data. The resulting cycle threshold (Ct) values were used to calculate the levels of expression of different genes relative to *PP2A,* as suggested by the manufacturer

(Applied Biosystems Inc., Foster City, CA). Primer sequences used for qRT-PCR are listed in Table 2.1.

Construction of vectors and generation of transgenic plants

The full-length *PIF1* open reading frame (ORF) was amplified by PCR using the primers listed in Table 2.1 and ligated into pENTR using the pENTR™/D-TOPO® Cloning Kit (Life Technologies Co., Carlsbad, CA, Cat No: K2400-20). The pENTR-PIF1 vector was recombined with pGWB14 (Nakagawa et al., 2007) to fuse a 3X HA tag at the C-terminus of PIF1. PIF1-HA-pGWB14 plasmid was transformed into the *TAP-SPA1* transgenic line. Transgenic seeds were selected on hygromycin to obtain homozygous lines with single inserts. The *COP1* ORF was PCR amplified and cloned into the pENTR vector as described above and the resulting pENTR-COP1 vector was recombined with the pGWB14 vector to fuse the 3X HA tag at the C-terminus of COP1. The COP1-HA-pGWB14 plasmid was transformed into *TAP-PIF1* transgenic plants. Transgenic seeds were selected on hygromycin to obtain homozygous lines with single inserts.

Protein extraction and immunoblot analyses

Seeds of various genotypes were grown in the dark for five days. For total protein extraction, 0.2 g tissue was collected and ground in 800 μL extraction buffer (1 M MOPS pH 7.6, 0.5 M EDTA, pH 8, 50% glycerol, 10% SDS, 40 mM β-mercaptoethanol, and 1×protease inhibitor cocktail [Sigma-Aldrich Co., St. Louis, MO, cat# 59], 2 mM PMSF, 25 mM β-GP, 10 mM NaF and 2 mM Na-orthovanadate) and cleared by centrifugation at 14,000 rpm for 15 min at 4ºC. After being boiled for 3 min, samples were centrifuged for 10 min and the total protein supernatants were separated on 8% SDS-PAGE gels, blotted onto polyvinylidene difluoride (PVDF) membranes, and probed with anti-HY5 (Hardtke et al., 2000) and anti-RPT5 (Enzo Life Sciences, Farmingdale, NY) antibodies. For the

secondary antibody, anti-rabbit IgG HRP conjugate (1:50000) (Kirkegaard & Perry Laboratories, Inc., Washington, DC) was used. Membranes were developed using a SuperSignal West Pico Chemiluminescent Substrate kit (Pierce Biotechnology Inc., Rockford, IL), and visualized on an X-ray film. The intensity of the HY5 and RPT5 bands from three independent blots was quantified using ImageJ software and the HY5 values were divided by the RPT5 values to generate a ratio for each sample. The dark control for the wild type sample was set to 1 from these ratios and the relative values of the other samples were calculated based on the wild type values. These relative values are shown as bar graphs in each figure under the blots.

Yeast Two-Hybrid analyses

The full-length open reading frame and various truncated forms of PIF1 were amplified by PCR using the primers listed in Table 2.1. These fragments were cloned into pEG202 and pJG4.5 (Ausubel et al., 1994) using the restriction sites included in the primers to generate LexA-PIF1, LexA-PIF1-N55, N150, N280, C328, C428 and AD-PIF1. All the clones were verified by restriction enzyme digestion and sequencing. Different HY5 and COP1 vectors used are as previously described (Ang et al., 1998; Saijo et al., 2003). These vectors were transformed into yeast strain EGY48-0 (Ausubel et al., 1994) and selected on minimal synthetic media without uracil, histidine and tryptophan for 3 days at 30ºC. Colonies were cultured overnight in liquid synthetic media without uracil, histidine and tryptophan supplemented with 2% (w/v) glucose. Aliquots of overnight cultures were then transferred to media supplemented with 2% (w/v) galactose and 1% (w/v) raffinose to induce the expression of the prey proteins. A β-galactosidase activity assay was performed as described (Saijo et al., 2003).

***In vivo/in vitro* co-immunoprecipitation assays**

For *in vivo* co-immunoprecipitation assays, seedlings were pretreated with MG132 as described (Shen et al., 2008). Total proteins were extracted from 0.4 g of dark-grown seedlings with 0.8 mL of native extraction buffer (50 mM Tris·Cl, pH 7.5, 150 mM NaCl, 1 mM EDTA, pH 8.0, 0.1% Tween20, 1×protease inhibitor cocktail [Sigma-Aldrich Co., St. Louis, MO, Cat# P9599], 1 mM PMSF, 20 μM MG132, 25 mM β-glycerophosphate, 10 mM NaF, and 2 mM Na orthovanadate) and cleared by centrifugation at 16,000 g for 15 min at 4°C. Anti-HA (Sigma-Aldrich Co., St. Louis, MO, Cat# H6908) antibody was incubated with Dynabeads (20 μL/μg antibody; Life Technologies Co**.,** Carlsbad, CA) for 30 min at 4°C, and the beads were washed twice with the extraction buffer to remove the unbound antibody. The bound antibody beads were added to 500 μg of total protein extracts in 0.8 mL and rotated for another 3 h at 4°C in the dark. The beads were collected using a magnet, washed three times with wash buffer, dissolved in 1×SDS-loading buffer, and heated at 65°C for 5 min. The immunoprecipitated proteins were separated on a 6.5% SDS-PAGE gel, blotted onto PVDF membranes, and probed with either anti-MYC (Sigma-Aldrich, Cat#: M4439) or anti-HA (Covance, Inc., Emeryville, CA, Cat# 16B12) antibody. Membranes were developed and visualized on an X-ray film as described above.

For *in vitro* coimmunoprecipitation assays, the full-length *COP1* ORF was PCR amplified and cloned into pENTR using the pENTR™/D-TOPO® Cloning Kit (Life Technologies Co**.,** Carlsbad, CA, Cat No: K2400-20). The pENTR-COP1 vector was recombined with the pVP13 destination vector (Jeon et al., 2005) to produce pVP-13-COP1. MBP-COP1 (Seo et al., 2003), GST-fusion protein with Arabidopsis HY5 (Hardtke et al., 2000) and HIS-PIF1 (Bu et al., 2011) were prepared as described previously. All protein combinations were incubated with 20 μL of amylose resin in the binding buffer (50 mM Tris-Cl, pH 7.5, 150 mM NaCl, 0.6% Tween-20, 1 mM DTT) for 3 h. The beads were

collected and washed six times with 5 min rotation each time in binding buffer. The bound HY5 were detected by anti-GST-HRP conjugate (RPN1236; GE Healthcare Bio-Sciences, Pittsburgh, PA). Membranes were developed and visualized as described above. The intensity of the GST-HY5 band from three independent blots was quantified using ImageJ software. The sample without PIF1 was set to 1 from these ratios and the relative values of the other samples were calculated based on this value. These relative values are shown as bar graphs.

***In vitro* ubiquitylation assays**

The His-PIF1 (Bu et al., 2011), GST-HY5 (Hardtke et al., 2000), MBP-COP1 (Seo et al., 2003), and E2 AtUBC8 (Lee et al., 2009) were prepared as described previously. All *in vitro* ubiquitylation assay procedures were performed as described (Saijo et al., 2003). Briefly, 2 μg of FLAG-Ubiquitin (U120; Boston Biochem Inc., Cambridge, MA), ~25 ng of E1 (UBE1, E-305; Boston Biochem Inc., Cambridge, MA), ~100 ng of E2 (AtUBC8), ~600 ng of MBP-COP1, ~400 ng of GST-HY5, and 100-200 ng MBP-PIF1 were used in the reaction. The FLAG-Ubiquitin conjugated HY5 and COP1 were detected by immunoblot with α-FLAG antibody (F1804; Sigma-Aldrich Co., St. Louis, MO). Anti-GST-HRP conjugate was used for HY5 detection. The intensity of the GST-HY5 bands detected by anti-FLAG antibody from three independent blots was quantified using ImageJ software. The sample without PIF1 was set to 1 and the relative values of the other samples were calculated based on this value. These relative values are shown as bar graph.

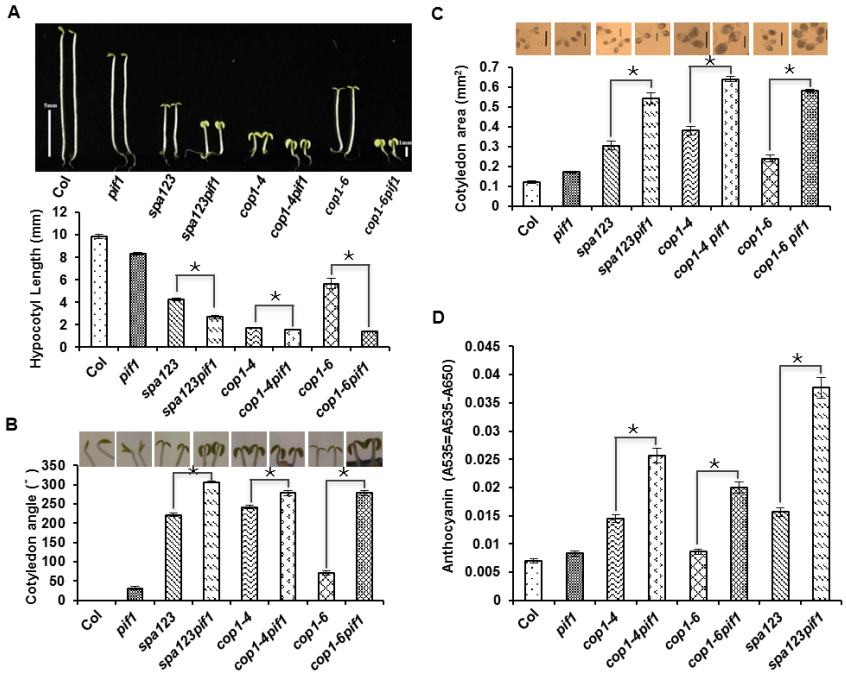

Figure 2.1: *pif1* and *cop1/spa123* mutants synergistically promote photomorphogenesis in the dark.

(A-C) (Top) Visible of the wild type (Col-0), *pif1*, *cop1*, *spa123* and various combinations of *pif1*, *cop1* and *spa123* mutant seedlings phenotypes as indicated. Seeds of various genotypes were grown on MS medium without sucrose for 5 days in the dark. (Bottom) Bar graph shows the mean hypocotyl lengths (A), cotyledon angles (B) and cotyledon areas (C) of the above genotypes (n>30, three biological replicates). Error bars indicate standard deviation. ***,** indicates significant difference ($p<0.05$). Bar = 1mm. (D) Bar graph shows the mean anthocyanin levels of the wild type (Col-0), *pif1*, *cop1*, *spa123* and various combinations of *pif1*, *cop1* and *spa123* mutant seedlings as indicated. Seedlings of various genotypes were grown on MS medium with sucrose for 3 days in the dark (n=50, three replicates). Error bars indicate standard deviation. *, indicates significant difference, $p<0.05$).

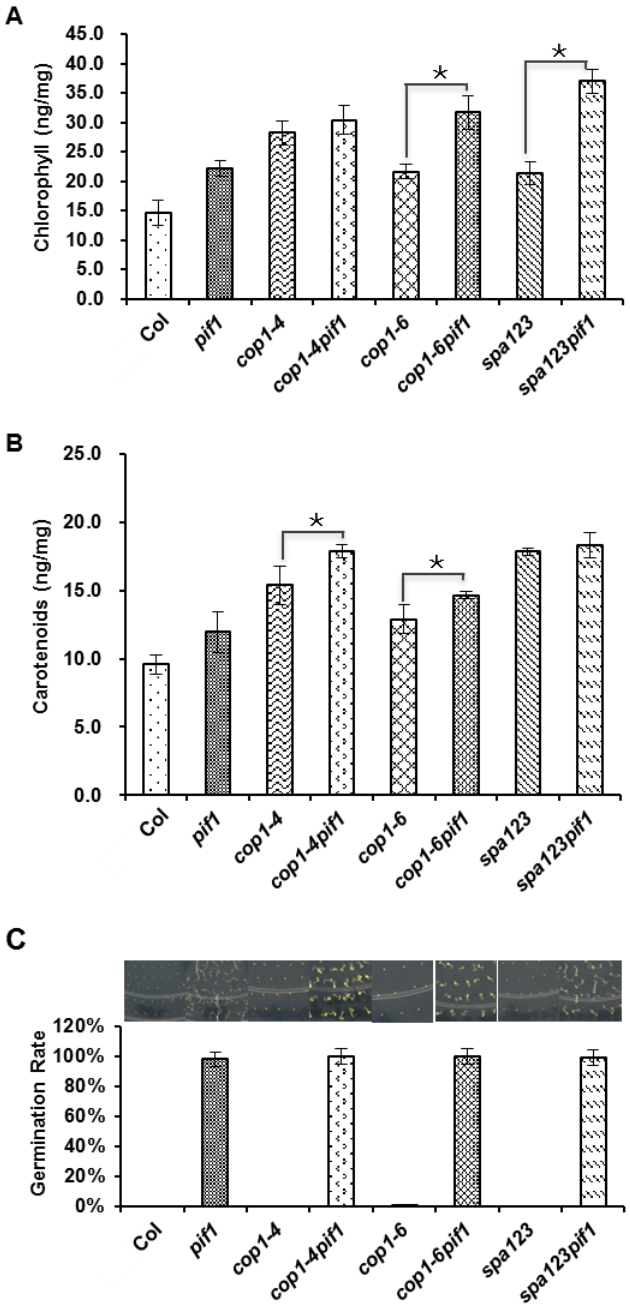

Figure 2.2: *pif1* enhances the accumulation of chlorophyll and carotenoid in the *cop1* and *spa123* backgrounds in the dark.

(A, B) Bar graphs show the amount of chlorophyll (A) and carotenoids (B) for various *pif1* combinations with *cop1-4, cop1-6* and *spa123* mutants. Seedlings were grown in the dark for 4 days and then exposed to white light for 5 hours before extraction of chlorophylls and carotenoids. *, indicates significant difference ($p<0.05$). Error bars indicate standard deviation. (C) The seed germination phenotype of *pif1* is not affected by *cop1-4, cop1-6* and *spa123* mutants. (Top) Photographs show the germinated and nongerminated seeds of various genotypes. (Bottom) Bar graph shows the percent of seeds germinated for various genotypes as indicated.

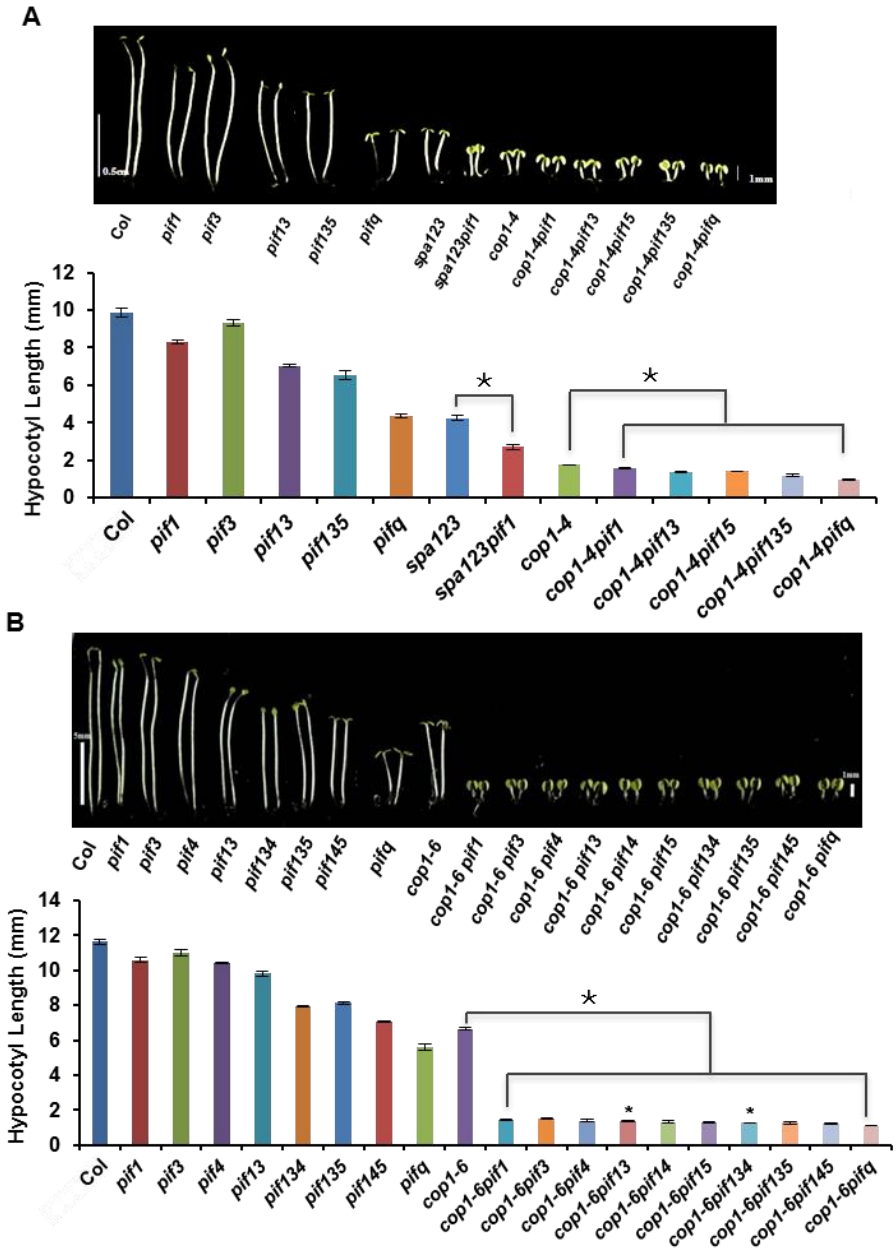

Figure 2.3: *pif*s enhance the photomorphogenic development synergistically with *cop1* and *spa123* in the dark.

(A) (Top) Photographs of seedlings of wild type (Col-0), *cop1-4*, *spa123*, and various *pif* combinations with and without *cop1-4* and *spa123*. (Bottom) Bar graph shows the

hypocotyl lengths of dark-grown seedlings of various genotypes as indicated. Seeds of various genotypes were grown on MS medium without sucrose for 5 days in the dark. Error bars indicate standard deviation. ***,** indicates significant difference ($p<0.05$). (B) (Top) Photographs of seedlings of wild type (Col-0), *cop1-6*, and various *pif* combinations with and without *cop1-6.* (Bottom) Bar graph shows the hypocotyl lengths of 5 day-old dark-grown seedlings of various genotypes as indicated. Error bars indicate standard deviation. ***,** indicates significant difference ($p<0.05$).

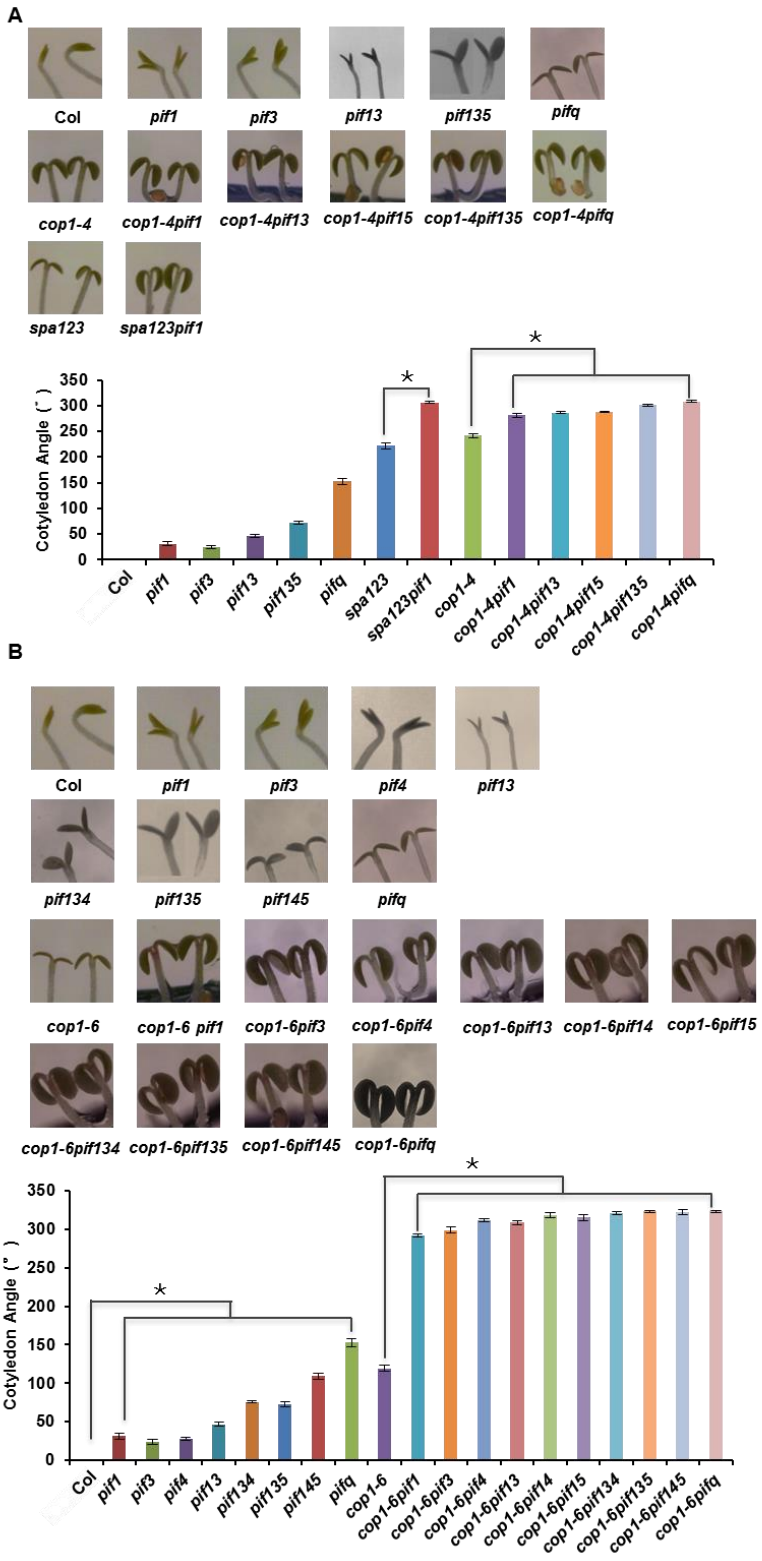

Figure 2.4: *pif*s increase the cotyledon angle of dark-grown seedlings synergistically

with *cop1* and *spa123*.

(A) (Top) Photographs of cotyledon angles of dark-grown seedlings of wild type (Col-0), *cop1-4*, *spa123*, and various *pif* combinations with and without *cop1-4* and *spa123*. (Bottom) Bar graph shows the cotyledon angles of dark-grown seedlings of various genotypes as indicated. Error bars indicate standard deviation. ***,** indicates significant difference ($p<0.05$). (B) (Top) Photographs of cotyledon angles of dark-grown seedlings of wild type (Col-0), *cop1-6*, and various *pif* combinations with and without *cop1-6.* (Bottom) Bar graph shows the cotyledon angles of dark-grown seedlings of various genotypes as indicated. Seeds of various genotypes were grown on MS medium without sucrose for 5 days in the dark. Error bars indicate standard deviation. ***,** indicates significant difference ($p<0.05$).

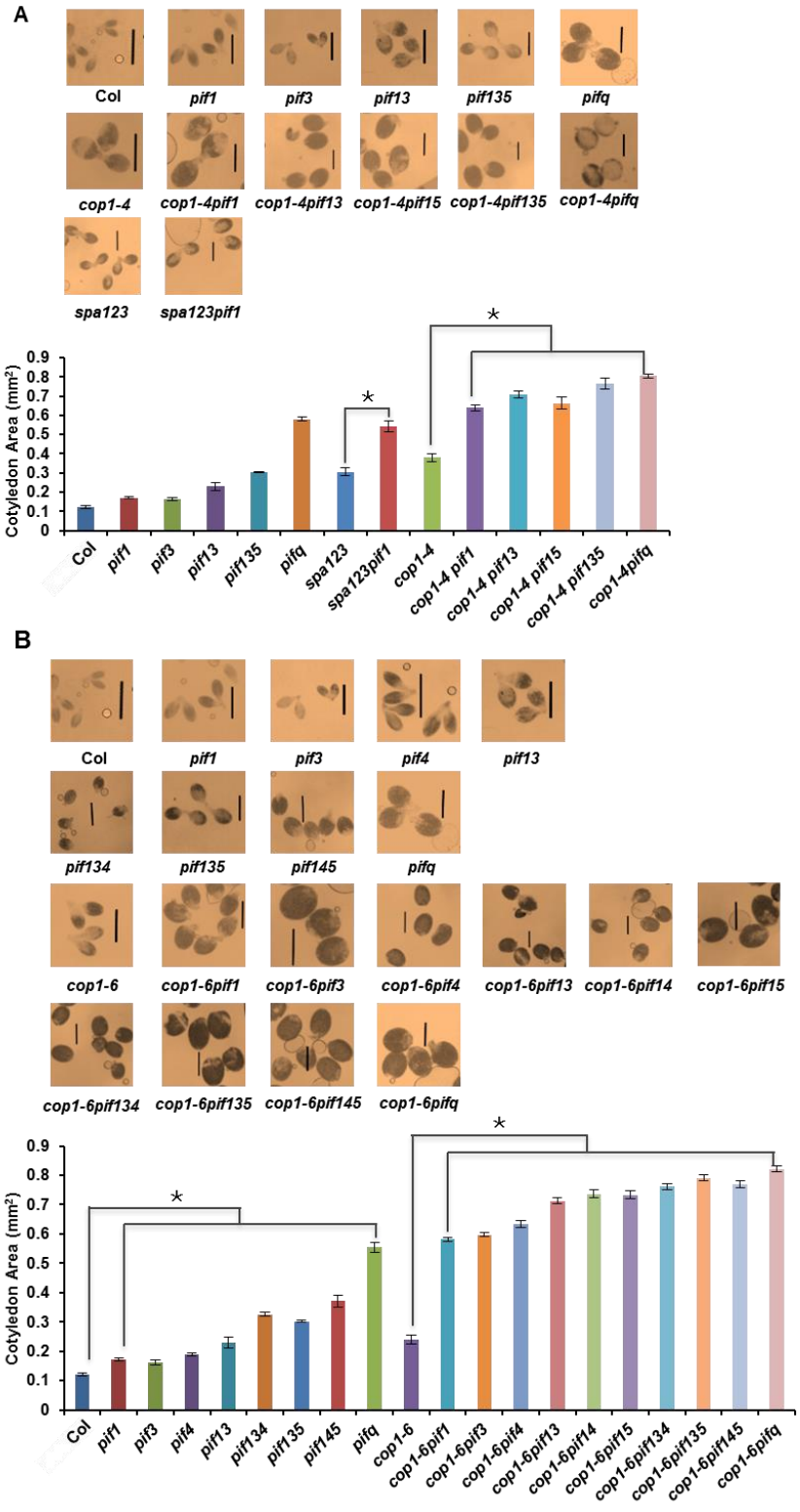

Figure 2.5: *pif*s increase the cotyledon area of dark-grown seedlings synergistically with

cop1 and *spa123*.

(A) (Top) Photographs of cotyledon areas of dark-grown seedlings of wild type (Col-0), *cop1-4*, *spa123*, and various *pif* combinations with and without *cop1-4* and *spa123*. Bar = 1mm. (Bottom) Bar graph shows the cotyledon areas of dark-grown seedlings of various genotypes as indicated. Error bars indicate standard deviation. ***,** indicates significant difference ($p<0.05$). (B) (Top) Photographs of cotyledon areas of dark-grown seedlings of wild type (Col-0), *cop1-6*, and various *pif* combinations with and without *cop1-6.* Bar = 1mm. (Bottom) Bar graph shows the cotyledon areas of dark-grown seedlings of various genotypes as indicated. Seeds of various genotypes were grown on MS medium without sucrose for 5 days in the dark. Error bars indicate standard deviation. ***,** indicates significant difference ($p<0.05$).

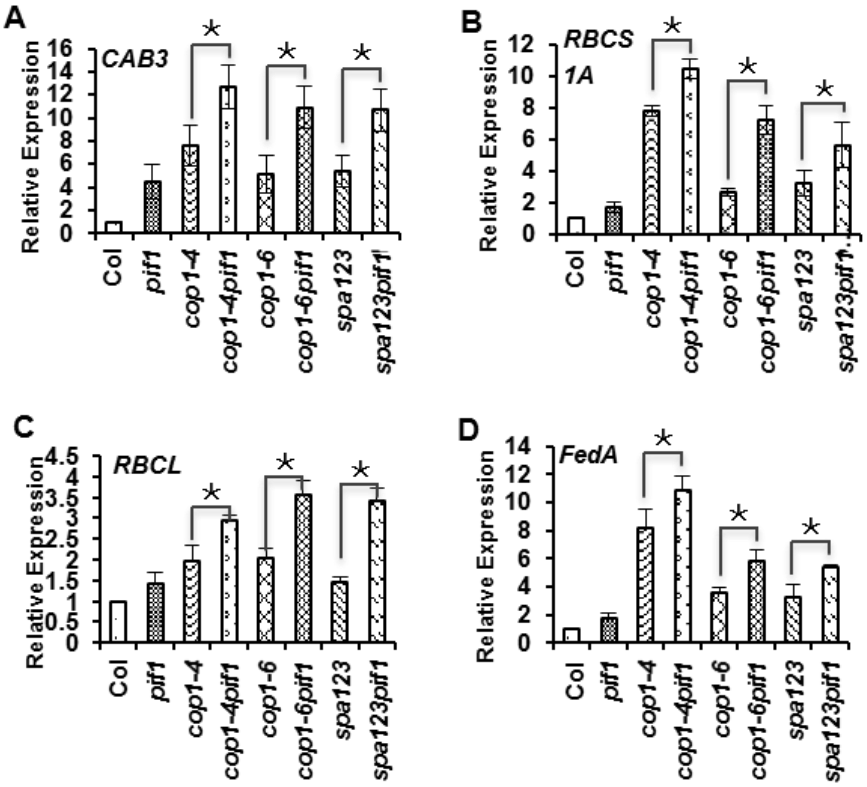

Figure 2.6: *pif1* and *cop1/spa123* mutants display synergistic promotion of light-regulated gene expression in the dark.

(A-D) Bar graphs show the expression of *CAB3* (A), *RBCS1A* (B), *RBCL* (C) and *FedA* (D) transcript levels in the wild type, *pif1*, *cop1*, *spa123* and various combinations of *pif1*, *cop1* and *spa123* mutant seedlings as indicated. Total RNA was isolated from 4 day-old dark-grown seedlings for qRT-PCR assays (n= 3 independent biological repeats). *PP2A* was used as an internal control. Wild type was set as 1 and the relative gene expression levels were calculated. Error bars indicate standard deviation. *, indicates significant difference ($p<0.05$).

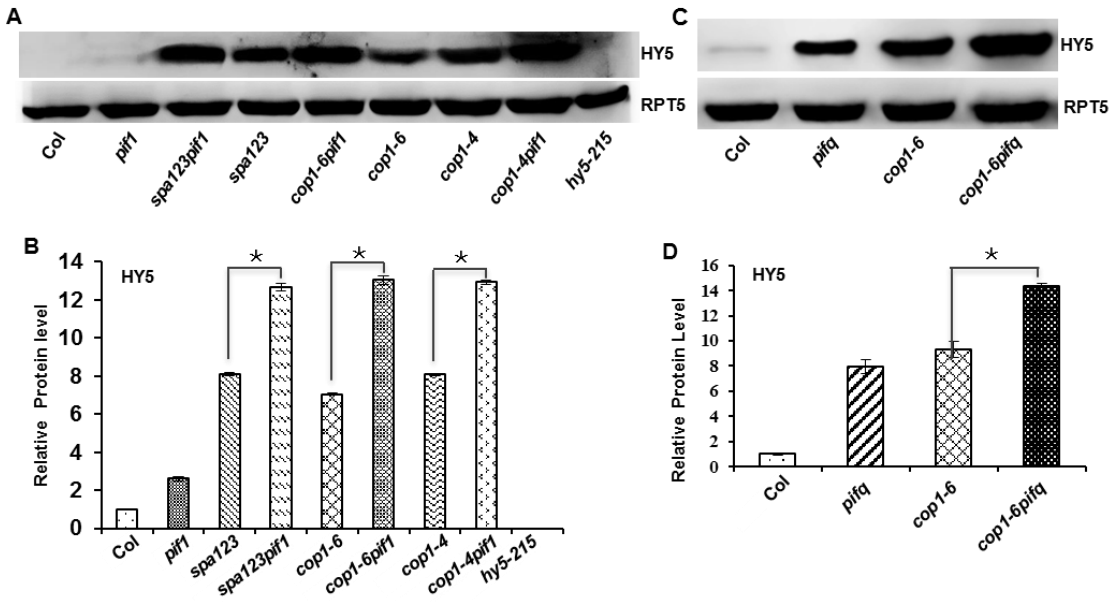

Figure 2.7: PIFs promote COP1 and SPA-mediated degradation of HY5 in the dark posttranslationally.

(A) Western blot shows the HY5 level in various genotypes as indicated. Total protein was extracted from 5 day-old seedlings grown on MS media without sucrose in darkness. Total protein was separated on an 8% SDS-PAGE gel, blotted onto PVDF membrane and probed with anti-HY5 or anti-RPT5 antibodies. (B) Bar graph showing the HY5 protein levels in the mutants indicated. For protein quantitation, HY5 band intensities were quantified from three independent blots using ImageJ, and normalized against RPT5 levels. Wild type was set as 1 and the relative proteins levels were calculated. Error bars indicate standard deviation. *, indicates significant difference ($p<0.05$). (C) Western blot shows the HY5 level in the wild type, *pifq*, *cop1-6* and *cop1-6pifq* backgrounds. An RPT5 blot shows a loading control. Seedlings were grown in the dark as described above. (D) Bar graph shows the quantified HY5 protein levels in the wild type (Col-0), *pifq*, *cop1-6* and *cop1-6 pifq*

backgrounds. Error bars indicate standard deviation. *, indicates significant difference ($p<0.05$).

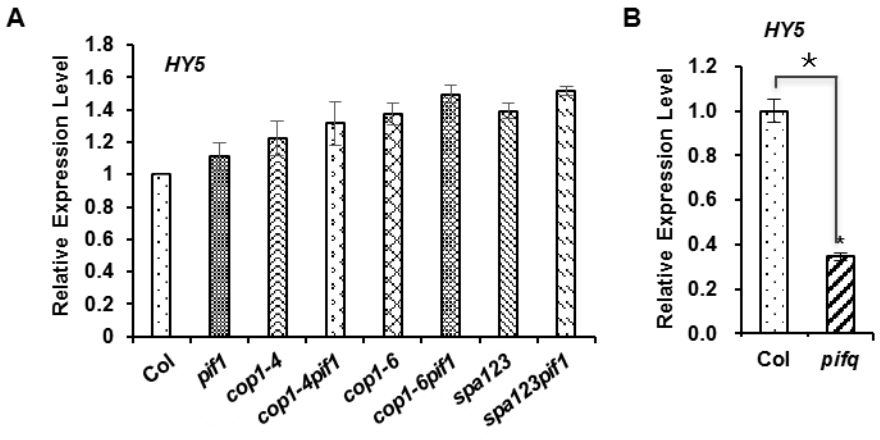

Figure 2.8: *HY5* mRNA level in various mutants compared to wild type.

(A) Bar graph showing the *HY5* mRNA levels in the mutants indicated. *HY5* mRNA level was determined using qRT-PCR assays. Total RNA was extracted from 4 day-old dark grown seedlings as described above. (B) Bar graph shows the *HY5* mRNA level in the wild type (Col-0) and *pifq* based on RNAseq data as described (Zhang et al., 2013). Error bars indicate standard deviation. ***,** indicates significant difference ($p<0.05$).

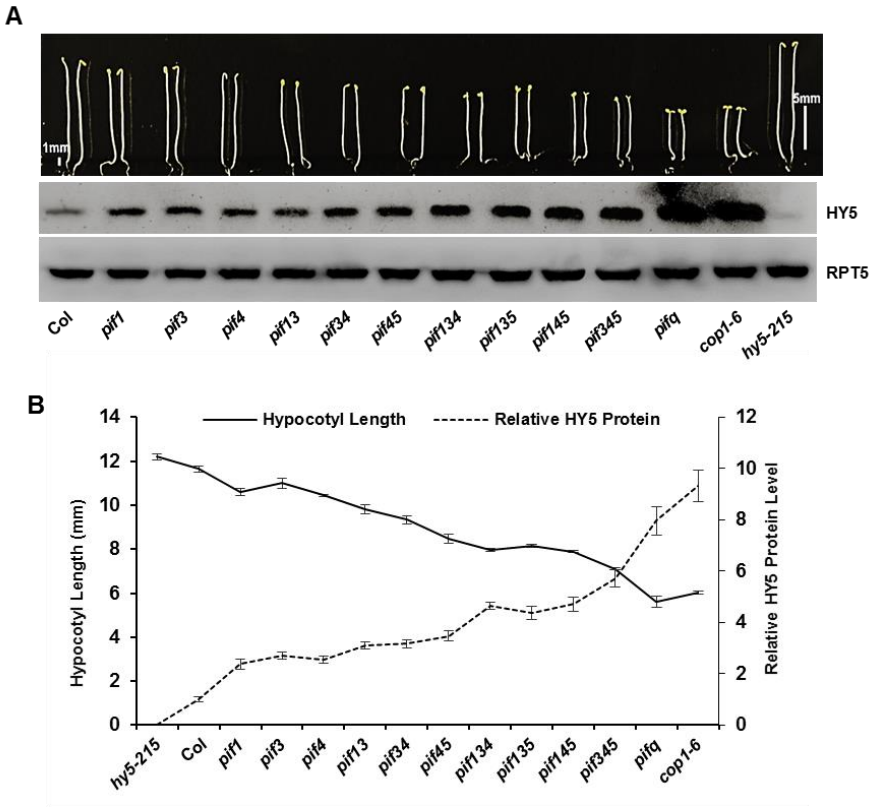

Figure 2.9: *pif*s redundantly regulate the level of HY5 in the dark.

(A) (Top) Visible phenotypes of the wild type, various *pif* single, double, triple and quadruple mutants, and *cop1-6* and *hy5-215* as controls. Seeds of various genotypes were grown on MS medium without sucrose for 5 days in the dark. (Bottom) Western blot shows the HY5 level in the above genotypes. RPT5 blot shows a loading control. Total protein was extracted from 5 day-old dark-grown seedlings grown on MS media without sucrose. (B) Line graph shows the inverse correlation between the hypocotyl lengths and the HY5 levels in the above genotypes. Band intensities were quantified from three independent blots using ImageJ, and normalized against RPT5 levels. Wild type was set as 1 and the relative proteins levels were calculated. Error bars indicate standard deviation.

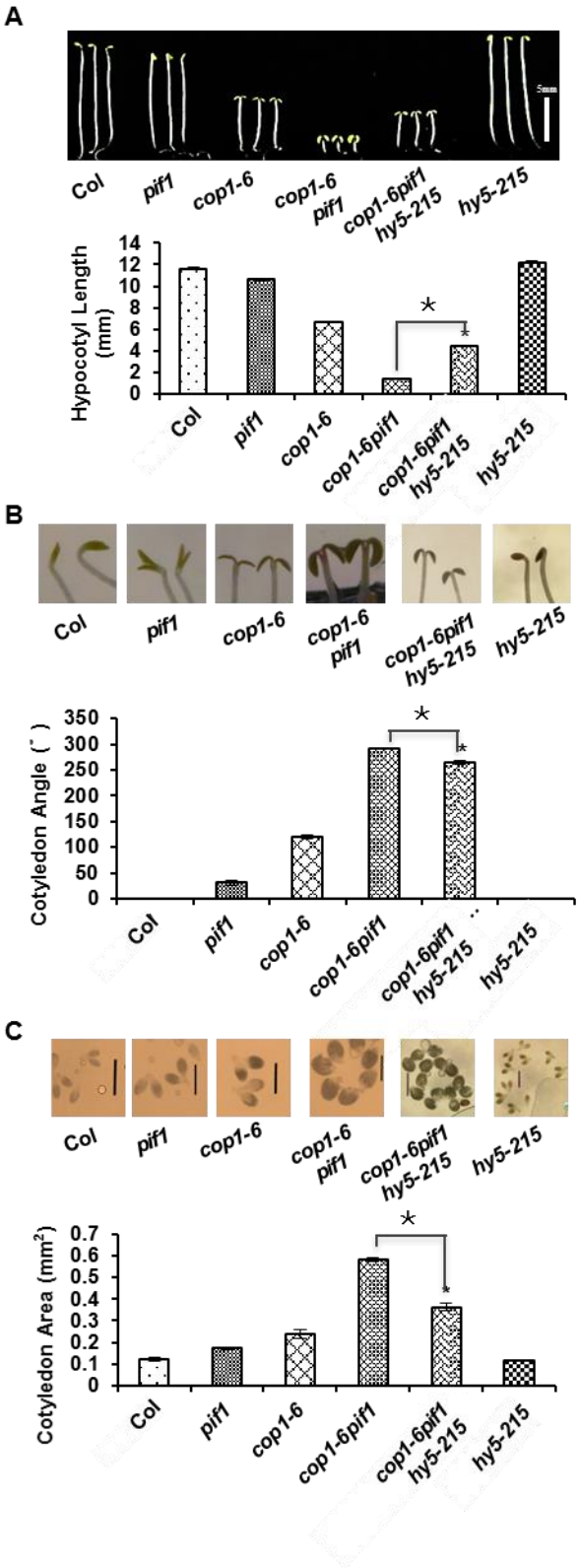

Figure 2.10: *hy5-215* partially suppresses the synergistic promotion of photomorphogenesis in the *cop1-6 pif1* background.

(A) (Top) Photographs of 5-day old dark grown seedlings of wild type, *pif1, cop1-6, cop1-6 pif1, hy5-215* and *cop1-6pif1 hy5-215*. (Bottom) Bar graph showing hypocotyl lengths of various genotypes as indicated. (B) (Top) Photographs of cotyledon angles of 5-day old dark grown seedlings. (Bottom) Bar graph showing cotyledon angles of various genotypes as indicated. (C) (Top) Photographs of cotyledon areas of 5-day old dark grown seedlings. (Bottom) Bar graph showing cotyledon areas of various genotypes as indicated. Error bars indicate standard deviation. *, indicates significant difference ($p<0.05$), ($n>30$, three biological replicates).

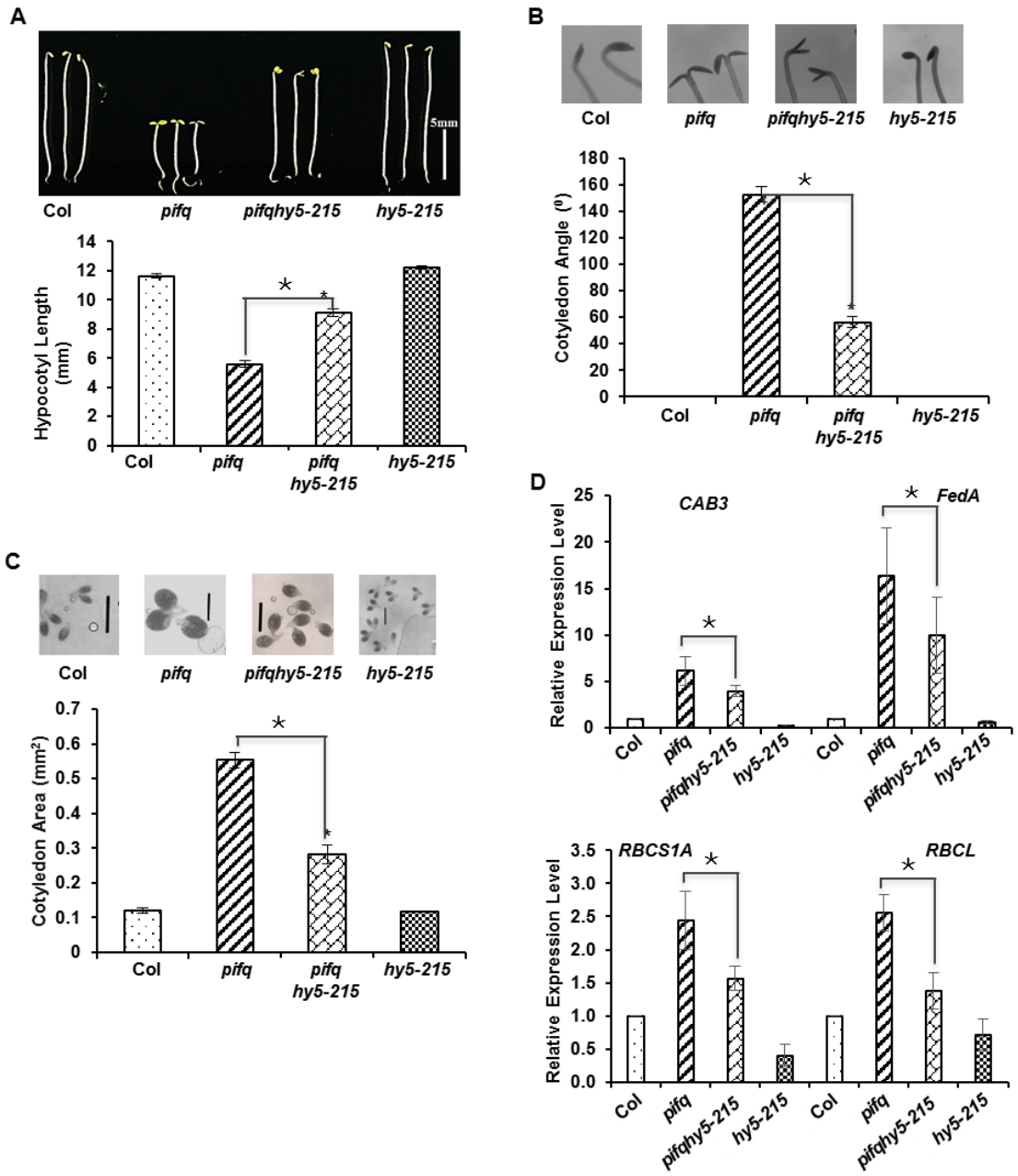

Figure 2.11: *hy5-215* partially suppresses the constitutive photomorphogenic phenotypes of *pifq*.

(A) (Top) Photographs of 5-day old dark grown seedlings of wild type, *pifq, pifq hy5-215* and *hy5-215*. (Bottom) Bar graph shows the hypocotyl lengths of various genotypes as indicated. (B) (Top) Photographs of cotyledon angles of 5-day old dark grown seedlings. (Bottom) Bar graph shows the cotyledon angles of various genotypes as indicated. (C) (Top) Photographs of cotyledon areas of 5-day old dark grown seedlings. (Bottom) Bar graph shows the cotyledon areas of various genotypes as indicated. Error bars indicate standard deviation. *, indicates significant difference ($p<0.05$), ($n>30$, three biological replicates). (D) Bar graphs show the expression of *CAB3*, *FedA, RBCS1A* and *RBCL* transcript levels in the wild type, *pifq, pifq hy5-215* and *hy5-215* mutant seedlings as indicated. Total RNA was isolated from 4 day-old dark-grown seedlings for qRT-PCR assays (n= 3 independent biological repeats). *PP2A* was used as an internal control. Wild type was set as 1 and the relative gene expression levels were calculated. Error bars indicate standard deviation. *, indicates significant difference ($p<0.05$).

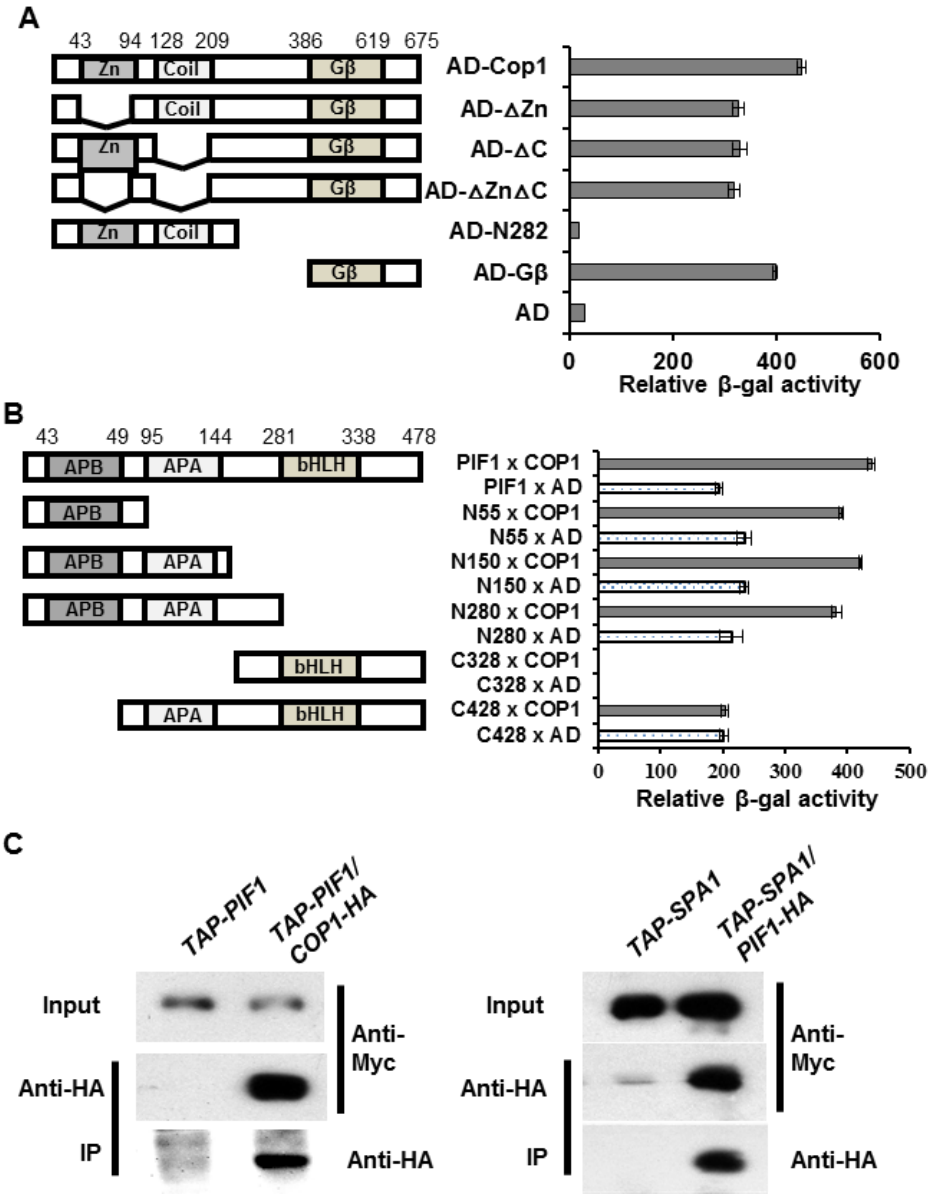

Figure 2.12: PIF1 interacts with COP1 and SPA1.

(A) The WD40 repeat domain of COP1 is necessary and sufficient to interact with PIF1 in Yeast-Two-Hybrid assays. Left panel shows the full-length and various deletion fragments of AD-COP1 fusion constructs. The zinc-binding ring finger (Zn), the coiled-coil domain (Coil) and the WD-40 repeats (Gβ) of COP1 are as indicated. Right panel shows the

corresponding β-galactosidase activities with LexA-full-length PIF1. The error bars represent standard deviation. (B) The amino terminal 55 amino acids containing the active phytochrome binding (APB) domain of PIF1 is necessary and sufficient for interaction with COP1 in Yeast-Two-Hybrid assays. Left panel shows the full-length and various deletion fragments of LexA-PIF1 fusion constructs. The APB, the active phyA binding (APA) and the basic helix-loop-helix (bHLH) domains of PIF1 are as indicated. Right panel shows the corresponding β-galactosidase activities with AD-full-length COP1. The error bars represent standard deviation. (C) PIF1 interacts with COP1 and SPA1 *in vivo*. Left panel illustrates interaction between PIF1 and COP1 in transgenic plants. Plants expressing TAP-PIF1 from the native *PIF1* promoter and COP1-HA from the constitutively active 35S promoter or plants expressing only TAP-PIF1 were grown in the dark for 4 days before protein extraction. TAP-PIF1 was immunoprecipitated using anti-HA (hemagglutinin) antibody and immunoblotted using anti-Myc or anti-HA antibody. Right panel illustrates interaction between PIF1 and SPA1 in transgenic plants. Plants expressing PIF1-HA from 35S promoter and TAP-SPA1 from 35S promoter or plants expressing only TAP-SPA1 were grown in the dark for 4 days before protein extraction. TAP-SPA1 was immunoprecipitated using anti-HA (hemagglutinin) antibody and immunoblotted using anti-Myc or anti-HA antibody.

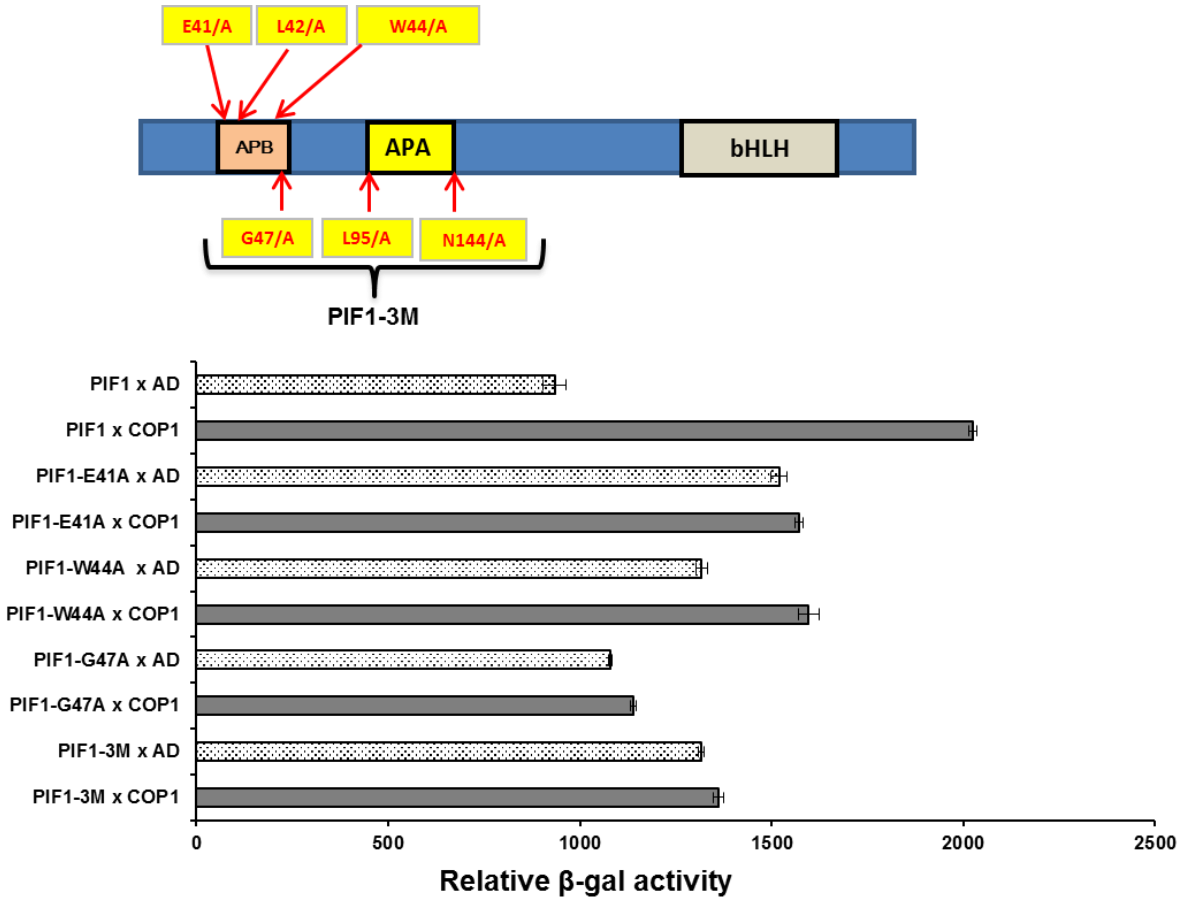

Figure 2.13: The APB domain of PIF1 is necessary for interaction with the full-length COP1 in Yeast Two-Hybrid assays.

(Top) Schematic diagram of PIF1 structure showing the position of APB, APA and bHLH domains. The point mutations in the APB and APA domains involved in phytochrome interaction are shown. (Bottom) The bar graph shows the b-galactosidase activities of various PIF1 wild type and point mutant versions with full-length AD-COP1. Error bars indicate standard deviation.

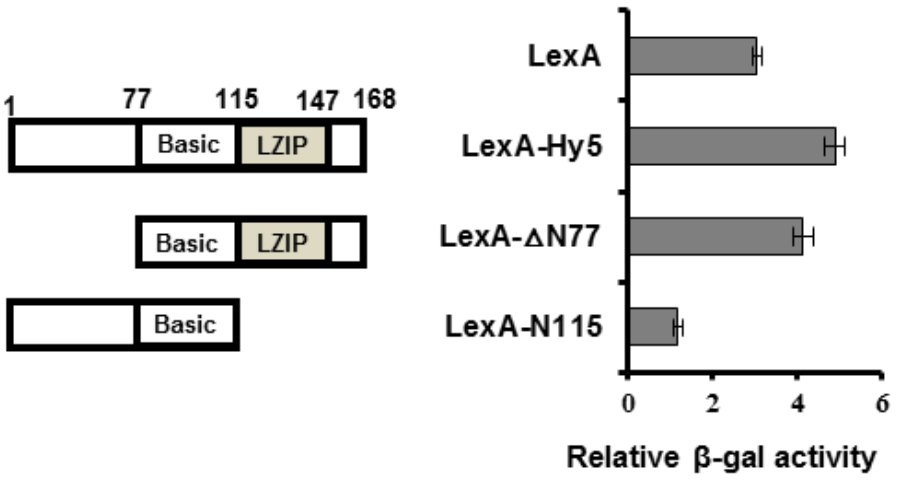

Figure 2.14: PIF1 interacts with the bZIP domain of HY5 in Yeast Two-Hybrid assays.

Left panel shows the full-length and various deletion fragments of LexA-HY5 fusion constructs. The basic and the Leucine zipper (LZIP) of HY5 are as indicated. Right panel shows the corresponding b-galactosidase activities with full-length AD-PIF1. Error bars indicate standard deviation.

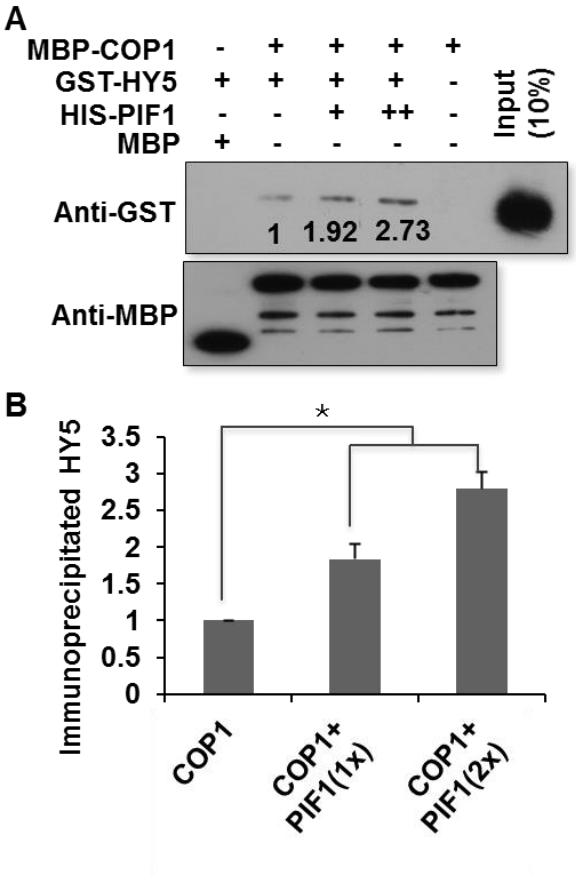

Figure 2.15: PIF1 promotes interaction between COP1 and HY5 in an *in vitro* pull-down assay.

Recombinant MBP-COP1, HIS-PIF1 and GST-HY5 fusions proteins were purified from *E. coli*. (A) GST–HY5 was precipitated by MBP–COP1 using maltose agarose beads in the absence and in the presence of increasing concentrations of HIS-PIF1. The pellet fraction was eluted and analyzed by immunoblotting using anti-GST and anti-MBP antibodies. Numbers on the blot indicate fold induction of interaction between COP1 and HY5. (B) Bar graph shows the enhancement of interaction between COP1 and HY5 in the presence of PIF1. Error bars indicate sem. *, indicates significant difference ($p<0.05$).

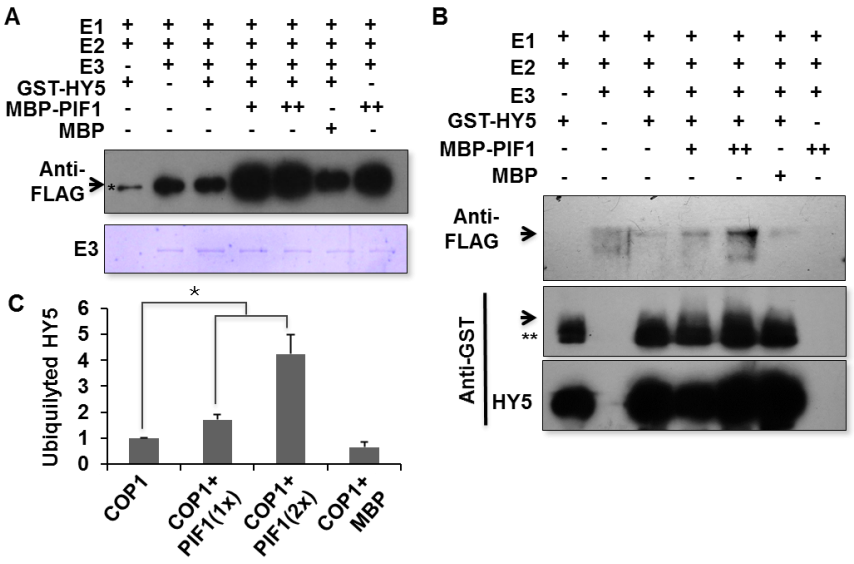

Figure 2.16: PIF1 enhances the auto- and trans-ubiquitylation activity of COP1.

Recombinant MBP-COP1, MBP-PIF1 and GST-HY5 fusions proteins were purified from *E. coli*. (A) PIF1 promotes autoubiquitylation of COP1 *in vitro*. *In Vitro* Ubiquitylation assay was performed using MBP-COP1 as E3, FLAG-Ubiquitin, GST-HY5 and increasing concentrations of MBP-PIF1. MBP was used as a control. The arrow indicates autoubiquitylated MBP-COP1 detected by anti-FLAG antibody. The amount of MBP-COP1 (E3) in each lane is shown below in Coomassie stained gel. *, indicates a non-specific band. (B) PIF1 promotes ubiquitylation of HY5 by COP1 *in vitro*. *In Vitro* Ubiquitylation assay was performed as described above. (Top panel) Arrow indicates ubiquitylated GST-HY5 detected by anti-FLAG antibody. (Middle panel) Arrow indicates ubiquitylated GST-HY5 detected by anti-GST antibody. **, indicates a non-specific band. (Bottom panel) Amount of GST-HY5 in each lane is shown as detected by anti-GST antibody. (C) Quantitation of the ubiquitylated HY5 level in the absence or presence of increasing concentration of PIF1 or GST as a control protein. Error bars indicate sem. *, indicates significant difference ($p<0.05$).

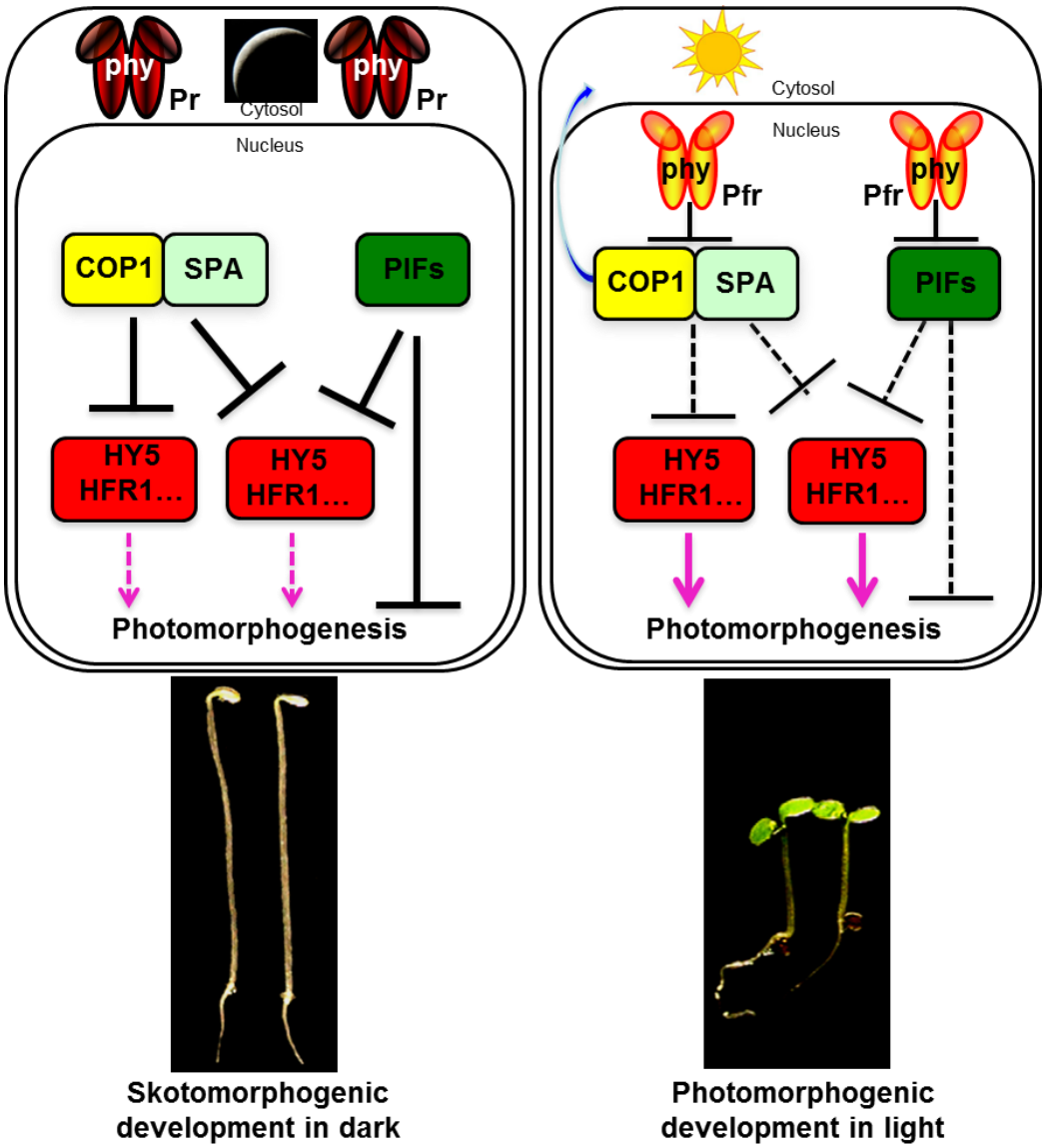

Figure 2.17: Model showing how PIFs and COP1-SPA proteins function synergistically as well as independently to repress photomorphogenesis in the dark.

(Left) phys are localized to the cytosol as an inactive Pr form, while PIFs and COP1/SPA proteins are constitutively localized to the nucleus in the dark. PIFs repress

photomorphogenesis by transcriptional repression of light-regulated genes. COP1/SPA proteins independently repress photomorphogenesis by targeting the positively acting transcription factors (e.g., HY5/HFR1/LAF1 and others) for Ub/26S proteasome mediated degradation. In addition, PIFs and COP1/SPA proteins also promote synergistic degradation of positively acting factors to repress photomorphogenesis in the dark. (Right) Light signals induce photo-conversion of the Pr form to the active Pfr form and thereby promote nuclear translocation of phys. Within the nucleus, the Pfr forms of phys interact with PIFs and induce phosphorylation, ubiquitylation and 26S proteasome-mediated degradation. In response to light, COP1/SPA complexes are also inactivated by phys in an unknown mechanism and/or by nuclear exclusion of COP1 under prolonged light (indicated by blue arrow) (Subramanian et al., 2004), thereby stabilizing the positively acting transcription factors. The light-induced degradation of PIFs as well as inactivation/nuclear exclusion of COP1 results in relieving the negative regulation to promote photomorphogenesis.

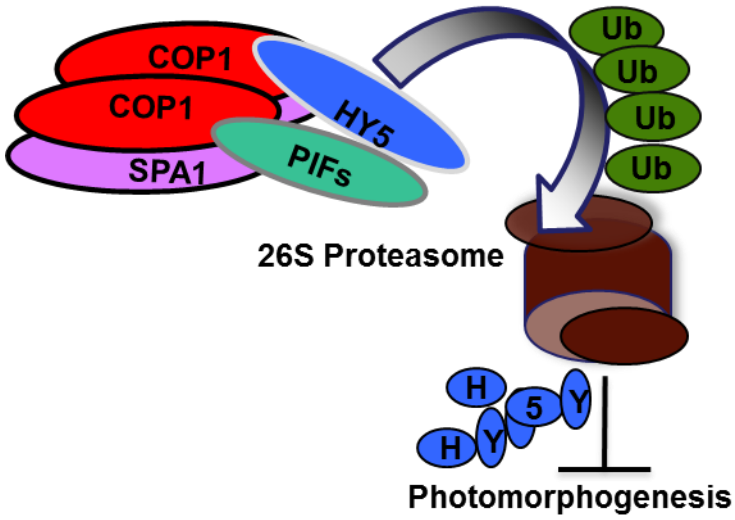

Figure 2.18: Model of how PIF1 promotes substrate recruitment, auto- and trans-ubiquitylation of HY5 to repress photomorphogenesis in the dark.

The amino terminal 55 amino acids containing the APB domain of PIF1 interacts with the WD40 repeat domain of COP1 and the bHLH domain of PIF1 interacts with the bZIP domain of HY5 (Figures 2.12-2.14) (Chen et al., 2013). PIF1 also interacts with full-length SPA1 *in vivo* (Figure 2.12). The amino terminal domain of HY5 interacts with the WD40 repeat domain of both COP1 and SPA1. In addition, both SPA1 and COP1 interact through their coil-coil domains. The resulting complex promotes ubiquitylation and subsequent degradation of HY5 through the 26S proteasome-mediated pathway.

Table 2.1: Primer sequences used in experiments described in the Chapter II.

Gene	Forward	Reverse
For qRT-PCR		
CAB3	GAGCTCAAGAACGGAAGATTGGC	CCGGGAACAAAGTTGGTTGC
RBCS1A	ACCTTCTCCGCAACAAGTGG	GAAGCTTGGTGGCTTGTAGG
RBCL	TCGGTG GAGGAACTTT AGGC	TGCAAGATCACGTCCCTCAT
Fed A	CTTCATTCATCCGTCGTTCC	AGGGTAAGCAGCACAAGTGA
HY5	GCTGCAAGCTCTTTACCATC	TCCGACAGCTTCTCCTCCAAACTC
PP2A	TATCGGATGACGATTCTTCGTGCAG	GCTTGGTCGACTATCGGAATGAGAG
For cloning		
PIF1	cgaGAATTCatgcatcattttgtccctgac	tgaGTCGACttaacctgttgtgtggtttccgtg
PIF1-N55	ctgGAATTCatgcatcattttgtccctgac	ctgGTCGACtctctggttttgaacaacaac
PIF1-N150	ctgGAATTCatgcatcattttgtccctgac	ctgGTCGACcagcctcgagaaattcatgaa
PIF1-C328	ctgGAATTCagaggggattttaataacgg	ctgGTCGACttaacctgttgtgtggtttcc
PIF1 pENTR	CACCatgcatcattttgtccctgacttcg	acctgttgtgtggtttccgtg
COP1 pENTR	CACCatggaagagatttcgacggatcc	cgcagcgagtaccagaactttgatgg

Chapter III: Suicidal co-degradation of the positive and negatively acting transcription factors fine tunes photomorphogenesis in Arabidopsis

ABSTRACT

LONG HYPOCOTYL IN FAR-RED1 (HFR1), a HLH transcription factor, has been shown to function as an important positive regulator of plant photomorphogenesis. HFR1 is degraded by the E3 Ubiquitin-ligase, CONSTITUTIVELY PHOTOMORPHOGENIC 1 (COP1) in the dark. Recently, it was shown that HFR1 heterodimerizes with Phytochrome Interacting Factor 1 (PIF1) and prevents transcriptional activation activity of PIF1 to regulate seed germination under red light. Here we show that HFR1 also promotes the degradation of PIF1 in the dark by direct heterodimerization. *hfr1* is hyposensitive to far-red light for seed germination response, consistent with previous roles of HFR1 under far-red light. By contrast, PIF1 also promotes the degradation of HFR1 in darkness. Genetic evidence shows that *hfr1* mutant partially suppresses the constitutive photomorphogenic phenotypes of the *cop1-6pif1* and *pifq* both in the dark and far red light conditions. GFP-HFR1 is synergistically stabilized in the *cop1 pif1* and *pifq* mutants both under dark and far-red light conditions. Biochemical evidence shows that PIF1 enhances the trans-ubiquitination of HFR1 by COP1 *in vitro*. In addition, the reciprocal co-degradation between PIF1 and HFR1 is dependent on the 26S-proteasome pathway *in vivo*. These data uncover a suicidal co-degradation mechanism between the positive and negative regulators to fine tune seed germination and seedling development during the dark to light transition.

KEYWORDS

bHLH transcription factor, E3 ligase, photomorphogenesis, suicidal co-degradation, ubiquitination, 26S proteasome.

INTRODUCTION

Plants undergo skotomorphogenesis in the dark and photomorphogenesis under light. Skotomorphogenic development is characterized by elongated hypocotyl, apical hook and small appressed cotyledons. In contrast, photomorphogenic development is characterized by short hypocotyl, and expanded green cotyledons. Light signals from the environment play an important role in promoting photomorphogenic development including seed germination, seedling de-etiolation, flowering time, shade avoidance, phototropism and other responses. These responses are mediated by a group of photoreceptors that track a majority of the visible wavelengths of the light spectrum. These include the UV-B-RESISTANCE 8 (UVR8) sensing UV-B light, the crytochromes (cry), phototropins (phot) and Zeitlupe family of F-box proteins for perceiving the UV-A/blue light signals and the phytochromes (phys) for perceiving red/far-red light (Bae and Choi, 2008; Galvão and Fankhauser, 2015).

The phytochromes are chromoproteins containing a ~120 kD polypeptide attached to a billin chromophore that is responsible for perceiving red/far-red light signals (Bae and Choi, 2008). Phytochromes are encoded by a small five-member family (phyA-phyE) in Arabidopsis, which can form homo and heterodimers *in vivo* (Sharrock, 2008; Clack et al., 2009). They are synthesized as the inactive Pr form. Upon sensing red light signals, phys undergo a conformational change to a biologically active Pfr form that can converted back to Pr form by exposure to far-red light. The Pfr form of all phys migrates into the nucleus with differential kinetics (Fankhauser and Chen, 2008), and regulates the expression of a large number of genes to promote photomorphogenesis (Tepperman et al., 2006).

Genetic screenings have identified two broad classes of mutants defective in phy signaling pathways: one shows light-dependent phenotypes and the other shows light-independent phenotypes (Huq and Quail, 2005). The light-independent group is also called

constitutively photomorphogenic (cop), suggesting that they display photomorphogenic phenotypes in the dark and consequently function as negative regulators of photomorphogenesis (Lau and Deng, 2012). The light-dependent group also includes the positive and negative regulators functioning in photomorphogenesis (Huq and Quail, 2005). For example, LONG HYPOCOTYL5 (HY5), HY5-HOMOLOG (HYH), LONG AFTER FAR-RED LIGHT1 (LAF1), LONG HYPOCOTYL IN FAR-RED1 (HFR1) and a B-BOX containing protein 22 (BBX22) are the major positive regulators of photomorphogenesis in phy signaling pathways (Oyama et al., 1997; Fairchild et al., 2000; Fankhauser and Chory, 2000; Ballesteros et al., 2001; Holm et al., 2002; Chang et al., 2011).

Among the negative regulators, Phytochrome Interacting Factors (PIFs) originally identified by both genetic and reverse genetic approaches have been shown to directly interact with phyA and/or phyB and inhibit photomorphogenic development (Castillon et al., 2007; Leivar and Quail, 2011; Leivar and Monte, 2014). PIFs consist of seven members (PIF1, PIF3-8) encoding bHLH transcription factors. They bind to the G-box (CACGTG) DNA sequence elements present in gene promoters and repress the light-inducible genes while activating the light-repressed genes in the dark. In response to light, phys directly interact with PIFs and induce their phosphorylation, ubiquitination and subsequent degradation to promote photomorphogenesis. In this process, both CUL3 and CUL4 based E3 ligases mediate light-induced ubiquitination of PIF1 and PIF3. In addition, Casein Kinase 2 and BIN2 have been shown to phosphorylate PIF1 and PIF4, respectively in a light-independent manner and affect light-induced degradation of these PIFs (Xu et al., 2015). However, PIFs are still degraded in these E3 ligase and kinase mutants, suggesting additional factors are functioning in these processes.

Although single *pif* mutants didn't display light-independent phenotypes, *pif1pif3pif4pif5* (*pifq*) quadruple mutants displayed constitutively photomorphogenic phenotypes suggesting PIFs are promoting skotomorphogenesis by inhibiting photomorphogenesis (Leivar et al., 2008; Shin et al., 2009). In addition, the CONSTITUTIVELY PHOTOMORPHOGENIC/DEETIOLATED/FUSCA (COP/DET/FUS) group of negative regulators suppress photomorphogenesis by promoting the degradation of the positive regulators (HY5/LAF1/HFR1 and others) in the dark (Lau and Deng, 2012; Xu et al., 2015). One of these factors, called CONSTITUTIVELY PHOTOMORPHOGENIC1 (COP1), that can function as an E3 ligase in vitro (Saijo et al., 2003; Seo et al., 2003). COP1 associates with SUPPRESSOR OF PHYA-105 (SPA1-4) family members and promotes degradation of positive regulators (Saijo et al., 2003; Hoecker, 2005; Zhu et al., 2008). Moreover, COP1/SPA forms complexes with CULLIN4, and the $CUL4^{COP1\text{-}SPA}$ complex degrades positively-acting transcription factors to repress photomorphogenesis in the dark (Chen et al., 2010). Strikingly, PIFs and COP1/SPA complex function synergistically to degrade HY5 to partially repress photomorphogenesis in the dark (Xu et al., 2014). Overall, multiple repressors are acting independently as well as synergistically to prevent photomorphogenesis in the dark. Light signals either degrade PIFs or inhibit COP1/SPA function by light-induced nuclear exclusion of COP1 to promote photomorphogenesis (Xu et al., 2015).

HFR1 is a basic helix-loop-helix transcription factor, which acts as an important positive regulator for both phytochrome A–mediated far-red and cryptochrome 1–mediated blue light signaling pathways (Fairchild et al., 2000; Fankhauser and Chory, 2000; Duek and Fankhauser, 2003). Previous studies have shown that HFR1 is degraded through the COP1/SPA-mediated ubiquitination pathway in darkness but is stabilized in response to light, irrespective of light quality (Yang et al., 2005). HFR1 also interacts with PIF4/PIF5

and inhibits their DNA binding and transcriptional activation activity to reduce the shade avoidance response (Lorrain et al., 2008; Hornitschek et al., 2009). More recently, it was shown that HFR1 also interacts with PIF1 and sequesters PIF1 activity to regulate red light-induced seed germination (Shi et al., 2013). In this study, we show that HFR1 also promotes seed germination under FR light. We further provide the biochemical and genetic evidence to support the hypothesis that PIF1 and HFR1 are undergoing suicidal co-degradation in the dark through the ubi/26S proteasome pathway during photomorphogenesis.

RESULTS

HFR1 promotes phyA-dependent seed germination under far red light conditions

PIF1 is a pivotal suppressor of seed germination in the dark (Oh et al., 2004), and a recent study showed that HFR1 sequesters PIF1 to regulate red light-induced phyB-dependent seed germination (Shi et al., 2013). However, HFR1 is mainly functional in the phytochrome A–mediated far-red and cryptochrome 1–mediated blue light signaling pathways (Fairchild et al., 2000; Fankhauser and Chory, 2000; Duek and Fankhauser, 2003). Thus, we performed seed germination assays for *hfr1* under increasing fluence of far red light conditions. Results showed that the *hfr1* single mutant also had a lower seed germination rate compared with wild type, suggesting that HFR1 is also functional in phyA-dependent seed germination responses (Figure 3.1). To further gain insight of genetic relationship between PIF1 and HFR1 for regulating phyA-dependent seed germination, we created *hfr1 pif1* double mutant and examined far-red light initiated seed germination. Results showed that *hfr1 pif1* double mutant displayed the same phenotype as the *pif1* single mutant (Figure 3.1). These data indicate that *pif1* is epistatic to *hfr1* in phyA-dependent seed germination.

HFR1 promotes the degradation of PIF1 both in the dark and red/far red light conditions

HFR1 heterodimerizes with PIF1 and sequesters PIF1 activity to promote seed germination under red light (Shi et al., 2013) (Bu et al., 2011). To examine if HFR1 regulates PIF1 protein level in the dark and light, we performed Western blots to examined native PIF1 protein level in the *hfr1* single mutant background under dark, red and far red light conditions. Strikingly, native PIF1 is strongly stabilized in the *hfr1* single mutant background under all these conditions (Figure 3.2A-C). The PIF1 level is much higher in the *hfr1* background under dark, and the difference in PIF1 level under light might be due to the dark level difference. These results suggest that HFR1 also promotes the degradation of PIF1 under dark. The increased level of PIF1 in the *hfr1* mutant under these conditions might partly explain the lower seed germination phenotype of the *hfr1* under red/far red light conditions (Figure 3.1)(Shi et al., 2013).

Previous studies have shown that upon light exposure, the active Pfr form of phytochrome could trigger the phosphorylation, ubiquitination and 26S proteasome-mediated degradation of PIFs (Castillon et al., 2007; Leivar and Quail, 2011; Ni et al., 2014; Xu et al., 2015; Zhu et al., 2015). However, PIF1 and other PIFs are known to be stable in the dark. Because PIF1 level is much higher in the *hfr1* background in the dark compared with wild type, we examined the native PIF1 protein level from the wild type Col-0 in the dark with and without a proteasome inhibitor (MG132) treatment and/or protein synthesis inhibitor cycloheximide (CHX). Very strikingly, the data show that PIF1 is degraded in the dark (Figure 3.2D). This degradation can be blocked by the proteasome inhibitor MG132 suggesting that PIF1 is degraded through the 26S proteasome mediated pathway in the dark.

Previous studies have shown that the COP1 E3 ligase interacts with HFR1 and induces its degradation through the ubi/26S proteasome pathway in the dark (Yang et al., 2005). Because PIF1 can interact with HFR1 and COP1 directly (Yang et al., 2005; Bu et al., 2011; Shi et al., 2013; Xu et al., 2014), it is possible that COP1, PIF1 and HFR1 form a complex that promotes the degradation of PIF1. To test this hypothesis, we created the *cop1-4 hfr1* double mutant and performed native PIF1 Western blot for *cop1-4,* and *cop1-4 hfr1* under both dark and far red light conditions. PIF1 is destabilized in the *cop1-4* background as previously shown. Strikingly, in the dark condition, PIF1 is significantly stabilized in the *cop1-4 hfr1* background compared to wild type (Figure 3.3A-B). Under far red light conditions, PIF1 protein was also stable in the *cop1-4* and much higher abundant in the *cop1-4 hfr1* background compared to wild type (Figure 3.3A-B). These data suggest that HFR1 promotes PIF1 degradation in the dark.

Previous study showed that the heterodimerization between HFR1 with PIF1 is necessary for the sequestration of PIF1 activity (Shi et al., 2013). In order to test if this heterodimerization is also responsible for the HFR1-mediated degradation of PIF1, we created is a mutant version of the HFR1 protein that interferes with the dimerization properties of the HLH domain of HFR1 by substituting Val172 Leu173 to Asp172Glu173 in the HLH domain (Figure 3.3C-D, Figure 3.4). These mutations have been shown to reduce heterodimerization both *in vitro* and *vivo* (Hornitschek et al., 2009). We made transgenic plants expressing the GFP-HFR1*. We then crossed both the wild type GFP-HFR1 and the mutant GFP-HFR1* into the *cop1-4 hfr1* background to generate *cop1-4 hfr1*/GFP-HFR1 and *cop1-4 hfr1*/GFP-HFR1*. Strikingly, the GFP-HFR1 in the *cop1-4 hfr1* background reduced the PIF1 level closer to wild type (Figures 3C-D). In contrast, the GFP-HFR1* failed to reduce the PIF1 level, suggesting that HFR1 promotes PIF1 degradation in a heterodimerization-dependent manner. These data also suggest that the

lower level of native PIF1 in *cop1-4* under dark might be due to the increased abundance of HFR1 that promotes the degradation of PIF1 in the cop1-4 background. Taken together, these data demonstrate that HFR1 regulates PIF1 level in the dark in both wild type and *cop1-4* backgrounds.

HFR1 promotes PIF1 degradation via ubi/26S proteasome mediated pathway

To examine if HFR1 mediated degradation of PIF1 is proteasome-dependent, we created the TAP-PIF1 transgenic plant in *cop1-4* and *cop1-4 hfr1* mutant backgrounds and performed Western blots in the presence and absence of the proteasome inhibitor Bortezomyb. Results show that the TAP-PIF1 degradation is blocked in the presence of the proteasome inhibitor (Bortezomib) treatment both in the *cop1-4* and *cop1-4 hfr1* mutant backgrounds under dark (Figures 3.5A-B). In addition, TAP-PIF1 level is higher in *cop1-4 hfr1* background than that in the *cop1-4* background, which is consistent with what we have shown for the native PIF1 level (Figures 3.5A-B). More strikingly, the stabilization of TAP-PIF1 in *cop1-4 hfr1* mutant background is significantly higher than in the *cop1-4* background. These data suggest that HFR1 promotes the degradation of PIF1 through the ubi/26S proteasome pathway.

It has been shown that some proteins can be degraded through the ubi/26S proteasome pathway independent of polyubiquitination due to the presence of unstructured regions or through interaction with another protein containing the unstructured region (van der Lee et al., 2014; Fishbain et al., 2015). To distinguish if the HFR1-mediated degradation of PIF1 is polyubiquitin dependent or independent, we immunopreciated the TAP-PIF1 from both the *cop1-4* and *cop1-4 hfr1* mutant backgrounds and then detected with anti-Myc and anti-Ub antibody. Results show that the immunopreciated TAP-PIF1 level detected by anti-Myc antibody is significantly higher in the *cop1-4 hfr1* background

than that in the *cop1-4* background as observed (Figure 3.5C, left panel; Figures 3.5A-B). But the ubiquitination level of the immunopreciated TAP-PIF1 detected by anti-Ub antibody is significantly reduced in the *cop1-4 hfr1* background than that in the *cop1-4* background (Figure 3.5C, right panel). The immunoprecipitated TAP-PIF1 is higher abundant but contains less polyubiquitination in the *cop1-4 hfr1* background, which support the hypothesis that HFR1 promotes the degradation of PIF1 in the dark via the 26S proteasome pathway by increasing the amount of polyubiquitination of PIF1.

hfr1 partially suppresses the photomorphogenic phenotypes in the *cop1-6 pif1* and *pifq* background

Previously, we have shown that *cop1-6 pif1* seedlings display synergistic effect in promoting the de-etiolation phenotypes in the dark due to the increased accumulation of HY5 in the *cop1-6 pif1* compared to the parental genotypes (Xu et al., 2014). However, *hy5* single mutant could only partially rescue the synergistic phenotype of the *cop1-6 pif1*. Since HFR1 is an important positive regulator of plant photomorphogensis (Jang et al., 2005; Yang et al., 2005), we hypothesize that HFR1 might be playing similar role as HY5. To test this hypothesis, we generated a *cop1-6 pif1 hfr1* triple mutant. Phenotypic analyses showed that all three de-etiolation phenotypes (shorter hypocotyl and expanded cotyledon angle and area) are partially suppressed in the *cop1-6 pif1 hfr1* triple mutant compared with those in the *cop1-6 pif1* double mutant both in the dark and different far red light conditions (Figures 3.6-3.7). Since the partial suppression of the *cop1-6 pif1* phenotype by *hfr1* might be due to the *hfr1*'s suppression for *cop1-6* only as shown previously (Yang et al., 2005), we further created *hfr1 pifq* quintuple mutant. The constitutive photomorphogenic phenotypes of the *pifq* are also partially suppressed by *hfr1* both under dark and far red light conditions (Figures 3.8A-D). These genetic data suggest that *hfr1* acts downstream of *cop1* and *pifq* in regulating photomorphogenesis.

PIFs promote the degradation of HFR1 posttranslationally in the dark and far-red light

Previous studies have shown that COP1-SPA complexes interact with HFR1 and induce its degradation through the ubi/26S proteasome pathway in the dark (Yang et al., 2005). To determine if the synergistic promotion of photomorphogenesis observed in the *cop1-6 pif1* mutant is also partially due to an increased abundance of HFR1 in the dark and far-red light, we generated the GFP-HFR1 transgenic plants in the Col, *pif1*, *cop1-6* and *cop1-6 pif1* backgrounds. Western blots showed that in both darkness and far red light conditions, the GFP-HFR1 protein is synergistically stabilized in the *cop1-6 pif1* background compared with that of the GFP-HFR1 in *pif1*, *cop1-6* single mutant backgrounds, respectively. This regulation is at the posttranslational level as the amount of the GFP-HFR1 mRNA is similar in these backgrounds (Figures 3.9A-B, Figure 3.10A). In addition, since *pifq* displays constitutive photomorphogenic phenotypes as *cop1*, we further created GFP-HFR1 transgenic plants in the *pifq* background. Strikingly, the GFP-HFR1 protein level, but not the *GFP* mRNA level, is significantly increased in the *pifq* compared to the wild type background (Figures 3.9C-D, Figure 3.10A). A recent study also showed that the native *HFR1* mRNA level is significantly reduced in the *pifq* background compared with the wild type (Figure 3.10B) (Zhang et al., 2013), suggesting that PIFs also transcriptionally activate the expression of *HFR1*. Taken together, these data suggest that, similar to HY5, HFR1 abundance is also regulated by PIFs and COP1 in a posttranslational manner.

PIF1 promotes HFR1 degradation in a polyubiquitination-dependent manner *in vivo*

Since HFR1 promotes PIF1 degradation in the dark by polyubiquitination through the 26S proteasome mediated pathway (Figure. 3.5), we examined whether PIF1 promotes HFR1 degradation in a similar manner. To answer this question, we immunoprecipitated

the GFP-HFR1 fusion protein from GFP-HFR1 and *pifq*/GFP-HFR1 and then detected with the anti-Ub and anti-GFP antibodies. Results show that the immunoprecipitated GFP-HFR1 level detected by anti-GFP antibody is significantly higher in the *pifq*/GFP-HFR1 than that in the GFP-HFR1 as observed (Figure 3.11, left panel; Figures 3.9C-D). However, the polyubiquitination level of the immunoprecipitated GFP-HFR1 detected by anti-Ub antibody is significantly reduced in the *pifq* background than that in the GFP-HFR1 background (Figure 3.11, right panel). These data suggest that the immunoprecipitated GFP-HFR1 has higher abundance but less polyubiquitination in the *pifq* background, which supports the hypothesis that PIF1 promotes the degradation of HFR1 in the dark via polyubiquitination followed by 26S proteasome mediated degradation pathway *in vivo*.

PIF1 enhances the COP1-mediated ubiquitination of HFR1

Previously, COP1 has been shown to directly ubiquitinate HFR1 *in vitro* (Jang et al., 2005; Yang et al., 2005). The polyubiquitination level is also reduced in the *pifq* background *in vivo* as shown above (Figure 3.11), suggesting that PIFs might enhance the ubiquitination activity of COP1 toward HFR1 as previously observed for HY5. To test this hypothesis, we performed an *in vitro* transubiquitination assay as described previously (Yang et al., 2005; Jang et al., 2005; Xu et al., 2014) using MBP-COP1, GST-HFR1 and different amount of MBP-PIF1. Immunoblotting with anti-Flag and anti-GST antibodies showed that COP1 functions as an E3 ligase to polyubiquitnate HFR1 as previously reported (Figure 3.12, lane 3) (Jang et al., 2005). In addition, PIF1 promotes the transubiquitination of COP1 to HFR1 in a concentration-dependent manner (Figure 3.12, lane 4 and 5). Taken together, these results demonstrate that PIF1 promotes the COP1-mediated degradation of HFR1.

DISCUSSION

Phytochrome-mediated light signaling pathways involve both bHLH factors (e.g., PIFs) acting as negative regulators and HLH factor (e.g., HFR1) acting as positive regulator (Duek and Fankhauser, 2005). The relationship between the bHLH and HLH has been documented in many eukaryotic system including plants (Littlewood, 1998; Toledo-Ortiz et al., 2003). In fact, HFR1 has been shown to sequester PIF1/PIF4/PIF5 to regulate red light-induced seed germination and shade avoidance responses (Hornitschek et al., 2009; Shi et al., 2013). Here we show that HFR1 also promotes seed germination under FR light conditions (Figure 3.1), consistent with its role under FR light in seedling de-etiolation. HFR1 promotes seed germination not only by sequestering PIF1, but also by negatively regulating PIF1 posttranslationally. HFR1 heterodimerizes with PIF1 and induces polyubiquitination and subsequent degradation of PIF1 in the dark through the ubi/26S proteasome pathway (Figures 3.2-3.5). This degradation requires direct heterodimerization as HFR1* mutants deficient in interaction with PIF1 failed to induce degradation of PIF1 (Figure 3.3C-D; Figure 3.4). Thus, bHLH-HLH interaction not only results in sequestration, but also posttranslational regulation of protein levels.

PIFs are known to be stable in the dark in general, and have been shown to undergo rapid degradation in response to red/far-red and blue light conditions (Leivar and Quail, 2011; Xu et al., 2015). In this process, phytochrome interaction is necessary for the light-induced phosphorylation, polyubiquitination and subsequent degradation (Al-Sady et al., 2006; Shen et al., 2008). In addition, both CUL3-LRB and CUL4-COP1-SPA complexes have been shown to function as E3 Ubiquitin ligases for the light-induced degradation of PIF3 and PIF1, respectively (Ni et al., 2014; Zhu and Huq, 2014; Zhu et al., 2015). However, the degradation of PIFs in the dark has not been shown yet. Our data showing that PIF1 is degraded in the dark when translation is blocked suggest that PIFs might also

be regulated in the dark. The PIF1 degradation in the dark is also ubi/26S proteasome-mediated, as it can be blocked by the proteasome inhibitor. In addition, HFR1 promotes the degradation of PIF1 in the dark by direct heterodimerization. Thus PIFs are posttranslationally regulated both in the dark and light conditions.

PIFs have been shown to display nontranscriptional roles in regulating HY5 posttranslationally (Xu et al., 2014). In this process, PIF1 increased the substrate availability of COP1, and enhanced the auto- and trans-ubiquitination activity of COP1 toward HY5. Another negative regulator named SHW1 also promotes COP1-mediated ubiquitination and degradation of HY5 (Srivastava et al., 2015). Because HFR1 is another COP1 substrate, and HFR1 interacts with PIFs and COP1 (Jang et al., 2005; Yang et al., 2005; Hornitschek et al., 2009; Bu et al., 2011; Shi et al., 2013), HFR1 might be subjected to similar regulation. We provide convincing biochemical and genetic evidence that PIF1 and COP1 synergistically regulate HFR1 posttranslationally. *In vitro*, PIF1 enhanced the COP1-mediated polyubiquitination of HFR1 (Figure 3.12). Consistently, HFR1 level is synergistically higher in the *cop1-6 pif1* double mutant compared to the *cop1-6* and *pif1* single mutants (Figure 3.9). In addition, genetic data show that *hfr1* partially suppresses the synergistic photomorphogenic phenotypes of the *cop1-6 pif1* double mutant (Figures 3.6-3.7). Moreover, *hfr1* also suppresses the constitutive photomorphogenic phenotypes of *pifq* in the dark and FR light (Figure 3.8). Thus, PIF1 is acting as a cofactor for COP1 to regulate multiple COP1 substrates *in vivo* as predicted (Xu et al., 2015). Overall, these data suggest that PIFs suppress photomorphogenesis not only by regulating the large-scale gene expression directly and indirectly in the dark (Leivar and Monte, 2014), but also work together with COP1-SPA complex to synergistically promote the degradation of the positive regulators of photomorphogeneis (Xu et al., 2014; Xu et al., 2015).

In summary, HFR1 promotes the degradation of PIF1 in the dark by direct heterodimerization. Conversely, PIF1 promotes the degradation of HFR1 in the dark by enhancing the COP1 activity toward HFR1. Thus, these two proteins are undergoing suicidal co-degradation in the dark (Figure 3.13). Recently, PIF3 and PhyB have been shown to undergo suicidal co-degradation in response to light via the $CUL3^{LRB}$ complex (Ni et al., 2014; Zhu and Huq, 2014). The co-degradation of PIF3 and PhyB appears to attenuate the incoming signals to protect plants by degrading the signal receptor as well as the primary signal acceptor in a mutually destructive manner (Ni et al., 2014; Zhu and Huq, 2014). The suicidal co-degradation of PIF1 and HFR1 found in our study also demonstrates a similar mechanism in the dark, where photomorphogenesis would not be over repressed by an excessively high abundance of the PIF repressors. This will allow the photomorphogenesis to proceed quickly upon incoming light signals.

MATERIALS AND METHODS

Plant materials, growth conditions and measurements.

Seeds of Colombia-0 (Col-0) ecotype of *Arabidopsis thaliana* was used for all experiments. The *pif1*, *pifq*, *cop1-6*, *cop1-6 pif1*, *hfr1*, *hfr1 pif1*, *cop1-4*, *cop1-4pif1*, GFP-HFR1, TAP-PIF1, *cop1-4*/TAP-PIF1 were used as described (Castillon et al., 2009; Xu et al., 2014; Zhu et al., 2015). For generation of *cop1-6 pif1 hfr1*, *cop1-6 hfr1*, *cop1-4 hfr1* and *hfr1 pifq*, *hfr1* was crossed with *cop1-6 pif1*, *cop1-6*, *cop1-4* and *pifq* to obtain F1 generation. Through genotyping, phenotypic characterization, and antibiotics selection of the large F2 and F3 population, we identified those mutant combinations. For generation of *pif1* GFP-HFR1, *pifq* GFP-HFR1, *cop1-6* GFP-HFR1, and *cop1-6 pif1* GFP-HFR1, GFP-HFR1 was crossed into those mutant backgrounds to obtain F1 generation. By genotyping, phenotypic characterization and antibiotic (Gentamycin for GFP-HFR1)

selection of large F2 and F3 population, we obtained these genetic materials. For generation of *cop1-4 hfr1*/GFP-HFR1 and *cop1-4 hfr1*/TAP-PIF1, *cop-4 hfr1* was crossed into GFP-HFR1 and TAP-PIF1, respectively to obtain F1 generation. Through genotyping and antibiotics selection (all of them are Gentamycin) of F2 and F3 generation, we obtained those genetic materials. The primers for genotyping were used as previously described (Castillon et al., 2009; Xu et al., 2014). To generate HFR1*GFP, HFR1* was first generated by site-directed mutagenesis with the primers listed in the table 3.1. HFR1 open reading frame was closed into pENTRY vector as previously described (Hornitschek et al., 2009). Then it was cloned into the GFP destination vector for transformation into *hfr1* single mutant background as described (Bu et al., 2011). To generate *cop1-4 hfr1* HFR1*GFP, *cop1-4 hfr1* was crossed to the *hfr1/* HFR1*GFP to obtain F1. By genotyping, antibiotic (Basta for HFR1*GFP) selection and phenotypic assay, *cop1-4 hfr1* HFR1*GFP was obtained.

Plants were grown in Metro-Mix 200 soil (Sun Gro Horticulture, Bellevue, WA) under 24-h light at 22 ± 0.5°C. Seeds were sterilized with ethanol and bleach and then plated on the Murashige and Skoog medium supplemented 0.9% agar without sucrose as described (Shen et al., 2005). After 3-4 days of cold treatment in the dark, seeds were exposed to white light for 3 hours at room temperature to trigger seed germination. For GFP-HFR1 Western blot, seeds were either placed back to the dark for 4 days or grown in the dark for 21 hours then transferred to continuous FRc (0.45 μmol/m^2/s) for 3 days. For PIF1 Western blot, seeds were placed back to the dark for 4 days to either directly harvest for protein extraction or exposed to a pulse of Rc (2 μmol m^{-2}) or FRc (30 μmol m^{-2}) and then incubated in the dark for 3/5 mins (Rc) or 10/20 mins (FRc). For gene expression and *in vivo* co-immunoprecipitation assays, seeds were placed back to the dark for 4 days to purify the protein. For de-etiolation phenotypic assays, seedlings are grown either in the

dark for 5 days or grown in the dark for 21 hours then transferred to continuous FRc (0.03 μmol/m^2/s, 0.06 μmol/m^2/s or 0.45 μmol/m^2/s) for 4 days before taking the pictures and measurement. For measurement of hypocotyl lengths, cotyledon areas, and cotyledon angles, digital pictures of dark or FRc grown seedlings as mentioned above were taken and at least 30 seedlings were measured using the public available software ImageJ (http://rsb.info.nih.gov/ij/). The phenotypic assays were replicated as least three times. The phyB (red light) and phyA (far red light)-dependent seed germination assays were performed as previously described (Zhu et al., 2015).

RNA isolation and quantitative RT-PCR

The quantitative RT-PCR (qRT-PCR) for seedlings was performed as previously described (Xu et al., 2014). Briefly, total RNA of 4-day-old dark grown seedlings were extracted with Spectrum plant total RNA kit (Sigma-Aldrich Co., St. Louis, MO). One μg of total RNA was used to reverse transcribe into cDNA using SuperScript III **(Life Technologies Co.,** Carlsbad, CA) after DNase I treatment to eliminate the genomic DNA. qRT-PCR was performed using the Power SYBR Green Kit (Applied Biosystems Inc., Foster City, CA) in a 7900HT Fast Real-Time PCR machine (Applied Biosystems Inc., Foster City, CA). *PP2A* (At1g13320) was used as a control. The resulting cycle threshold (Ct) values were used for calculation of the relative expression level for *GFP* genes relative to *PP2A*. The value of GFP-HFR1 was set as 1 to calculate the relative values of other genotypes. Primers of qRT-PCR are listed in the table 3.1.

Protein extraction and immunoblot analyses

For GFP-HFR1 and native PIF1 Western blots, seedling materials were grown as described above. For TAP-PIF1 Western blot, after seed germination induction, seeds were kept in darkness for 4 days, one batch of seedlings for each genotype was treated with

proteasome inhibitor (40 mM Bortezomib) for 3 hours before protein extraction. For all the different Western blots, after harvesting their samples, proteins were purified in extraction buffer (1 M MOPS PH 7.6, 10% SDS, 50% glycerol, 0.5 M EDTA pH 8, 1×protease inhibitor cocktail (Sigma-Aldrich Co., St. Louis, MO), 40 mM β-mercaptoethanol, 2 mM PMSF, 25 mM β-GP, 10 mM NaF and 2 mM Na-orthovanadate), followed by boiling in water for 3 mins. Then the samples were centrifuged at maximum speed for 10 mins and then loaded the supernatant on either 8% (for GFP-HFR1 and native PIF1) or 6.5% (for TAP-PIF1) SDS-PAGE gel. After blotting the protein onto polyvinylidene difluoride (PVDF) membranes, the same membrane was first blotted with anti-GFP (Santa Cruz Biotech, Dallas, TX), anti-PIF1 (Shen et al., 2008) or anti-Myc (EMD Millipore, Billerica, MA) antibodies followed by anti-RPT5 antibody (Enzo Life Sciences, Farmingdale, NY) after stripping. For the quantification of the GFP-HFR1 protein level, native PIF1 degradation kinetics and TAP-PIF1 protein with/without Bortezomib treatment, we used publicly available ImageJ software to measure band intensities of RPT5 and GFP-HFR1, native PIF1, or TAP-PIF1 based on at least three independent biological repeats data.

***In vivo* immunoprecipitation assays**

To detect the ubiquitination of TAP-PIF1 and GFP-HFR1 in *pifq* background *in vivo*, immunoprecipitation from 4-d-old dark-grown seedlings of each genotype were performed as previously described with minor modification (Shen et al., 2008). Briefly, total protein was extracted from 4 day-old dark grown seedlings pretreated with the proteasome inhibitor (40 mM Bortezomib) for 3 hours before protein extraction. Total proteins were extracted from the same amount of seedling tissues (~0.4 g) with 1 mL urea extraction buffer (8M urea, 10mM Tris, pH 8.0, 100 mM NaH_2PO_4, 100mM NaCl, 0.05% Tween 20, 1×protease inhibitor cocktail [Sigma-Aldrich Co., St. Louis, MO], 2 mM PMSF,

10 mM MG132, 25 mM β-glycerophosphate, 10 mM NaF, 2 mM Na-orthovanadate, and 100 nM calyculin A) and centrifuged in the dark at maximum speed for 15 mins at 4°C. TAP-PIF1 or GFP-HFR1 was immunoprecipitated from the supernatants with Dynabeads Protein A (Life Technologies Co., Carlsbad, CA) bound with either anti-Myc (Rabbit, Sigma-Aldrich Co., St Louis, MO) or anti-GFP (Rabbit, Invitrogen, Carlsbad, CA) antibodies, respectively. Then the pellets were washed and heated with SDS-Laemmli buffer for 5 min at 65°C before loading to either 6.5% (for TAP-PIF1) or 8% (for GFP-HFR1) SDS-PAGE gels. Same blot was first probed with anti-Ub (Santa Cruz Biotech, Dallas, TX) antibody followed by either anti-Myc (Mouse, EMD Millipore, Billerica, MA) or anti-GFP (Mouse, Santa Cruz Biotech, Dallas, TX) antibody after stripping for TAP-PIF1 or GFP-HFR1 blot, respectively.

***In vitro* ubiquitination assays**

The *in vitro* ubiquitination assay was performed as previously described with minor modification (Jang et al., 2005; Yang et al., 2005; Xu et al., 2014). For preparations of the proteins, MBP-PIF1 was purified from *E.coli* as previously described (Xu et al., 2014). HFR1 was digested from the HFR1-GAD (Castillon et al., 2009), and then cloned into pGEX4T-1 vector to obtain GST-HFR1. Both MBP-COP1 and GST-HFR1 proteins were purified freshly from *E.coli* as previously described but in lower induction temperature (~15°C) for increasing protein solubility (Hardtke et al., 2000; Xu et al., 2014). Flag-tagged ubiquitin (Flag-Ub), UBE1 (E1) and UbcH5b (E2) were used as previously described (Jang et al., 2005) (Boston Biochem, Cambridge, MA). For the *in vitro* ubiquitination reaction, 5μg of Flag-Ubiquitin, ~25ng of E1, ~25ng of E2, ~500ng of MBP-COP1, ~200ng of GST-HFR1, and 50 or 100ng MBP-PIF1 were added in the reaction buffer containing 50 mM Tris, pH7.5, 2 mM ATP, 5 mM $MgCl_2$, and 2 mM DTT. MBP-COP1 was pretreated with

20 μM $ZnCl_2$ for 45min at 22°C before adding into the reaction system. Reactions were carried out at 30°C for 2 hr, and then the samples were heated at 95°C with SDS loading buffer. Reaction mixtures were then loaded onto a 8% polyacrylamide SDS gel and blotted onto PVDF membranes. Ubiquitinated GST-HFR1 was first detected with α-Flag antibody (F1804; Sigma-Aldrich Co., St. Louis, MO) and same blot was then probed with anti-GST-HRP conjugate (GE Healthcare Bio-Sciences, Pittsburgh, PA).

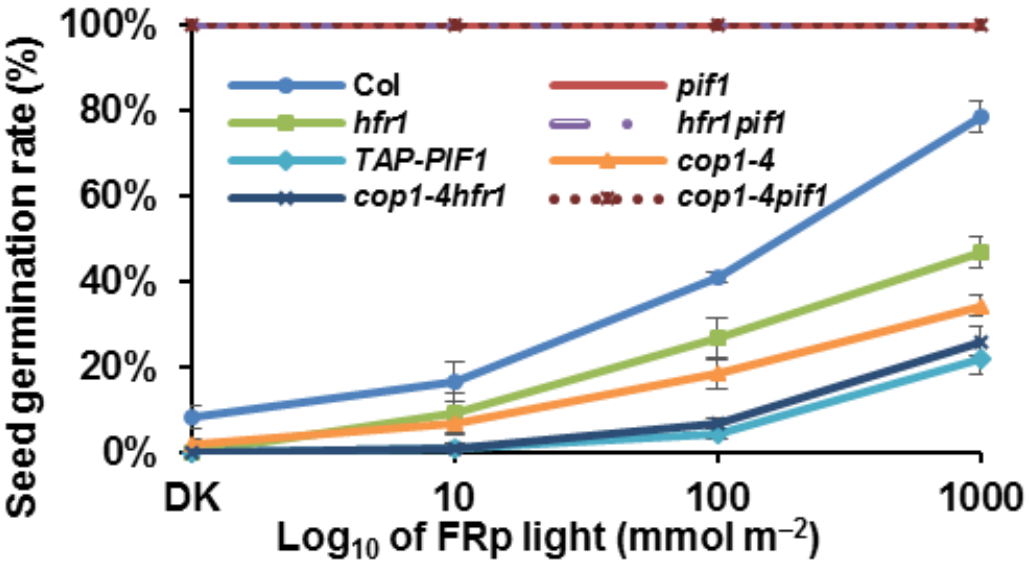

Figure 3.1: HFR1 promotes seed germination under far-red light.

Line graph shows the percent of seeds germinated for various genotypes as indicated in the dark and an increasing amount of far red light intensities. Same stage seeds of Col, *pif1*, *hfr1*, *hfr1pif1*, *TAP-PIF1OX*, *cop1-4*, *cop1-4hfr1* and *cop1-4pif1* were surface sterilized within 1 hour of imbibition and plated on MS plates. They were exposed to far red light (34 μmol/m^2/s) for 5 mins before being kept in the dark for 48 hours. The seeds were then either kept in the dark continuously or treated with increasing amount of far-red light as indicated and then wrapped again to keep in the dark for 6 additional days before being quantified. The error bars indicate STDEV (n=50, three biological replicates).

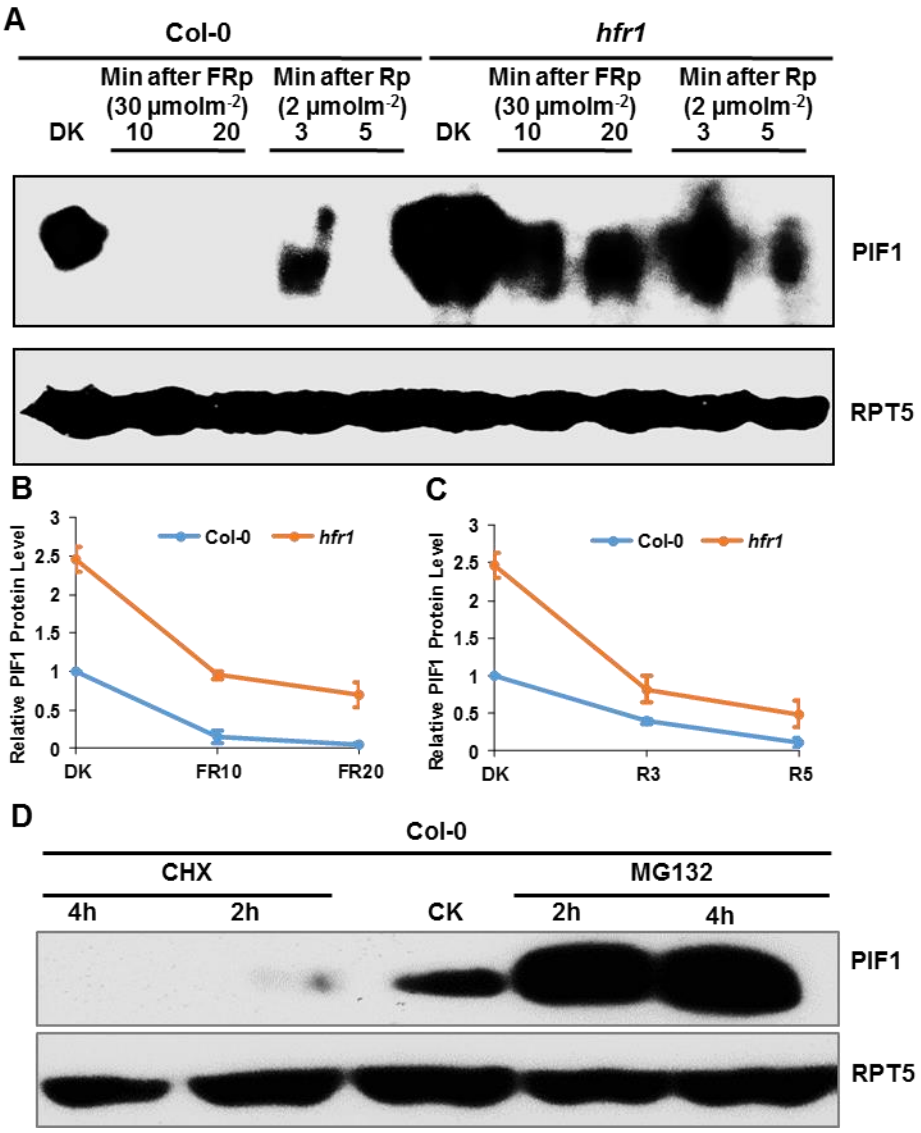

Figure 3.2: PIF1 is more abundant in the *hfr1* single mutant under dark, Rc and FRc light conditions compared to wild type.

(A) Western blot shows reduced degradation of native PIF1 in the *hfr1* background both in the dark, Rc and FRc light compared with wild-type seedlings. Four-day-old dark-grown seedlings were either kept in darkness or exposed to a pulse of Rc (2 µmol m^{-2}) or FRc (30

μmol m^{-2}) light and then incubated in the dark for the duration indicated. The seedlings were harvested for protein extraction. Total protein was separated on an 8% SDS–PAGE gel, transferred to PVDF membrane and probed with anti-PIF1 and anti-RPT5 antibodies. (B) Quantification of PIF1 levels in response to FR light condition is shown. RPT5 was used as a control. The PIF1 protein level of Col-0 in the dark was set as 1 for normalization. The error bars indicate standard deviation (n=3). (C) Quantification of PIF1 degradation kinetics in response to R light is shown. RPT5 was used as a control. The PIF1 protein level of Col-0 in the dark was set as 1 for normalization. The error bars indicate standard deviation (n=3). (D) Western blot shows the PIF1 level in 5 day-old wild type Col-0 dark grown seedlings treated with cycloheximide (CHX) or a proteasome inhibitor (MG132) for the indicated hours before protein extraction in the dark. CK is a control without any treatment in the dark. Total protein was separated on an 8% SDS-PAGE gel, blotted onto PVDF membrane and probed with anti-PIF1 or anti-RPT5 antibodies.

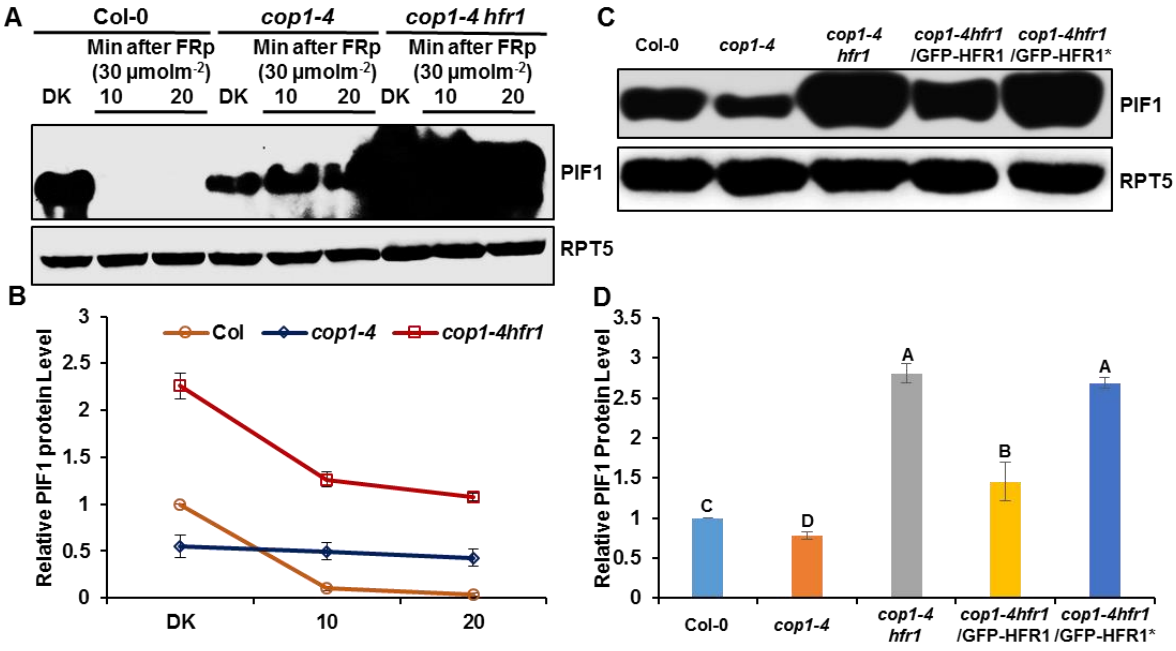

Figure 3.3: HFR1 promotes PIF1 degradation both in the dark and FR light in the *cop1-4* background.

(A) Western blot shows reduced degradation of native PIF1 in the *cop1-4 hfr1* background both in the dark and in response to FR light compared with wild-type and *cop1-4* seedlings. Four-day-old dark-grown seedlings were either kept in darkness or exposed to a pulse of FR light and then incubated in the dark for the duration indicated before protein extraction. Total protein was separated on an 8% SDS–PAGE gel, transferred to PVDF membrane and probed with anti-PIF1 and anti-RPT5 antibodies. * indicates a non-specific band. (B) Quantification of PIF1 levels in response to FR light is shown. RPT5 was used for normalization. The error bars indicate standard deviation (n=3). (C) Western blot shows the PIF1 level in wild type Col-0, *cop1-4*, *cop1-4hfr1* and *cop1-4hfr1*/GFP-HFR1. Total protein was extracted from 4 day-old dark-grown seedlings grown on MS media. Total protein was separated on an 8% SDS-PAGE gel, blotted onto PVDF membrane and probed

with anti-PIF1 or anti-RPT5 antibodies. (D) Quantification of PIF1 protein level using RPT5 as a control. The letters "A" to "D" indicate statistically significant differences between means of protein levels. ($p<0.05$). The error bars indicate standard deviation (n=3).

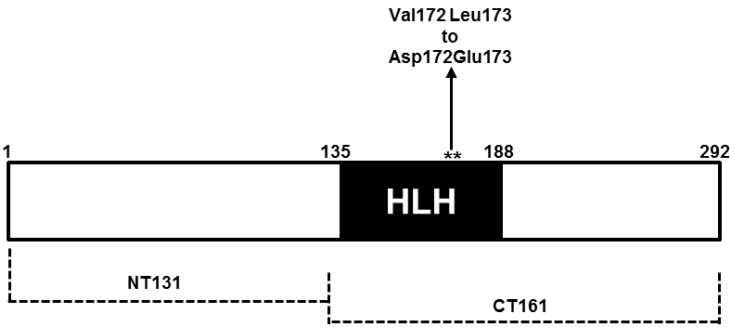

Figure 3.4: The functional structure of HFR1

Revised from Yang et al., 2005 and Shi et al., 2015. N-terminal 131 domain of HFR1 is responsible for interaction with COP1 and triggered the 26 proteasome mediated degradation, the C-terminal 161 domain (CT161) is involved in forming heterodimer with PIF1 to block PIF1's transcriptional activity for binding to DNA. The ** indicate mutation version of the HFR1 protein (HFR1*) that substitutes two conserved residuesVal172 Leu173 to Asp172Glu173 in the HLH domain, which can interfere the dimerization.

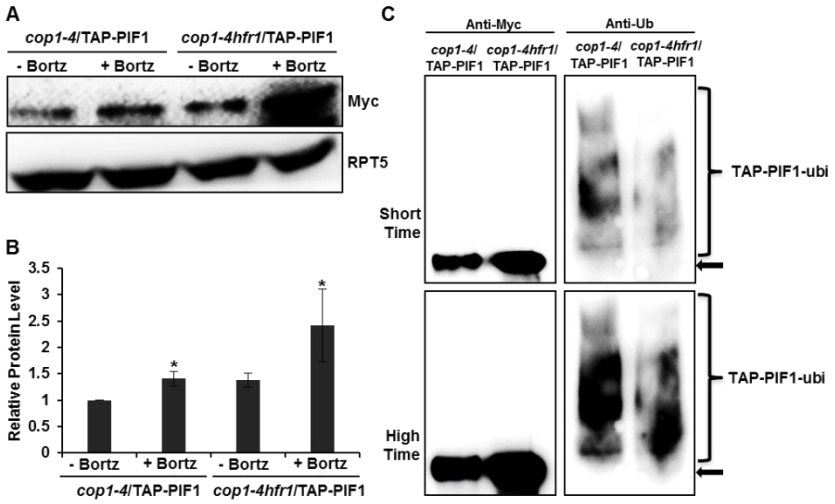

Figure 3.5: HFR1-mediated PIF1 degradation is ubi/26S proteasome dependent.

(A) Western blot shows the TAP-PIF1 level in *cop1-4* and *cop1-4hfr1* background. Total protein was extracted from 4 day-old seedlings grown on MS media in darkness. One batch of seedlings was pretreated with the proteasome inhibitor (40 mM Bortezomib) for 3 hours before protein extraction. Total protein was separated on an 6.5% SDS-PAGE gel, blotted onto PVDF membrane and probed with anti-Myc or anti-RPT5 antibodies. (B) Quantification of TAP-PIF1 protein level using RPT5 as a control. The * indicate statistically significant differences compared with non-Bortezombib treatment ($p<0.05$). The error bars indicate standard deviation (n=3). (C) TAP-PIF1 level is higher but the ubiquitination level is lower in the *cop1-4hfr1* compared with *cop1-4* background in darkness. Total protein was extracted from 4 day-old dark grown seedlings with the proteasome inhibitor (40 mM Bortezomib) pretreatment for 3 hours before protein extraction. TAP-PIF1 was immunoprecipitated using anti-Myc antibody (rabbit) from protein extracts. The immunoprecipitated samples were then separated on 6.5% SDS-PAGE gels and probed with anti-Myc (left, Mouse) or anti-Ub (right) antibodies. Top panel is shorter time exposure, bottom panel is longer time exposure. Arrow indicates the TAP-PIF1.

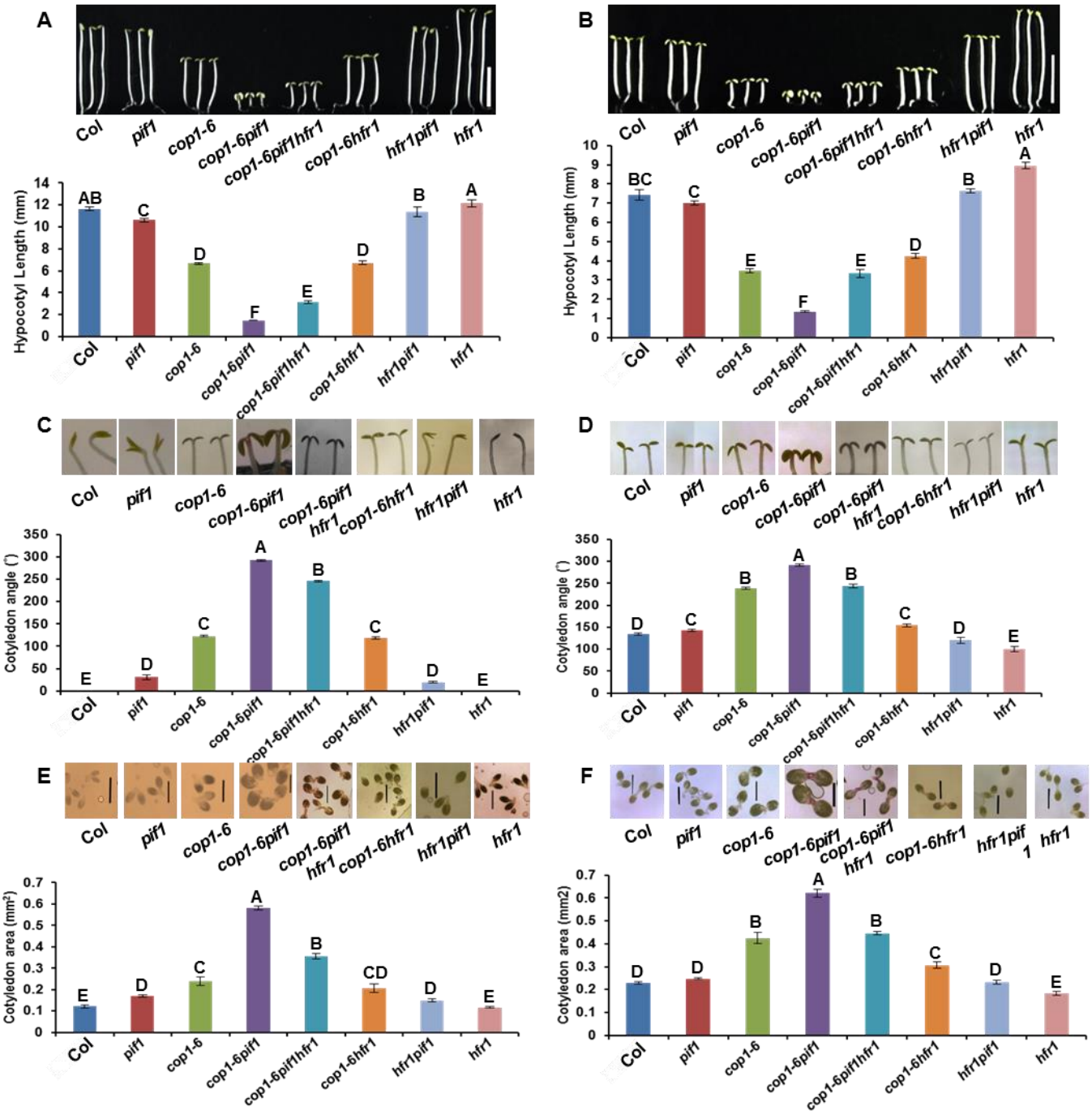

Figure 3.6: *hfr1* partially suppresses the synergistic promotion of photomorphogenesis in the *cop1-6pif1* background in the dark and FRc.

(A-B) (Top) Photographs of seedlings of wild type, *pif1, cop1-6, cop1-6pif1, cop1-6pif1hfr1, cop1-6hfr1, hfr1pif1* and *hfr1*. Seedlings were grown either in the dark for 5 days or grown in the dark for 21 hours then transferred to continuous FRc (0.06 μmol/m^2/s) for 4 days. (Bottom) Bar graph showing hypocotyl lengths of various genotypes as indicated. (C-D) (Top) Photographs of cotyledon angles of dark and FRc light grown seedlings. (Bottom) Bar graph showing cotyledon angles of various genotypes as indicated. (E-F) (Top) Photographs of cotyledon areas of dark and FRc light grown seedlings. (Bottom) Bar graph showing cotyledon areas of various genotypes as indicated above. Error bars indicate standard deviation. The letters "A" to "F" indicate statistically significant differences between means for hypocotyl lengths, cotyledon angle and cotyledon area of the indicated genotypes, ($p<0.05$), ($n>30$, three biological replicates).

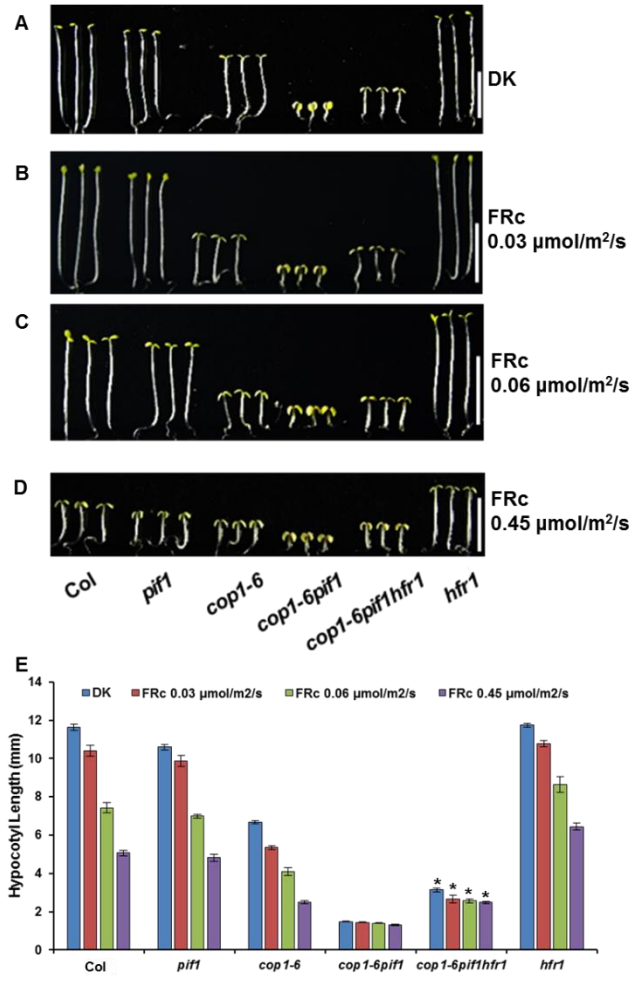

Figure 3.7: *hfr1* partially suppresses the synergistic promotion of photomorphogenesis in the *cop1-6pif1* background in the dark and different amounts of FRc conditions.

(A-D) Photographs of seedlings of wild type, *pif1, cop1-6, cop1-6 pif1, cop1-6 pif1 hfr1,* and *hfr1*. Seedlings are grown either in the dark for 5 days (A) or grown in the dark for 21 hours and then transferred to continuous FRc (0.03 µmol/m^2/s) (B), (0.06 µmol/m^2/s) (C) or (0.45 µmol/m^2/s) (D) for 4 days. (D) Bar graph showing hypocotyl lengths of various genotypes in different conditions as indicated. Error bars indicate standard deviation. *,

indicates significant difference ($p<0.05$) compared with *cop1-6pif1*. (n>30, three biological replicates).

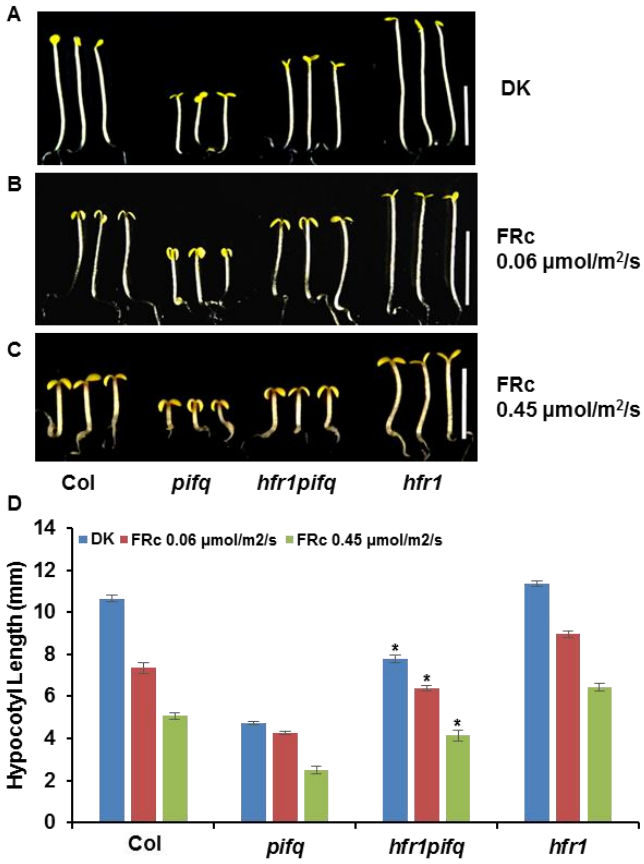

Figure 3.8: *hfr1* partially suppresses the constitutive photomorphogenic phenotypes of *pifq* in the dark and different FRc light conditions.

(A-C) Photographs of seedlings of wild type, *pifq, hfr1pifq,* and *hfr1*. Seedlings were grown either in the dark for 5 days (A) or grown in the dark for 21 hrs then transferred to continuous FRc (0.06 µmol/m^2/s) (B) or FRc (0.45 µmol/m^2/s) (C) for 4 additional days. (D) Bar graph showing hypocotyl lengths of various genotypes as indicated above. Error bars indicate standard deviation. *, indicates significant difference ($p<0.05$) compared with *pifq*. (n>30, three biological replicates).

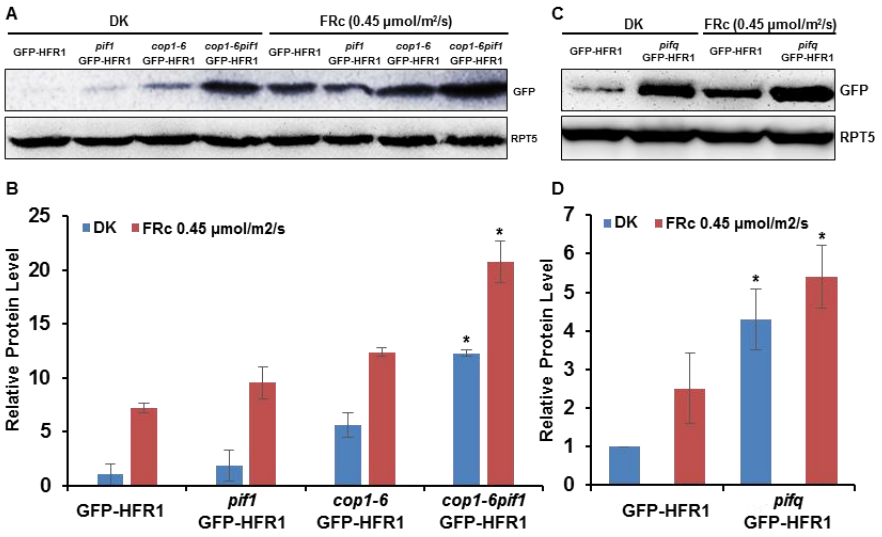

Figure 3.9: PIFs promote the degradation of HFR1 posttranslationally in the dark and far-red light.

(A) Western blot shows the HFR1 protein level in the *GFP-HFR1* transgene in the *hfr1* mutant and *pif1*, *cop1-6* and *cop1-6pif1,* respectively, harboring the *GFP-HFR1* transgene. Seedlings are grown either in the dark for 4 days or grown in the dark for 21hrs and then transferred to continuous FRc (0.45 µmol/m^2/s) for 3 days. Total protein was separated on an 8% SDS-PAGE gel, blotted onto PVDF membrane and probed with anti-GFP or anti-RPT5 antibodies. (B) Bar graph shows the GFP-HFR1 protein levels in the mutants indicated. For protein quantitation, GFP-HFR1 band intensities were quantified from three independent blots using ImageJ, and then normalized against RPT5 levels. Wild type was set as 1 and the relative proteins levels were calculated. Error bars indicate standard deviation. *, indicates significant difference ($p<0.05$) between double and single mutants background. (C) Western blot shows the HFR1 protein level in the GFP-HFR1 and *pifq*/GFP-HFR1. An RPT5 blot shows a loading control. Seedlings were grown in the dark or FRc light as described above. (D) Bar graph shows the quantified GFP-HFR1 protein

levels in the GFP-HFR1 and *pifq*/GFP-HFR1. Error bars indicate standard deviation. *, indicates significant difference ($p<0.05$).

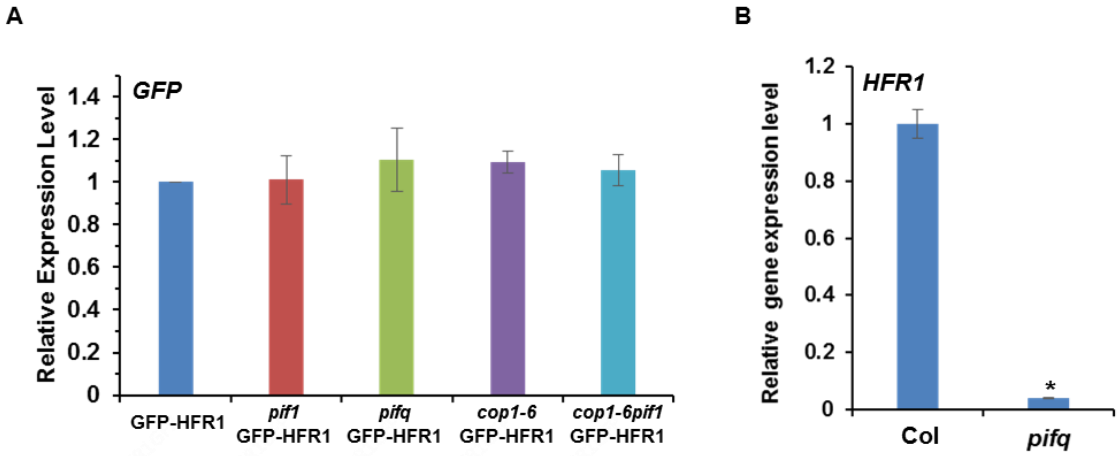

Figure 3.10: *GFP* mRNA and native *HFR1* mRNA level in various backgrounds.

(A) Bar graph showing the *GFP* mRNA levels in the different genotypes as indicated. *GFP* mRNA level was determined using qRT-PCR assays with primers designed from the *GFP* region. Total RNA was isolated from 4 day-old dark-grown seedlings for qRT-PCR assays (n= 3 independent biological repeats). *PP2A* was used as an internal control. GFP-HFR1 was set as 1 and the relative gene expression levels were calculated. Error bars indicate standard deviation. (B) Bar graph shows the native *HFR1* mRNA level in the wild type (Col-0) and *pifq* based on RNAseq data as described (Zhang et al., 2013). Error bars indicate standard deviation. *, indicates significant difference ($p<0.05$).

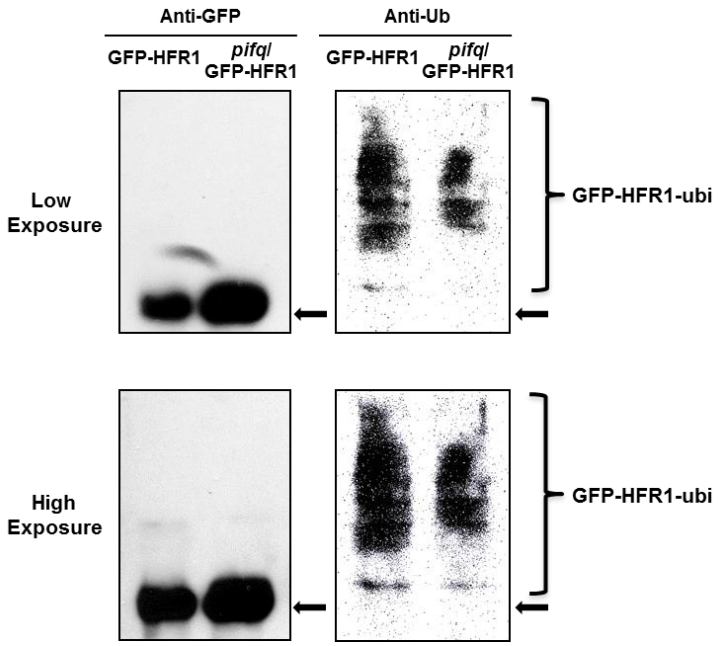

Figure 3.11: PIF1 promotes HFR1 degradation in a polyubiquitination-dependent manner *in vivo*.

The protein level of GFP-HFR1 is higher but the ubiquitination level of GFP-HFR1 is lower in the *pifq* compared with GFP-HFR1 background in darkness. Total protein was extracted from 4 day-old dark grown seedlings pretreated with the proteasome inhibitor (40 mM Bortezomib) for 3 hours before protein extraction. GFP-HFR1 was immunoprecipitated using anti-GFP antibody (rabbit) from protein extracts prepared using 4-d-old dark-grown seedlings. The immunoprecipitated samples were then separated on 8% SDS-PAGE gels and probed with anti-GFP (left, Mouse) or anti-Ub (right) antibodies. Top panel is lower exposure, bottom panel is higher exposure. Arrow indicates the GFP-HFR1 size.

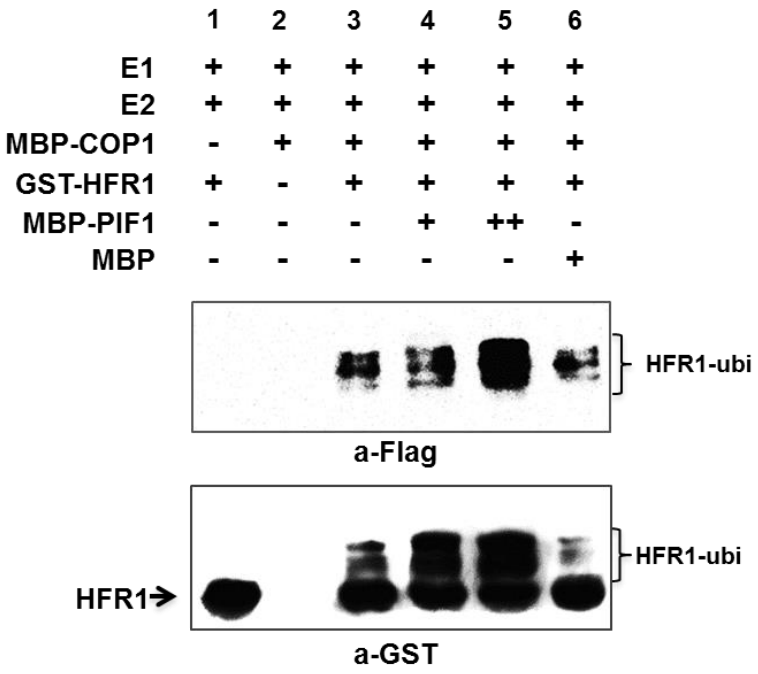

Figure 3.12: PIF1 enhances the COP1-mediated ubiquitination of HFR1.

PIF1 promotes the ubiquitination of HFR1 by COP1 *in vitro*. Recombinant MBP-COP1, MBP-PIF1 and GST-HFR1 fusions proteins were purified from *E. coli*. *In Vitro* Ubiquitination assay was performed using MBP-COP1 as E3 Ubiquitin ligase, GST-HFR1 as a substrate, Flag-Ubiquitin, UBE1 (E1), UbcH5b (E2), and increasing concentrations of MBP-PIF1. MBP was used as a control. (Top panel) Ubiquitinated GST-HFR1 detected by anti-Flag antibody. (Bottom panel) Ubiquitinated GST-HFR1 detected by anti-GST antibody. Arrow indicates the non-ubiquitinated GST-HFR1.

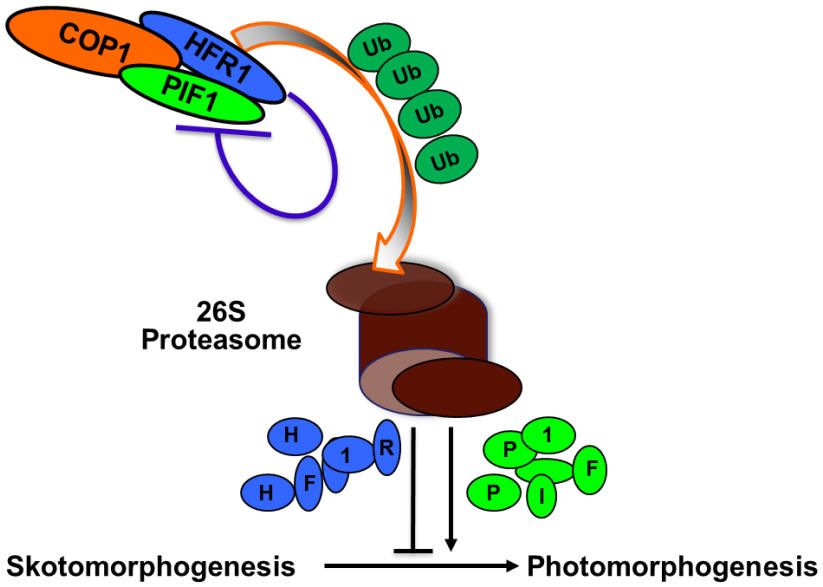

Figure 3.13: Model showing suicidal co-degradation of PIF1 and HFR1 by COP1 during photomorphogenesis.

PIF1, COP1 and HFR1 directly interact with each other to form a complex. PIF1 promotes the COP1-mediated ubiquitination and subsequent degradation of HFR1 through the 26S proteasome-mediated pathway. At the same time, PIF1 is also ubiquitinated and co-degraded together with HFR1 by the 26S proteasome.

Table 3.1: Primer sequences used in experiments described in the Chapter III.

Gene	Forward	Reverse
For qRT-PCR		
GFP	AAGCTGACCCTGAAGTTCATCTGC	CTTGTAGTTGCCGTCGTCCTTGAA
PP2A	TATCGGATGACGATTCTTCGTGCAG	GCTTGGTCGACTATCGGAATGAGAG
For HFR1*GFP site directed mutagenesis		
HFR1-pENTRY Cloning	CACCATGTCGAATAATCAAGCTTTCATGG	TAGTCTTCTCATCGCATGGGAAGAAAAATCC
HFR1-Mutagenesis	CAAGACGGACAAGGTTTCGGATGAGGACAAGACCATAGAG	CTCTATGGTCTTGTCCTCATCCGAAACCTTGTCCGTCTTG

Chapter IV: PIF1 promotes HECATE2 degradation via COP1 to regulate photomorphogenesis and flower development

ABSTRACT

Light signals perceived by photoreceptors play crucial roles regulating different aspects of plant developmental processes. The bHLH transcription factors PHYTOCHROME-INTERACTING FACTORs (PIFs) were shown to be the central regulatory node for signaling crosstalks between light signals and other internal and external signals, like hormone, circadian clock, temperature, and sugar. However, how light signals impinge upon reproductive development is still unclear. Recently we revealed that the HECATE bHLH transcription factors (HEC1, 2 and 3) play a role in promoting photomorphogenesis by antagonizing the activity of the PIFs through their direct interaction (Zhu et al., 2016). The HECs were originally identified as the regulators for female reproductive development in *Arabidopsis*. Thus, we hypothesize that light might also play a role on reproductive development via the regulatory hub between HECs and PIFs. Here we show that HECs also antagonize PIFs to regulate the expression of the class E MADS-box genes *SEPALLATA1* and *3* (*SEP1* and *3*) in flowers. Conversely, PIF1 promotes the degradation of HEC2 via E3 ligase Constitutively Photomorphogenic 1 (COP1), which is another major regulator in light signaling pathway. Combining *pif1* single or *pif1pif3pif4pif5* quadruple mutants (*pifq*) with *cop1-6* resulted in floral defects (stigmatic flower tissue overgrowth) similar to those of *HEC* mis-expressing plants. Conversely, *hec1 hec2* largely suppressed the phenotype of *cop1-6 pif1* flowers. In summary, these studies expand the repertoire of developmental programs under the control of light signaling factors, and uncover a link between light signaling and flower development.

KEYWORDS

Arabidopsis, HLH transcription factors (HECATEs), E3 ligase COP1, bHLH transcription factors (PIFs), photomorphogenesis, flower pattern development.

INTRODUCTION

As sessile organism, plants use light as an important signal to regulate growth and development. A broad spectrum of light signals including visible and UV wavelengths have profound effect on plant life cycle, including seed germination, seedling etiolation, phototropic growth, flowering time, circadian clock, shade avoidance response and others (Bae and Choi, 2008; Casal, 2013; Fankhauser and Christie, 2015). To perceive the diverse spectrum of light signals, plants have evolved different photoreceptors to sense the signals and regulate the plant growth and development accordingly. These include phytochrome (phy) perceiving red/far-red light, UVB-RESISTANCE 8 (UVR8) sensing UV-B light, the crytochromes (CRY), phototropins (PHOT) and Zeitlupe family for perceiving the UV-A/Blue light signals (Casal, 2013; Galvão and Fankhauser, 2015).

The phy family consists of five members (phyA-phyE) encoding apoproteins in Arabidopsis (Mathews and Sharrock, 1997). They can form homo- and hetero-dimers among the family members (Sharrock and Clack, 2004). These apoproteins are attached to a billin chromophore necessary for perceiving light signals. Upon red light exposure, the dimeric holophytochrome of all family members allosterically changes its conformation to a biologically active Pfr form and migrates into nucleus with differential kinetics (Fankhauser and Chen, 2008). The active Pfr form can be reverted back to the inactive Pr form by exposure to far-red light. This interconversion makes phys a unique photoreceptor whose activity can be reversibly regulated by light. After nuclear migration, the active Pfr form interacts with a number of unrelated proteins including the Phytochrome Interacting basic helix-loop-helix transcription factors called PIFs (Castillon et al., 2007; Leivar and

Quail, 2011). PIFs function as negative regulators of photomorphogeneis, opposing all the activities of active phytochromes. Thus, phys are promoting photomorphogenesis in response to light while PIFs are promoting skotomorphogenic development in darkness.

Genetic studies have identified another group of mutants that are constitutively photomorphogenic (*cop* mutants) in the dark, suggesting that these factors also function as negative regulators of light signaling pathways (Lau and Deng, 2012). One of these proteins called CONSTITUTIVELY PHOTOMORPHOGENIC1 (COP1) functions as an E3 Ubiquitin ligase (Osterlund et al., 2000). COP1 forms complexes with SUPPRESSOR OF PHYA (SPA1-4) and targets the positive regulators (including LONG HYPOCOTYL 5 (HY5), LONG HYPOCOTYL IN FAR-RED (HFR1), LONG AFTER FAR-RED LIGHT 1 (LAF1) and others) for ubiquitination and subsequent degradation in the dark, thereby repressing precocious photomorphogenesis in darkness (Saijo et al., 2003; Seo et al., 2003; Jang et al., 2005; Yang et al., 2005; Zhu et al., 2008). COP1 also targets many other substrates including CONSTANS (CO), EARLY FLOWERING 3 (ELF3), and GIGANTEA (GI) for regulation of the flowering time and circadian clock (Liu et al., 2008; Yu et al., 2008; Lau and Deng, 2012; Xu et al., 2015). Very recently, COP1 has been shown to target EBF1 and EBF2 to regulate seedling emergence through soil by functioning together with the ethylene signaling pathway (Shi et al., 2016). The COP1/SPA complex also interacts with PIFs and synergistically regulates the positively acting transcription factor HY5 in the dark. In this process, PIFs are exerting their non-transcriptional role in enhancing the E3 ligase activity of COP1 (Xu et al., 2014; Xu et al., 2015). Thus, the COP1/SPA complex and PIFs play a wide role in regulating plant growth and development.

To promote photomorphogenesis, the active Pfr form of phys migrates into the nucleus and inhibits both of these negative regulators by distinct mechanisms. For COP1/SPA complex, both phyA and phyB physically interact with SPA1 in response to

light and reorganize the COP1/SPA complex, thereby inhibiting COP1 activity (Lu et al., 2015; Sheerin et al., 2015; Xu et al., 2015). Phys also induce nuclear exclusion of COP1 under prolonged light, thereby reducing the availability of its substrates for degradation (Subramanian et al., 2004). In case of PIFs, phys induce rapid phosphorylation, ubiquitination and subsequent degradation by the 26S proteasome pathway (Leivar and Quail, 2011). Strikingly, COP1/SPA in association with CULLIN4 (CUL4) is functioning positively during the dark-to-light transition. The $CUL4^{COP1-SPA}$ E3 Ubiquitin ligase recruits phosphorylated form of PIF1 and induces rapid ubiquitination and degradation in response to light (Zhu et al., 2015). In addition, PIF3 and PHYB are co-degraded by the CULLIN 3 $^{\text{Light Response BTB}}$ ($CUL3^{LRB}$) E3 Ubiquitin ligase (Ni et al., 2014). Inhibition and/or removal of COP1/SPA and PIFs by phys initiate a gradual progression to photomorphogenesis.

In addition to these posttranslational regulations of PIFs, recent studies showed that the helix-loop-helix (HLH) transcription factor, HFR1, sequesters PIF1/PIF4/PIF5 by forming a heterodimer with these PIFs to prevent DNA binding to their target gene promoters (Hornitschek et al., 2009; Shi et al., 2013). Very recently, we have identified another small family of HLH transcription factors, HECATEs (HEC1, 2 and 3), that promotes photomorphogenesis by negatively regulating the function of PIF1 and possibly other PIFs (Zhu et al., 2016). HEC2 is also degraded in the dark and stabilized under light, suggesting HEC2 might be a COP1 substrate. HECs were initially identified as factors regulating female reproductive tract develop in Arabidopsis and more recently have been shown to regulate stem cells in Arabidopsis (Gremski et al., 2007; Crawford and Yanofsky, 2011; Schuster et al., 2014). Constitutive overexpression of *HECATE 1* showed overproliferation of stigmatic tissue phenotype in which all primary shoots terminate in a stigma (Gremski et al., 2007). The flowers in *35S::HECATE2* transgenic plants have

ectopic stigmatic tissues on sepals. Flowers of *35S::HECATE3* also transform into carpelloid stalks capped by stigmas (Gremski et al, 2007). Interestingly, all the *cop1 pif* mutant combinations that we created in a previous study also showed similar overproliferated stigmatic tissue phenotype in the adult plant flowers, especially for the terminal inflorescence (Xu et al., 2014). Because HEC2 is unstable in the dark and because PIFs and COP1 synergistically promote degradation of the positively acting factors (Xu et al., 2015), we hypothesize that HEC2 might be a COP1 substrate that is also under synergistic regulation by COP1 and PIFs. In this study, we demonstrate that the light signaling factors are not only regulating photomorphogenesis at the seedling stage, but also playing a role in regulating the development of flower patterns. We provide genetic and biochemical evidence that COP1/SPA and PIFs are posttranslationally controlling HEC2 and possibly other HEC family members at the flower stage to regulate flower pattern development. This study uncovers a new function of light signaling factors and underscores the broader roles played by these factors in promoting plant growth and development.

RESULTS

cop1-6 and *pif* mutant combinations and *spaQ* display ectopic overproliferation of stigma phenotype in a *hec*-dependent manner

In a previous study, we created different mutant combinations between *cop1-6* and *pif1, 3, 4, 5* to demonstrate that COP1 and PIFs synergistically suppress photomorphogenesis in the dark (Xu et al., 2014). When these mutants were grown under continuous white light in green house, the adult plant flowers displayed ectopic overproliferation of stigmatic tissue (carpels) phenotype especially in the terminal stage flowers (Figure 4.1A). In contrast, the parental genotypes including *pif1*, *pifq*, and *cop1-6* showed normal flower phenotype similar to wild type (Figure 4.1A-B). The mutant phenotype was observed at both early stage flowers examined under scanning electron

microscope (Figure 4.1A, top panel) and later stage imaged by optical microscope (Figure 4.1A, middle and bottom panel). The *spaQ* (*spa1, 2, 3, 4* quadruple) mutant also displayed similar mutant flower phenotype (Figure 4.2A-B). Because not all the flowers of an individual plant showed the mutant flower phenotype, and not all the plants in each population displayed the mutant flower due to low penetrance, we selected the percentage of plants displaying the mutant flower phenotype in a population as the key phenotype to analyze. Strikingly, the quantitative data showed that, with more *pif* mutants incorporated into the *cop1-6* mutant, the penetrance of the mutant phenotype in each population is significantly increased. In the *cop1-6 pifq* mutant background, ~50% of the plants in each population displayed the phenotype compared to only 12.5% in the *cop1-6 pif1* background (Figure 4.1B). In addition, ~20% of the *spaQ* plants displayed this mutant flower pattern phenotype (Figure 4.2C).

Previous studies showed that overexpression of *HECs* showed very similar overproliferation of stigmatic tissue phenotype as we observed in the *cop1-6 pifq* and *spaQ* mutants (Figures 4.1A-B; Figures 4.2A-B). HECs are HLH transcription factors that play important roles in regulating the female reproductive organ development. Loss of function *hec* mutants causes severe defects in stigma of the gynoecium (Gremski et al., 2007). These data suggest that the *cop1-6 pifq* and *spaQ* mutant phenotypes might be due to an increased abundance of HECs. To test this hypothesis, we created the *cop1-6 pif1* HEC2-GFP and *cop1-6 pif1 hec1 hec2* quadruple mutant to employ both the gain of function and loss of function analyses. Strikingly, HEC2-GFP in the *cop1-6 pif1* background strongly enhanced the *cop1-6 pif1* mutant phenotype similar to the *cop1-6 pifq* background (Figure 4.3B). Conversely, while the *hec1 hec2* displayed normal flower phenotype similar to the wild type, *hec1 hec2* almost completely suppressed the overproliferation of stigmatic tissue phenotype in the *cop1-6 pif1 hec1 hec2* background, suggesting that *hec1 hec2* is epistatic

to *cop1-6 pif1* (Figures 4.1A-B). The small difference between the wild type and *cop1-6 pif1 hec1 hec2* might be due to a third member in the HECATE family called HEC3 (Gremski et al., 2007). Overall, these gain of function and loss of function data provide convincing evidence that the light signaling factors are involved in regulating flower pattern development.

PIFs and COP1 promote the degradation of HEC2 posttranslationally in flowers.

To determine if the HECs are more abundant in the *cop1-6 pif* combination mutants compared to the parental controls at the flower stage, we crossed HEC2-GFP into these backgrounds. We performed Western blots to test the HEC2-GFP protein level in the HEC2-GFP and various mutant backgrounds of *pif1*, *pifq*, *cop1-6* and *cop1-6 pif1*, respectively, containing the HEC2-GFP transgene (Figures 4.3A-B). Strikingly, both the *pifq* HEC2-GFP and *cop1-6* HEC2-GFP displayed much higher amount of HEC2-GFP protein compared to the HEC2-GFP flowers (Figures 4.3A-B). In addition, the HEC2-GFP protein level is significantly higher in the *cop1-6 pif1* double mutant backgrounds compared to either single mutant (Figures 4.3A-B). We examined the *HEC2-GFP* mRNA levels in these backgrounds using the qRT-PCR assays to test if the above differences in HEC2-GFP protein levels are at the post-translational level. The data show that there is no significant difference in *HEC2-GFP* mRNA level among these different genetic backgrounds (Figure 4.3B).

Previously, SPA proteins have been shown to function synergistically with COP1 to degrade positively acting factors in light signaling pathways (Saijo et al., 2003; Seo et al., 2003). To test if SPA proteins are involved in regulation of HEC2 in flowers, we crossed HEC2-GFP into *spaQ* mutant background. Western blots of flower samples showed that the HEC2-GFP is highly abundant in the *spaQ* mutant background compared

to wild type (Figures 4.4A-B), which is consistent with the overproliferation of the stigmatic tissue phenotype that we observed in the *spaQ* mutants (Figures 4.2A-B). Overall, these data suggest that COP1/SPA complex and PIFs regulate the abundance of HEC2 and possibly other HECs in a posttranslational manner.

hec1 hec2 **partially suppressed the synergistic promotion of photomorphogenic phenotypes of the** ***cop1-6 pif1*** **and the constitutive photomorphogenic phenotypes of** ***pifq***

Recently, we have shown that HECs are a new group of positive regulators for plant photomorphogenesis (Zhu et al., 2016). In the dark, COP1 suppresses photomorphogenesis by degrading the positive regulators (ELONGATED HYPOCOTYL 5, HY5; LONG HYPOCOTYL in FAR-RED1, HFR1; LONG AFTER FAR-RED LIGHT1, LAF1 and others) by forming the COP1/SPA complexes (Osterlund et al., 2000; Saijo et al., 2003; Seo et al., 2003; Jang et al., 2005; Xu et al., 2015). We have also shown that *cop1* and *pif1* mutant combinations synergistically promote photomorphogenesis by degrading the positively acting transcription factor HY5 (Figure 4.5A) (Xu et al., 2014). To examine if *hec1 hec2* can suppress the synergistic phenotypes of the *cop1-6 pif1*, we created the *cop1-6 hec1 hec2* and *pif1 hec1 hec2* triple and *cop1-6 pif1 hec1 hec2* quadruple mutants (Figure 4.5A). Phenotypic analyses of the hypocotyl lengths for these mutants showed that *hec1 hec2* partially suppressed the synergistic promotion of photomorphogeneis of the *cop1-6 pif1* double mutant (Figure 4.5A). In addition, *hec1 hec2* significantly rescued the hypocotyl length phenotype of the *cop1-6* mutant, suggesting that *hec1 hec2* acts downstream of *cop1* mutant.

Previous studies also showed that *pifq* displayed constitutive photomorphogenic phenotypes similar to the *cop1* mutant seedlings (Leivar et al., 2008; Shin et al., 2009; Xu et al., 2015). To test if *hec1 hec2* acts downstream of *pifq*, we created *pifq hec1 hec2*

sextuple mutant. Analyses of the hypocotyl length phenotype showed that *hec1 hec2* significantly suppressed the constitutive photomorphogenic phenotypes of *pifq* (Figure 4.5B). Overall, these data suggest *hec1* and *hec2* are acting downstream of *cop1* and *pifq* mutants.

PIFs and COP1 promote the degradation of HEC2 posttranslationally in etiolated seedlings.

To provide biochemical evidence in support of the hypothesis that increased abundance of HECs in the *cop1 pif* mutant combination seedlings contribute to the synergistic photomorphogenic phenotypes, we examined both the HEC2-GFP protein and mRNA levels at the etiolated seedlings stage grown in the dark. The results show that the HEC2-GFP protein, but not the *HEC2-GFP* mRNA, level is significantly stabilized in the *cop1-6 pif1* double mutant compared with that in *cop1-6* and *pif1* single mutant backgrounds, respectively (Figures 4.6A-B). Because *hec1 hec2* could also partially suppress the constitutive photomorphogenic phenotypes of the *pifq*, we also examined the HEC2-GFP protein and mRNA levels in the *pifq* HEC2-GFP seedlings. Results show that there is significantly higher amount of HEC2-GFP protein, but not the *HEC2-GFP* mRNA, in the *pifq* mutant background compared with the wild type and *pif1* single mutants, respectively, indicating that the constitutive photomorphogenic phenotypes of the *pifq* might be partly due to an increased abundance of HEC2 in the dark (Figures 4.6A-B). Taken together, these data suggest that PIFs and COP1 regulate the abundance of HEC2 and possibly other HECs posttranslationally in a synergistic manner in darkness.

To further validate this hypothesis, we created COP1-HA/HEC2-GFP double transgenic plants and performed Western blots. Results show that the overexpression of COP1 significantly reduces the abundance of HEC2-GFP in etiolated seedlings (Figure 4.7). The degradation of HEC2-GFP in the COP1-HA background can be significantly

blocked by the proteasome inhibitor (Bortezomib) treatment (Figure 4.7). These data further support the hypothesis that HEC2 is degraded by COP1 through the 26S proteasome mediated pathway.

PIFs and HEC1/HEC2 antagonistically regulate the expression of *SEP1* and *SEP3* genes in flowers.

Recently we have shown that HEC2 antagonistically regulate PIF function to promote photomorphogenesis by directly interacting with PIF1 and preventing the DNA binding and transcriptional activation activity of PIF1 (Zhu et al., 2016). Since PIFs and HECs are oppositely regulating the overproliferation of stigma phenotype as shown above (Figures 4.1A-B; Figures 4.3A-B), we examined if these factors are also antagonistically regulating flower pattern gene expression. Previous studies have shown that all four PIFs (PIF1, 3, 4, 5) preferentially bind to the core G-box DNA-sequence motif (CACGTG), which a variant of the canonical E-box (Martinez-Garcia et al., 2000; Huq and Quail, 2002; Huq et al., 2004; Al-Sady et al., 2008; de Lucas et al., 2008). We first examined ~2 kb promoter sequences of all the ABCE classes of flower pattern genes, including *APETALA1* (*AP1*), *APETALA 2* (*AP2*), *APETALA 3* (*AP3*), *PISTILLATA* (*PI*), *AGAMOUS* (*AG*), *SEPALLATA 1* (*SEP1*), *SEPALLATA 2* (*SEP2*), *SEPALLATA 3* (*SEP3*), *SEPALLATA 4* (*SEP4*) (Krizek, 2015), and also *FRUITFULL* (*FUL*), whose overexpression caused compound terminal flower phenotype similar to the overproliferation of stigmatic phenotype of the *cop1-6 pif1* mutants (Figure 4.1) (Varkonyi-Gasic et al., 2011). Strikingly, all these genes have the E-box motifs in their promoter regions. More interestingly, the promoters of *SEP1* and *SEP3* have G-box motifs, which are the preferential binding sites of PIFs (Figure 4.8B). *SEP1* and *SEP3* are two of the four MADS-box flower pattern E class genes that have been shown to function redundantly for controlling the petal, stamen and carpel development (Pelaz et al., 2000). Thus, we hypothesized that PIFs might directly

bind to the G-box motifs of the promoters of *SEP1* and *SEP3* to regulate the expression of *SEP1* and *SEP3*.

To test this hypothesis, we performed the qRT-PCR analyses for the *SEP1* and *SEP3* genes using RNA isolated from inflorescence tissues from the *pifq* and *hec1 hec2* mutants. Strikingly, the expression of both genes is significantly higher in the *pifq* mutant background. In contrast, the expression of *SEP1* and *SEP3* are significantly reduced in the *hec1 hec2* mutant backgrounds (Figures 4.8A). These data further support the hypothesis that PIFs suppress the expression of *SEP1* and *SEP3*, while HECs might activate the expression of *SEP1* and *SEP3* by negatively regulating the function of PIFs. Moreover, the chromatin immunoprecipitation (ChIP) assay showed that the binding of Myc-PIF1, Myc-PIF3, Myc-PIF4, and Myc-PIF5 was highly enriched in the G-Box region of promoters of both *SEP1* and *SEP3* genes compared to the control regions (Figure 4.8C). The enrichment is ~1.8 to 2.5-fold compared with the control region (Figure 4.8C). These data suggest that PIFs and HECs are functioning antagonistically to regulate the expression of flower pattern genes.

PIF1, HEC1 **and** ***HEC2*** **co-express in developing carpels and inflorescence tissues**

To examine if PIF1, HEC1 and HEC2 are co-expressed in flower tissues, we analyzed their expression pattern using the β-glucuronidase (GUS) reporter gene constructs, pHEC1:GUS, pHEC2:GUS and pPIF1:GUS that has been described recently (Zhu et al., 2016). Results show that HEC1 and HEC2 genes are expressed in the developing septum, transmitting tract and stigma at stage 12 of flower development as previously reported (Figures 4.9A-B, left panels) (Gremski et al., 2007; Crawford and Yanofsky, 2011). PIF1 also expresses in the same tissues in similar pattern at stage 12 flower (Figure 4.9C, left panel). In addition, PIF1, HEC1 and HEC2 are also co-expressed

in the inflorescence tissues (Figures 4.9A-C, right panels). Taken together, the gene expression data further suggest that the ectopic overproliferation of carpels phenotype might be due to the antagonistic regulation of PIFs and HECs on the flower pattern genes.

HEC1 and HEC2 physically interact with COP1, SPA1 and PIF1.

Because HEC2-GFP is more abundant in the *cop1-6 pif1* double mutant and *pifq* mutant backgrounds compared to the *cop1-6* and *pif1* single mutants, we further examined if PIF1 and COP1 can directly interact with HEC1 and HEC2, respectively. Yeast two-hybrid assays show that the full length COP1 interacts with both the HEC1 and HEC2 (Figure 4.10A). Moreover, we performed *in vivo* immunoprecipitation (co-IP) assays using COP1-HA as a bait to co-IP HEC2-GFP from double transgenic seedlings. Since overexpression of COP1-HA significantly degraded HEC2-GFP (Figure 4.7), we pretreated the COP1-HA/HEC2-GFP double transgenic seedling samples with proteasome inhibitor (Bortezomib) to block the degradation of HEC2-GFP. *In vivo* co-IP assays under these conditions show that COP1-HA robustly interacts with HEC2-GFP (Figure 4.10B). In addition, bimolecular fluorescence complementation (BiFC) assays show that COP1 directly interacts with HEC1, HEC2, and HEC3 in a transient assay in tobacco (Figures 4.10C-E). PIF1 also interacted with HEC2 in a BiFC assay (Figure 4.11), consistent with the interaction assays recently described (Zhu et al., 2016). Taken together, these data suggest that PIF1, HEC1, HEC2 and COP1 form protein complexes together.

COP1 has been shown to form complexes with SPA1-4 and synergistically degrade COP1 targets including, HY5, HFR1, LAF1 (Lau and Deng, 2012). In addition, SPA1 interacted with all the COP1 targets. Since HEC2 interacts with COP1, we further examined if SPA1 also interacts with HEC1 and HEC2. Yeast two-hybrid assays show that the full length of SPA1 interacts with HEC1 and HEC2 (Figure 4.12A). Similar to COP1,

overexpression of SPA1 also triggered degradation of HEC2-GFP *in vivo,* which was blocked by the proteasome inhibitor, Bortezomib (Figure 4.12B, C). Thus, we pretreated the TAP-SPA1/HEC2-GFP double transgenic seedling samples with proteasome inhibitor (Bortezomib) and performed *in vivo* interaction (Figure 4.12C). Results show that TAP-SPA1 interacted with HEC2-GFP *in vivo*. Overall, these data suggest that COP1, SPA1 and PIF1 form complexes with HEC1 and HEC2.

COP1 directly ubiquitinates HEC2 *in vitro* and PIF1 promotes the trans-ubiquitination activity of COP1.

The higher abundance of HEC2-GFP protein in *cop1* mutant background and the lower amount of HEC2-GFP protein in COP1-HA overexpression background suggest that COP1 might act as an E3 Ubiquitin ligase to directly ubiquitinate HEC2 and trigger its subsequent degradation. To test this hypothesis, we performed *in vitro* ubiquitination assay using *E.coli* purified MBP-COP1 as the E3 ligase and GST-HEC2 as the substrate in the presence of Flag-Ubiquitin, UBE1 (E1), and UbcH5b (E2). The results showed that HEC2 was polyubiquitinated in the presence of COP1 as detected by the anti-GST and anti-Flag antibodies (Figure 4.13, lanes 1-3). In addition, we have shown that PIF1 promotes the degradation of COP1 substrate by enhancing the transubiquitination activity of COP1 toward the substrates (Xu et al., 2015). To examine this hypothesis, we performed the *in vitro* ubiquitination assay using GST-HEC2, MBP-COP1 and different amount of MBP-PIF1 or MBP as a control. Results showed that, in the presence of PIF1, the ubiquitination level of HEC2 was significantly increased in a PIF1 concentration-dependent manner (Figure 4.13, lane 4-5). In contrast, the addition of MBP control protein did not affect the COP1-mediated ubiquitination of HEC2 (Figure 4.13, lane 6). Taken together, these data strongly suggest that HEC2 is a new substrate for COP1 E3 Ubiquitin ligase that can be

directly polyubiquitinated by COP1. Moreover, PIF1 enhanced the COP1-mediated ubiquitination of HEC2 in a concentration dependent manner.

DISCUSSION

Light has a profound effect on plant growth and development not only as an energy source for photosynthesis, but also as an environmental signal throughout the life cycle of plants. Previous research in light signaling mainly focused on developmental pathways that prepare plants for autotrophic growth by maximizing the solar energy utilization and ensure reproductive growth to complete the life cycle. Here we show that light signaling factors not only regulate photomorphogenesis, but also flower pattern development, expanding the role of these factors in plant growth and development.

COP1-SPA complex and PIFs not only suppress photomorphogenesis but also regulate the development of flower patterns.

COP1-SPA complex and PIFs are well-established negative regulators of photomorphogenesis, both of which function independently as well as synergistically to repress photomorphogeneis in the dark (Leivar and Quail, 2011; Lau and Deng, 2012; Xu et al., 2015). Here we show that these factors synergistically regulate flower pattern development by controlling the amount of a HLH transcription factor called HEC2 and possibly other HEC family members. While *cop1* and *pif* single mutants didn't display any flower development phenotype, combination mutants between *cop1-6* and *pif1* displayed ectopic flower phenotype including overproliferation of stigmatic tissues (Figures 4.1A-B). This phenotype was enhanced by the overexpression of HEC2 in the *cop1-6 pif1* background similar to a level displayed by the *cop1-6pifq* mutant (Figure 4.1B). In addition, *spaQ* displayed significant overproliferation of stigma tissue phenotype compared to the wild type (Figure 4.2). Conversely, *hec1 hec2* suppressed the overproliferation of stigma tissue phenotype of the *cop1-6 pif1* mutant. This genetic

relationship is also observed at the seedling stage where *cop1-6 pif1* displayed synergistic photomorphogenesis as previously reported (Xu et al., 2014), and *hec1 hec2* partially suppressed the photomorphogenic phenotypes of the *cop1-6 pif1* and *pifq* mutants (Figure 4.5). Previously, HECs have been shown to regulate stigmatic tissue development. Overexpression of all three HECs (HEC1, HEC2 and HEC3) induced overproliferation of stigmatic tissue phenotype similar to that observed for the *cop1-6 pif1*, *cop1-6 pifq* and *cop1-6 pif1 HEC2-GFP* lines (Gremski et al., 2007; Crawford and Yanofsky, 2011). Overall, these data suggest that HECATE proteins are functioning downstream of the COP1-SPA and PIFs in regulating photomorphogenesis and flower pattern development.

Although light signaling factors have not been shown to regulate flower pattern development, flower pattern genes have been shown to regulate light signaling pathways. For example, the flower pattern factors APETALA3 and PISTILLATA negatively regulate the expression of *BANQUO* genes (Mara et al., 2010). BNQs in turn interact with HFR1 and control its function to regulate hypocotyl lengths and greening process in petals and sepals (Mara et al., 2010). Thus, light signaling and flower development factors might have dual roles in regulating both processes.

COP1 directly ubiquitinates HEC2 and PIF1 enhances the COP1-mediated ubiquitination of HEC2 *in vitro*

Consistent with the above genetic evidence, the biochemical data presented here strongly suggest that HEC2 is a new substrate of COP1 E3 Ubiquitin ligase. First, HEC2-GFP protein level is more abundant in the *pif1*, *cop1-6*, *pifq,* and *cop1-6 pif1* backgrounds at the adult flower and seedling stages compared to HEC2-GFP in wild type background (Figure 4.3; Figure 4.6). Conversely, overexpression of COP1 reduces the amount of HEC2-GFP in the COP1-HA/HEC2-GFP double transgenic line, which can be increased by the treatment of proteasome inhibitor Bortezomib (Figure 4.7). Second, COP1, SPA1

and PIF1 directly interact with HEC2 in yeast-two-hybrid, BiFC and *in vivo* co-IP assays (Figures 4.10-4.12). Third, COP1 directly poly-ubiquitinates HEC2 in the presence of the E1 and E2 enzymes *in vitro* (Figure 4.13). Moreover, this poly-ubiquitination is enhanced by the increasing concentration of PIF1 and not by an unrelated control protein. These data are consistent with our previous report that HEC2 is degraded in the dark and is stabilized by light at seedling stage (Zhu et al., 2016). Overall, these data suggest that COP1 and PIFs regulate both seedling de-etiolation and flower pattern development by directly regulating the abundance of HEC2 and possibly other HEC proteins (Figure 4.14).

HECs and PIFs antagonistically regulate the expression of flower patterning genes

Previously, we have shown that PIFs and HECs are co-expressed at the seedling stage and antagonistically regulate photomorphogenesis (Zhu et al., 2016). PIFs activate *HEC* expression, while HEC2 and possibly other HECs negatively regulate PIF1 function by heterodimerization, thereby, forming a negative feedback loop to fine tune photomorphogenesis. The phenotypic and promoter:reporter assays presented here also show that *PIF1, HEC1* and *HEC2* are co-expressed at the flower tissues and functioning antagonistically to regulate flower pattern development (Figures 4.8-4.9). In addition, PIFs and HECs are oppositely regulating the expression of *SEP1* and *SEP3,* two flower patterning genes that have the G-box in their promoter regions, which are the preferential binding sites of PIFs (Figure 4.8A). The ChIP assays show that all four PIFs directly bind to the promoters of *SEP1* and *SEP3* genes (Figure 4.8C). Because HEC2 have been shown to interact with PIF1 and inhibit its DNA binding and transcriptional activation of target genes in etiolated seedlings, these data suggest that *SEP1* and *SEP3* are regulated by PIFs and HECs in a similar manner in flowers. However, the enrichment of Myc-PIFs on the G-boxes of promoters of *SEP1* and *SEP3* genes is only ~1.8 to 2.5-fold in flowers of light-

grown adult plants, which is relative lower than the enrichment of Myc-PIFs on their target genes in dark-grown etiolated seedlings (Figure 4.8C) (Zhu et al., 2016). This is because the Myc-PIFs are relative low abundant in continuous white light due to the phytochrome mediated degradation of PIFs (Xu et al., 2015). Overall, all these data suggest that PIFs and HECs are functioning antagonistically to regulate the expression of flower pattern genes.

Although, the *sep1sep2sep3* triple mutant lacks the petals, stamens and carpels (Pelaz et al., 2000), and PIFs directly repress *SEP1* and *SEP3* expression in flower tissue (Figure 4.8), the 2-4-fold mis-regulation of these genes in the *pifq* background appears to be insufficient to induce flower patterning defect as *pifq* didn't display this phenotype (Figure 4.1). Thus, a threshold level of HEC2-GFP is critical to induce this phenotype. This threshold appears to be present in the *cop1-6 pif1* and *cop1-6 pifq* backgrounds that showed the phenotype, but not in the *cop1-6*, *pif1* and *pifq* backgrounds that lack the phenotype. HECs have been shown to interact with other bHLH proteins including, SPT and ALC (Kristina Gremski, Gynoecium patterning in *Arabidopsis thaliana*: control of transmitting tract development by the *HECATE* genes, PhD thesis, University of California, San Diego, 2006), both of which form homo- and hetero-dimers and regulate critical aspects of gynoecium and fruit development including stigma tissue growth (Heisler et al., 2001; Rajani and Sundaresan, 2001; Groszmann et al., 2011; Schuster et al., 2015). In addition, SPT has been shown to regulate seed germination and seedling growth in response to cold and light, respectively (Penfield et al., 2005). Thus, HECs might control the function of multiple bHLH factors to regulate light signaling and flower patterning. Another closely related atypical bHLH protein, INDEHISCENT (IND) also interacts with SPT and regulates flower and fruit patterning (Liljegren et al., 2004; Girin et al., 2011). It is possible that IND is also under post-translational regulation by the COP1-SPA complex and PIFs.

Because most of the ABCE flower pattern genes have the E/G-box present in their promoter regions, the PIF-SPT-HEC regulatory network might control many if not all these genes to regulate flower development.

MATERIALS AND METHODS

Plant materials, growth conditions and measurements

Seeds of wild type (Col-0) and various mutants (*pif1*, *pifq*, *cop1-6*, *cop1-6 pif1*, *cop1-6 pifq*, *spaQ*) in the Col-0 background were used (Laubinger et al., 2004; Xu et al., 2014). HEC2-GFP, *hec1 hec2* double mutant, *pHEC1:GUS, pHEC2:GUS* and *pPIF1:GUS* have been described (Zhu et al., 2016). For generation of *cop1-6 pif1 hec1 hec2*, *cop1-6 hec1 hec2*, *pif1 hec1 hec2* and *pifq hec1 hec2*, *hec1 hec2* was crossed with *cop1-6 pif1*, *cop1-6*, *pif1* and *pifq* to obtain F1 generation. Through genotyping and phenotypic characterization of the large F2 and F3 population, we identified the mutant combinations. For generation of *pif1* HEC2-GFP, *pifq* HEC2-GFP, *cop1-6* HEC2-GFP, and *cop1-6 pif1* HEC2-GFP, HEC2-GFP was crossed into those mutant backgrounds to obtain F1 generation. Through genotyping, phenotypic characterization and antibiotic (Basta for HEC2-GFP) selection of large F2 and F3 population, we created those genetic materials. For generation of COP1-HA/HEC2-GFP double transgenic plants, COP1-HA was crossed into HEC2-GFP to produce F1 seeds. Through antibiotic selection and phenotypic characterization of F2 and F3 generation, double transgenic plants were obtained for *in vivo* co-immunoprecipitation assays. Primers for genotyping were used as previously described (Schuster et al., 2014; Xu et al., 2014).

Plant were grown in Metro-Mix 200 soil (Sun Gro Horticulture, Bellevue, WA) under 24-h light at 22 ± 0.5°C. Seeds were surface-sterilized and plated on Murashige and Skoog (MS) growth medium containing 0.9% agar without sucrose as described (Shen et

al., 2005; Xu et al., 2014). After 4 days of cold treatment at 4°C in the dark, seeds were exposed to 3hrs of white light at room temperature to induce the germination. Then seeds were placed back to dark for either 4 days for seedling Western blots or 5 days for phenotypic assays. For flower phenotypic assay, same stage flowers were harvested for phenotypic assays.

For measurement of hypocotyl lengths, digital pictures of 5 day-old dark-grown seedlings were taken by camera. Hypocotyl lengths of at least 30 seedlings for each genotype were measured by ImageJ (http://rsb.info.nih.gov/ij/). At least three biological repeats were carried out. For quantification of percentage of multiple stigmatic tissue (carpel) phenotype, at least 50 plants for each genotype were grown for each population. The percentage of multiple stigmatic tissue (≥2 carpels) phenotype = number of plants showing the phenotype/total number of plants in each population. At least three biological repeats were done for each genotype.

RNA extraction and quantitative RT-PCR

The qRT-PCR assays were performed as previously described (Xu et al., 2014). For seedlings, four day-old dark-grown seedlings were used. For flower tissue, same stage of flowers were harvested and frozen in liquid nitrogen. Total flower RNA was isolated using the Spectrum plant total RNA kit (Sigma-Aldrich Co., St. Louis, MO). One μg of total RNA was reverse transcribed into cDNA using the SuperScript III **(**Life Technologies Co.**,** Carlsbad, CA) as per the manufacturer's protocol and then treated with DNase I to eliminate genomic DNA. Real-time PCR was performed using the Power SYBR Green RT-PCR Reagents Kit (Applied Biosystems Inc., Foster City, CA) in a 7900HT Fast Real-Time PCR machine (Applied Biosystems Inc., Foster City, CA). *PP2A* (At1g13320) was used as a control for normalization. The cycle threshold (Ct) values were used for

calculation of the relative expression level for *GFP* genes relative to *PP2A*. The HEC2-GFP or wild type Col-0 value was set as 1 to calculate the relative values of other samples. Primer used for qRT-PCR is listed in the table 4.1.

Protein extraction and Western blots analyses

For Western blots, same amount of four day-old dark-grown seedlings or flowers from light-grown plants were harvested for protein extraction in extraction buffer (50% glycerol, 10% SDS, 0.5 M EDTA pH 8, 1 M MOPS PH 7.6, 1×protease inhibitor cocktail (Sigma-Aldrich Co., St. Louis, MO, cat# 59), 40 mM β-mercaptoethanol, 2 mM PMSF, 25 mM β-GP, 10 mM NaF and 2 mM Na-orthovanadate). After boiling for 3 mins, samples were centrifuged at 14,000 rpm for 10 mins. Total protein supernatants were loaded on 8% SDS-PAGE gels and blotted onto polyvinylidene difluoride (PVDF) membranes. The same membrane was first blotted with anti-GFP antibody (Santa Cruz Biotech, Dallas, TX) followed by anti-RPT5 antibody (Enzo Life Sciences, Farmingdale, NY) after stripping. For secondary antibody, anti-mouse or anti-rabbit IgG HRP conjugate (1:50000) (Kirkegaard & Perry Laboratories, Inc., Washington, DC) was used for GFP and RPT5 respectively. Membranes were developed with SuperSignal West Pico Chemiluminescent substrate kit (Pierce Biotechnology Inc., Rockford, IL), and visualized on a camera or X-ray film. For the quantification of GFP and RPT5 protein level, the blots of three biological repeats were measured by ImageJ and the relative protein levels represent the ratio of GFP values divided by the RPT5 values. The HEC2-GFP was set as 1 to calculate the values of other samples for making the bar graph under the blot of each figure.

Chromatin Immunoprecipitation followed by quantitative PCR (ChIP-qPCR)

The ChIP-qPCR assays were performed as previously described (Gómez-Mena et al., 2005; Moon et al., 2008; José Ripoll et al., 2015) with minor modification. Briefly,

same amount of Myc-PIF1, Myc-PIF3, Myc-PIF4, Myc-PIF5 flower tissue (~2g, including open flowers and stage 13-14 fruits) were harvested for each of the three biological repeats. The tissues were immediately cross-lined with 1% formaldehyde for 45min under vacuum as previously described (Gómez-Mena et al., 2005). The cross-linking reaction was stopped by adding glycine to a final concentration of 0.125 M followed by sufficient wash with water. The samples were then frozen in liquid nitrogen and ground into a fine powder. The nuclei were extracted with Nuclei isolation buffer (2M sucrose, 0.5M PIPES, 1M $MgCl_2$, 1M KCl, 5M NaCl, 20% Triton X-100, 200mM PMSF and 1×protease inhibitor cocktail (Sigma-Aldrich Co., St. Louis, MO, cat# 59)) and then lysed with Nuclei Lysis buffer as previously described (Moon et al., 2008). After sonication to shear DNA into ~500bp fragment, the suspension was centrifuged at 14,500 rpm for 5min at 4°C. The solubilized chromatin was pre-absorbed overnight with 5 µl anti-Myc antibody (EMD Millipore, Billerica, MA) at 4°C for overnight. 40µl of dynabead protein A was added into each sample and rotated for another hour at 4°C. Immunoprecipitated samples were sequentially washed by low salt wash buffer (0.2% SDS, 150mM NaCl, 0.5% Triton X-100, 2mM EDTA and 20mM Tris·Cl pH 8.0), high salt wash buffer (0.2% SDS, 150mM NaCl, 0.5% Triton X-100, 2mM EDTA and 20mM Tris·Cl pH 8.0), LiCl wash buffer (0.5% NP-40, 0.25M LiCl, 0.5% Deoxycholate Sodium Salt, 1mM EDTA and 10mM Tris·Cl pH 8.0) and TE buffer (1mM EDTA and 10mM Tris·Cl pH 8.0). Immunocomplexes were eluted from the beads using the elution buffer (50 mM Tris-HCl pH8.0, 10 mM EDTA, 1% SDS) at room temperature with gentle rotation and crosslinking was reversed by incubation with 10µl 5M NaCl at 65°C for overnight, followed by Proteinase-K treatment for 1 hour. DNA was then purified with using QIAEX II Gel Extraction Kit (Qiagen, Cat. No. 20051). qRT-PCR was performed for the quantification of the immunoprecipitated DNAs at different

region by using the primers listed in the table 4.1. Input DNAs were used as control for normalization. Three technical qRT-PCR repeats were done for each 3 biological replicate.

Histology and microscopy

Flower GUS-Staining was performed as previously described (Ripoll et al., 2006; Alonso-Cantabrana et al., 2007; Crawford and Yanofsky, 2011). Briefly, same stage of flowers and inflorescence were harvested and treated with 90% ice-cold acetone for each line and then washed with the washing buffer for 5min and incubated with staining buffer at 37°C as described (Ripoll et al., 2006). Some of the flowers were dissected to check the carpel staining under dissecting microscope for imaging. For the flower phenotype, later stage flowers were imaged under dissecting microscope, earlier stage flowers were dissected and examined by scanning electron microscopy (SEM). SEM was carried out as described with minor modification (Ripoll et al., 2006). Briefly, same stage of flowers for different genotypes were harvested and fixed with 4% glutaraldehyde and 2% paraformaldehyde solution. Samples were then washed sequentially with 50%, 75%, 95% and 100% ethanol prior to critical point drying with CO_2 (Tousimis Samdri 790 CPD). Specimens were sputter-coated with either gold or Pt/Pd (Cressington 208 Benchtop Sputter Coater) and visualized under the scanning electron microscope (Zeiss Supra40 SEM-Electron Microscope).

Yeast two-hybrid analyses

Full-length of HEC1 and HEC2 were cut from GAD-HEC1 and GAD-HEC2 (Zhu et al., 2016). Then they were cloned into pEG202 (Ausubel et al., 1994) using the restriction sites included in the primers to generate LexA-HEC1 and LexA-HEC2 followed by verification of sequencing and restriction enzyme digestion. AD-COP1 and AD-SPA1 were used as previously described (Xu et al., 2014; Zhu et al., 2015). The different

combinations of these vectors were transformed into yeast EGY48-0 (Ausubel et al., 1994). After growing on - uracil, -histidine and –tryptophan (-ura-his-try) media for 3 days at 30ºC, same size colonies were cultured in liquid -ura-his-try media supplemented with 2% (w/v) glucose for overnight (O/N). Then aliquots of O/N cultures were transferred into liquid -ura-his-try media supplemented with 1% (w/v) raffinose and 2% (w/v) galactose to induce the protein expression. β-galactosidase activity assay was performed and quantified as described (Ausubel et al., 1994).

***In vivo* co-immunoprecipitation assays**

Four day-old dark-grown COP1-HA/HEC2-GFP and TAP-SPA1/HEC2-GFP seedlings were pretreated with 40 μmol bortezomib (LC Laboratories, Woburn, MA) for 4hrs as previously described to block the HEC2 degradation (Zhu et al., 2015). HEC2-GFP and wild type were used as controls. Total protein was purified from 0.4g of dark grown seedlings with 800 μl native extraction buffer (100 mM phosphate buffer, pH 7.8, 150 mM NaCl, 0.1% NP40, 1×protease inhibitor cocktail (Sigma-Aldrich Co., St. Louis, MO, Cat. No: P9599), 1 mM phenylmethylsulfonyl fluoride (PMSF), 40 μM bortezomib, 25 mM β-glycerophosphate, 10 mM sodium fluoride (NaF), and 2 mM Na orthovanadate). Anti-HA (Abcam, Cambridge, MA, Cat. No: ab9110) or anti-Myc antibody (Sigma-Aldrich Co., St Louis, MO) was incubated with Dynabeads (20 μL/μg antibody; Life Technologies Co., Carlsbad, CA) for 30mins at 4°C. The beads were then washed twice with extraction buffer to get rid of unbound antibody. After 15min centrifuge of protein extracts at 16,000g at 4°C in the darkroom, the supernatants were added into the beads bound with antibody for incubation for 3hrs with rotation at 4°C in the dark. The beads were then washed three times with 1ml extraction buffer with 0.2% NP40 to remove the unbound antibody. Immunoprecipitated proteins were eluted with 1× SDS loading buffer and heated at 65°C

for 5min. The samples were then separated on an 6.5% SDS-PAGE gel, blotted onto PVDF membranes, and probed with either anti-GFP (Santa Cruz Biotech, Dallas, TX) or anti-HA (Covance, Inc., Emeryville, CA, Cat# 16B12) or anti-Myc (EMD Millipore, Billerica, MA) antibody. Membranes were developed and visualized on an X-ray film or camera as described above.

Bimolecular fluorescence complementation (BiFC) assay

BiFC assay was performed as previously described (José Ripoll et al., 2015) (Ripoll et al., 2015; Rodríguez-Cazorla et al., 2015). Briefly, coding sequences of COP1, PIF1, HEC1, and HEC2 were either cut from the yeast vectors as previously described (Zhu et al., 2015) or amplified from their cDNAs using Phusion PCR (New England Biolabs, Ipswich, MA). Then they were cloned into either the pBJ36-SPYNE or pBJ36-SPYCE plasmids, containing the N-terminal (nt) and C-terminal (ct) halves of the yellow fluorescent protein (YFP) (YFPnt and YFPct), respectively as described in the figures (Rodríguez-Cazorla et al., 2015). The following cloning, transformation, and YFP visualization were carried out as previously described (Rodríguez-Cazorla et al., 2015).

***In vitro* ubiquitination assays**

The MBP-PIF1 and MBP-COP1 were purified from *E.coli* as previously described (Zhu et al., 2015), HEC2 ORF was digested from the GAD-HEC2 (Zhu et al., 2016) and then cloned into pGEX4T-1 vector. GST-HEC2 protein was purified from *E.coli* using the Pierce Glutathione Agarose beads followed by the proteins purification protocols from Thermo scientific (Rockford, IL). UBE1 (E1), UbcH5b (E2), Flag-tagged ubiquitin (Flag-Ub) were purchased from Boston Biochem (Cambridge, MA). The *in vitro* ubiquitination assays were performed as previously described with minor modification (Saijo et al., 2003; Seo et al., 2003; Zhao et al., 2013; Xu et al., 2014). Briefly, 5µg of Flag-Ubiquitin, ~25ng

of E1, ~25ng of E2, ~500ng of MBP-COP1, ~300ng of GST-HEC2, and 50-100ng MBP-PIF1 were used in the reaction. MBP-COP1 was treated with 20 μM $ZnCl_2$ for 45min at 22°C before the ubiquitination assay. The reaction buffer contains 50 mM Tris, pH7.5, 5 mM $MgCl_2$, 2 mM ATP, and 2 mM DTT. After incubation at 30°C for 2hrs, the reaction mixtures were stopped by the addition of SDS sample buffer and heated at 95°C before electrophoresis on an 8% SDS/polyacrylamide gels. After blotted onto PVDF membranes, the Anti-GST-HRP conjugate (GE Healthcare Bio-Sciences, Pittsburgh, PA) was used for GST-HEC2 detection and the Flag-Ubiquitin conjugated HEC2 was detected by α-Flag antibody (F1804; Sigma-Aldrich Co., St. Louis, MO).

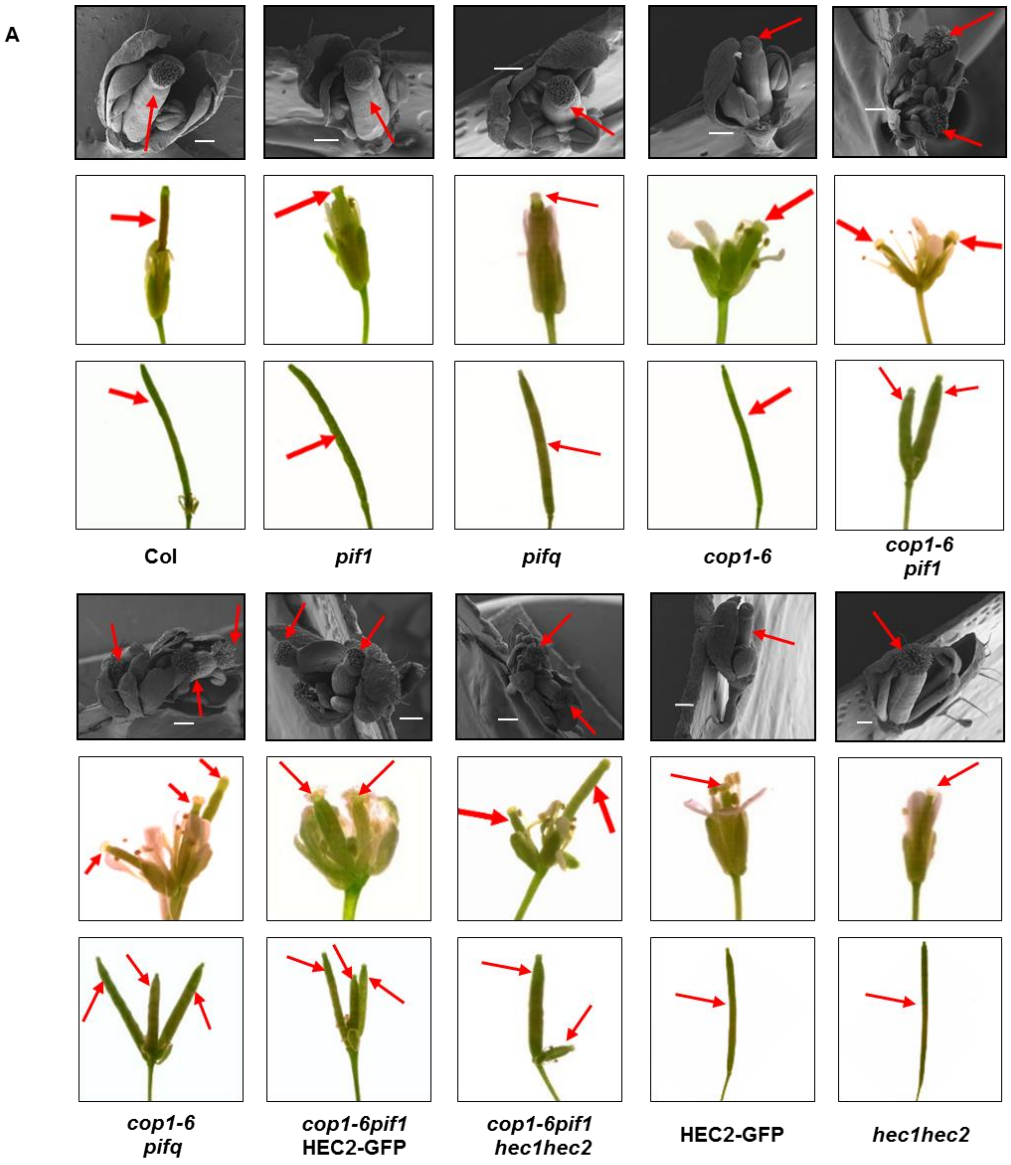
A
Col
pif1
pifq
cop1-6
cop1-6 pif1
cop1-6 pifq
cop1-6pif1 HEC2-GFP
cop1-6pif1 hec1hec2
HEC2-GFP
hec1hec2
B
Percentage of overproliferation of stigmatic tissue (carpels) phenotypes
60%
50%
40%
30%
20%
10%
0%
D
D
D
D
B
A
A
C
D
D
Col
pif1
pifq
cop1-6
cop1-6 pif1
cop1-6 pifq
cop1-6pif1 HEC2-GFP
cop1-6pif1 hec1hec2
HEC2-GFP
hec1hec2

Figure 4.1: *cop1-6* and *pif* mutant combinations display ectopic overproliferation of the stigmatic tissue phenotype in a *hec*-dependent manner.

(A) The multiple carpel/silique (overproliferation of stigmatic tissue) phenotypes of the *cop1-6pif* mutant combinations and *cop1-6pif1*HEC2-GFP along with control plants under both scanning electron microscope for early stage (top panel) and optical microscope for later stage (middle and bottom panel). The red arrows indicate the carpels that develop into siliques. Scale bars = 200μm. (B) The quantification of percentage of overproliferation of stigmatic tissue (carpels) phenotypes for Col-0, *pif1*, *pifq*, *cop1-6*, *pif1*, *cop1-6pif1*, *cop1-6pifq*, *cop1-6pif1*HEC2-GFP, *cop1-6pif1hec1hec2*, HEC2-GFP and *hec1hec2*. Percentage = number of plants showing the mutant flower phenotype/total number of plants in each population. Error bars indicate standard deviation. The letters "A" to "D" indicate statistically significant differences between means of percentages of overproliferation of stigmatic tissue phenotype ($p<0.05$), ($n>50$, three biological replicates).

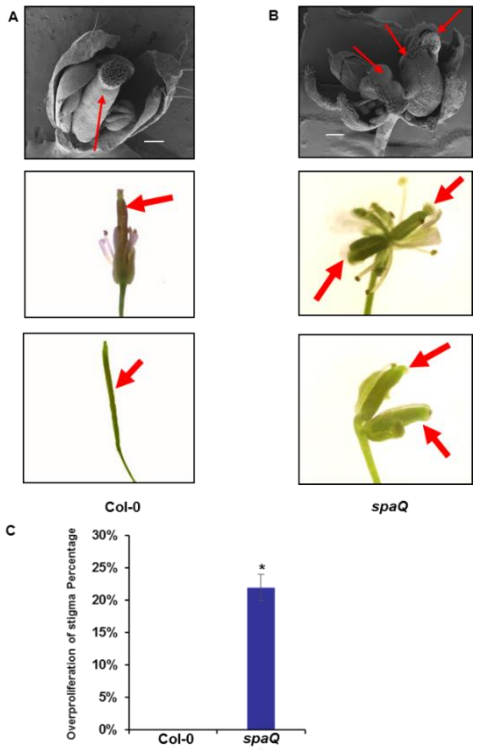

Figure 4.2: Overproliferation of stigmatic tissue phenotypes of the *spaQ* mutant.

(Top) Scanning electron micrographs of wild type Col-0 (A) and *spaQ* (B) flowers at stage 11. Scale bars = 200µm. The red arrows indicate the multiple carpel (Overproliferation of stigmatic tissue) in one single flower of the wild type and *spaQ* mutant. (Middle) Photographs of stage 15 flowers from wild type (A) and *spaQ* mutant (B) grown under continuous white light. (Bottom) Photographs of siliques from wild type (A) and *spaQ* mutant (B) grown under continuous white light. (C) The quantification of overproliferation of stigmatic tissue phenotypes for Col-0 and *spaQ*. Percentage = number of plants showing the mutant flower phenotype/total number of plants in each population. Error bars indicate standard deviation. *, indicates significant difference ($p<0.05$), ($n>50$, three biological replicates).

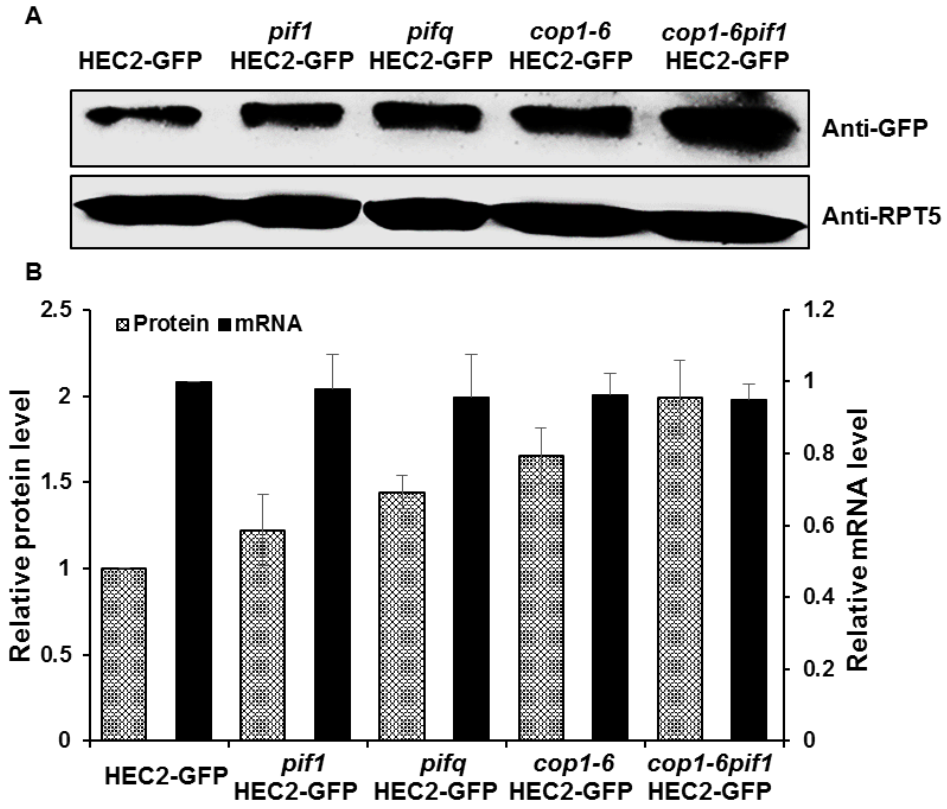

Figure 4.3: PIFs and COP1 promote the degradation of HEC2 posttranslationally in flowers.

(A) Western blots show the HEC2-GFP protein level in HEC2-GFP and various mutant backgrounds of *pif1*, *pifq*, *cop1-6* and *cop1-6pif1*, respectively, containing the HEC2-GFP transgene. Plants are grown in continuous white light until they flower. Same stage flowers were collected and frozen in liquid nitrogen. Total protein was purified and separated on an 8% SDS-PAGE gel, blotted onto PVDF membrane and probed with anti-GFP or anti-RPT5 antibodies. (B) Bar graph showing the HEC2-GFP protein (left Y-axis) and *HEC2-GFP* mRNA (right Y-axis) levels in the flowers of the mutants indicated. For protein quantitation, HEC2-GFP band intensities were quantified from three independent blots

using ImageJ, and normalized against RPT5 levels. HEC2-GFP was set as 1 and the relative proteins levels were calculated. *HEC2-GFP* mRNA level was determined using qRT-PCR assays with primers from the *GFP* region. Total RNA was extracted from same stage flowers, *PP2A* was used as an internal control. HEC2-GFP was set as 1 and the relative gene expression levels were calculated. Error bars indicate standard deviation (n=3).

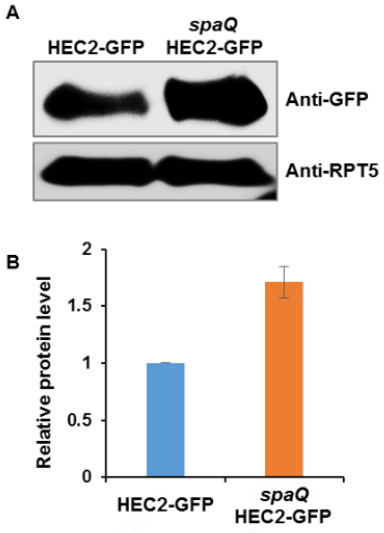

Figure 4.4: HEC2 is highly abundant in flowers of *spaQ*.

(A) Western blots show the HEC2-GFP protein level in HEC2-GFP and spaQ mutant background containing the HEC2-GFP transgene. Plants are grown in continuous white light until they flower. Same stage flowers were collected and frozen in liquid nitrogen. Total protein was purified and separated on an 8% SDS-PAGE gel, blotted onto PVDF membrane and probed with anti-GFP or anti-RPT5 antibodies. (B) Bar graph showing the HEC2-GFP protein levels in the flowers of HEC2-GFP and spaQ/HEC2-GFP. For protein quantitation, HEC2-GFP band intensities were quantified from three independent blots using ImageJ, and normalized against RPT5 levels. HEC2-GFP was set as 1 and the relative proteins levels were calculated. Error bars indicate standard deviation (n=3).

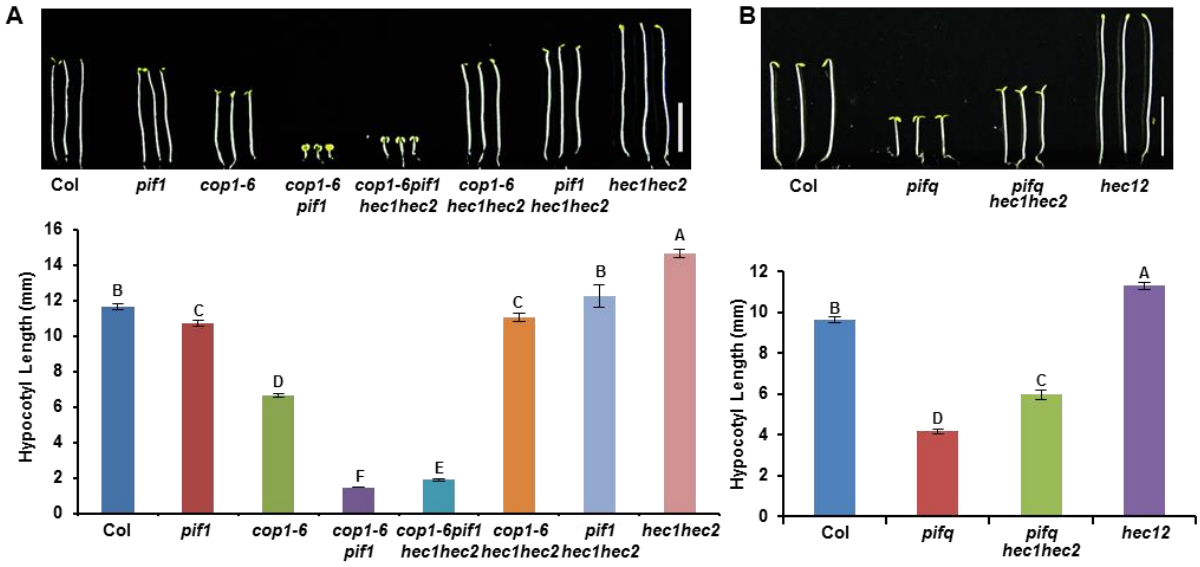

Figure 4.5: *hec1 hec2* partially suppressed the synergistic promotion of photomorphogenic phenotypes of the *cop1-6 pif1* and the constitutive photomorphogenic phenotypes of *pifq*.

(A) (Top) Photographs of seedlings of wild type, *pif1, cop1-6, cop1-6pif1, cop1-6pif1hec1hec2, cop1-6hec1hec2, pif1hec1hec2* and *hec1hec2* mutants. Seedlings are grown in the dark for 5 days. (Bottom) Bar graph showing hypocotyl lengths of various genotypes as indicated. (B) (Top) Photographs of seedlings of wild type, *pifq, pifqhec1hec2* and *hec1hec2*. Seedlings are grown in the dark for 5 days. (Bottom) Bar graph showing hypocotyl lengths of various genotypes as indicated. Error bars indicate standard deviation. The letters "A" to "F" indicate statistically significant differences between means of hypocotyl lengths among the genotypes after T-test ($p<0.05$), ($n>30$, three biological replicates)

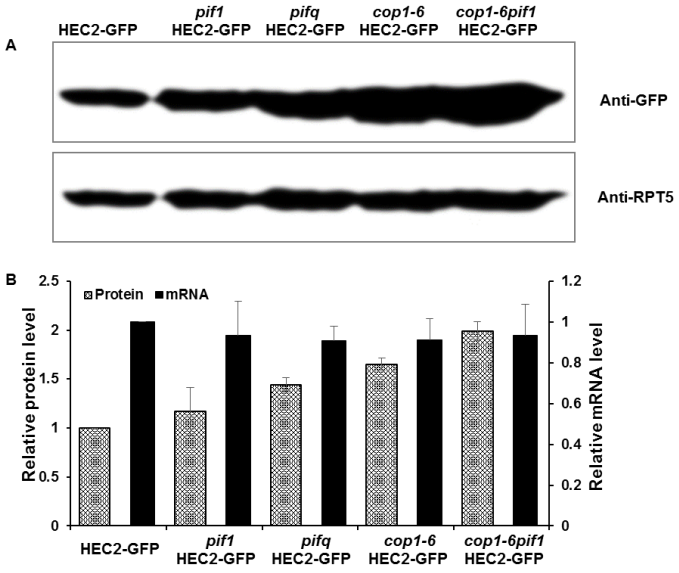

Figure 4.6: PIFs and COP1 promote the degradation of HEC2 posttranslationally in etiolated seedlings.

(A) Western blots show the HEC2-GFP protein level in the HEC2-GFP and various mutant backgrounds of *pif1*, *pifq*, *cop1-6* and *cop1-6pif1*, respectively, harboring the HEC2-GFP transgene. Seedlings are grown in the dark for 4 days. Total protein was separated on an 8% SDS-PAGE gel, blotted onto PVDF membrane and probed with anti-GFP or anti-RPT5 antibodies. (B) Bar graph showing the HEC2-GFP protein (left Y-axis) and *HEC2-GFP* mRNA (right Y-axis) levels in the seedlings of the mutants indicated. For protein quantitation, HEC2-GFP band intensities were quantified from three independent blots using ImageJ, and normalized against the RPT5 levels. HEC2-GFP was set as 1 and the relative protein levels were calculated. *HEC2-GFP* mRNA level was determined using qRT-PCR assays with primers from the *GFP* region. Total RNA was extracted from 4 day-old dark grown seedlings, *PP2A* was used as an internal control. HEC2-GFP was set as 1 and the relative gene expression levels were calculated. Error bars indicate standard deviation (n=3).

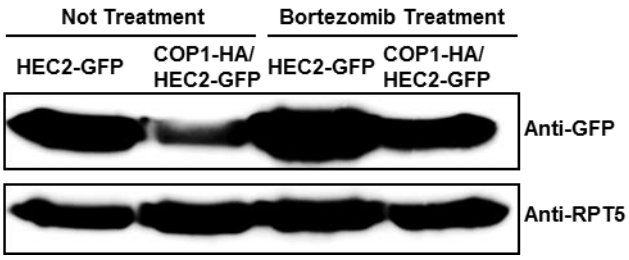

Figure 4.7: Overexpression of COP1-HA causes the degradation of HEC2-GFP through the 26S proteasome mediated pathway.

Western blot shows the HEC2-GFP protein level in the HEC2-GFP and COP1-HA/HEC2-GFP double transgenic lines, respectively, with and without proteasome inhibitor (40 mM Bortezomib, 3hrs) treatment. Seedlings are grown in the dark for 4 days. Total protein was separated on an 8% SDS-PAGE gel, blotted onto PVDF membrane and probed with anti-GFP or anti-RPT5 antibodies.

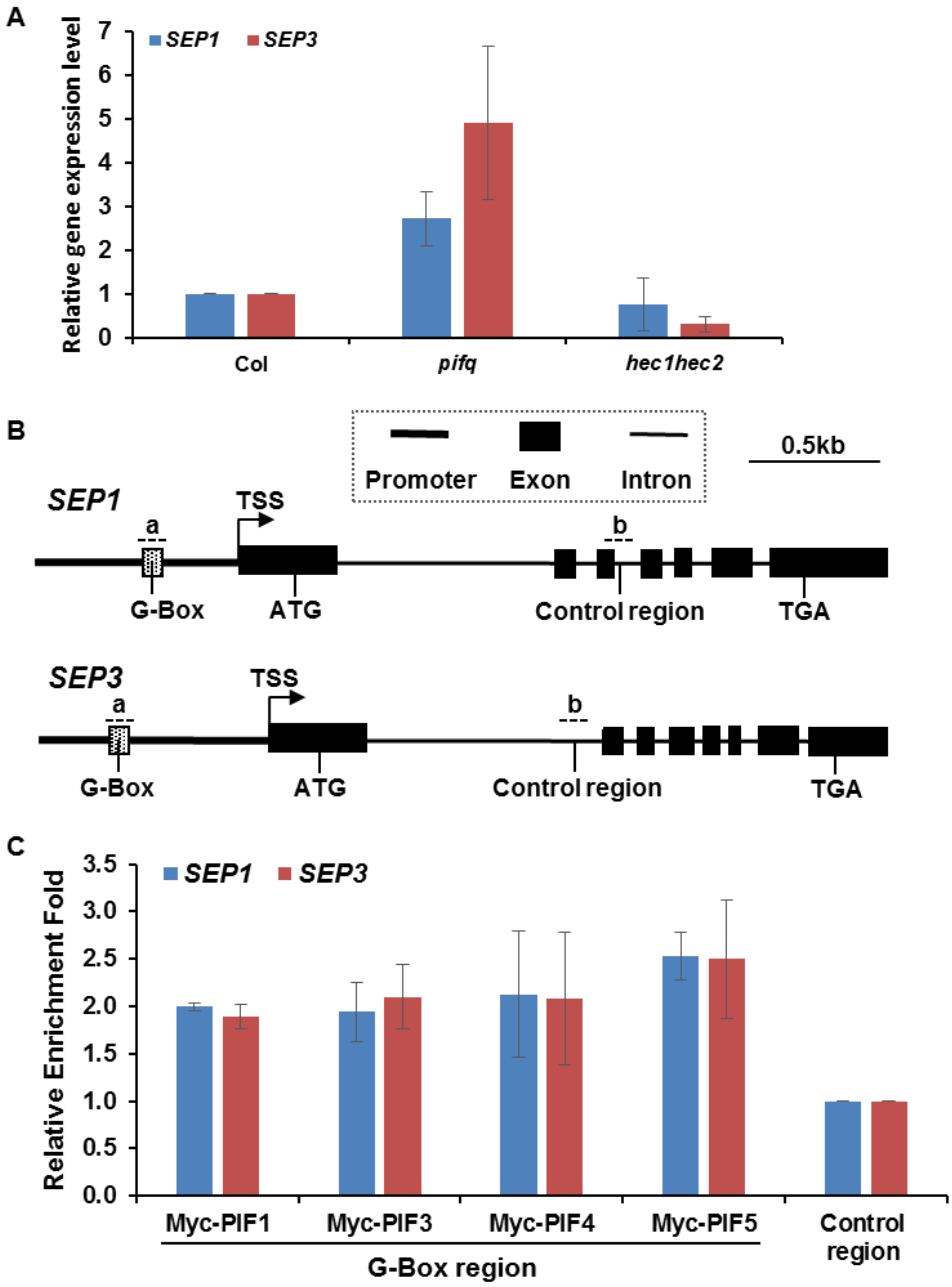

Figure 4.8: PIFs and HEC1/HEC2 antagonistically regulate the expression of *SEP1* and *SEP3* genes in flowers.

(A) Bar graph shows the expression of *SEP1* and *SEP3* transcript levels in the wild type, *pifq* and *hec1hec2* mutant seedlings as indicated. Total RNA was isolated from same stage inflorescences for qRT-PCR assays (n= 3 independent biological repeats). *PP2A* was used as an internal control. Wild type was set as 1 and the relative gene expression levels were calculated. Error bars indicate standard deviation. (B) Gene structures of the *SEP1* or *SEP3* genes analyzed in the chromatin immunoprecipitation (ChIP) experiment. The G-Box in the promoter region of *SEP1* or *SEP3* and the control regions are labeled as indicated. The dash lines show the positions of the PCR fragments in ChIP analyses for either *SEP1* or *SEP3* in their G-Box and control regions. (C) The chromatin immunoprecipitation (ChIP) assays using the Myc-PIF1, Myc-PIF3, Myc-PIF4, Myc-PIF5 show that the G-box region of the promoters of either *SEP1* or *SEP3* is more highly enriched compared to control regions. Same stage inflorescences of Myc-PIFs are harvested and fixed for ChIP assay. Anti-Myc antibody was used to immunoprecipitate Myc-PIFs and associated DNA fragment. DNA was amplified by qRT-PCR by using the primers indicated on the genes structures of *SEP1* and *SEP3* (B).

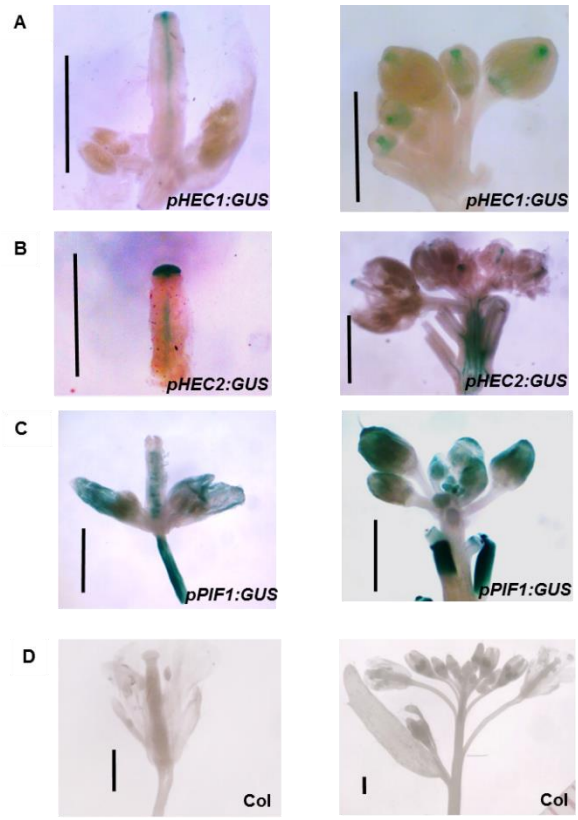

Figure 4.9: *PIF1*, *HEC1* and *HEC2* co-express in developing carpels and inflorescence tissues.

(A-D) GUS staining assay was performed for *pHEC1:GUS, pHEC2:GUS* and *pPIF1:GUS* in developing carpels at stages 12 (left panes) and inflorescences (right panels). Col-0 was used as a control. The expression patterns of *PIF1* and *HEC1/HEC2* are similar in these tissues. Scale bars = 1mm.

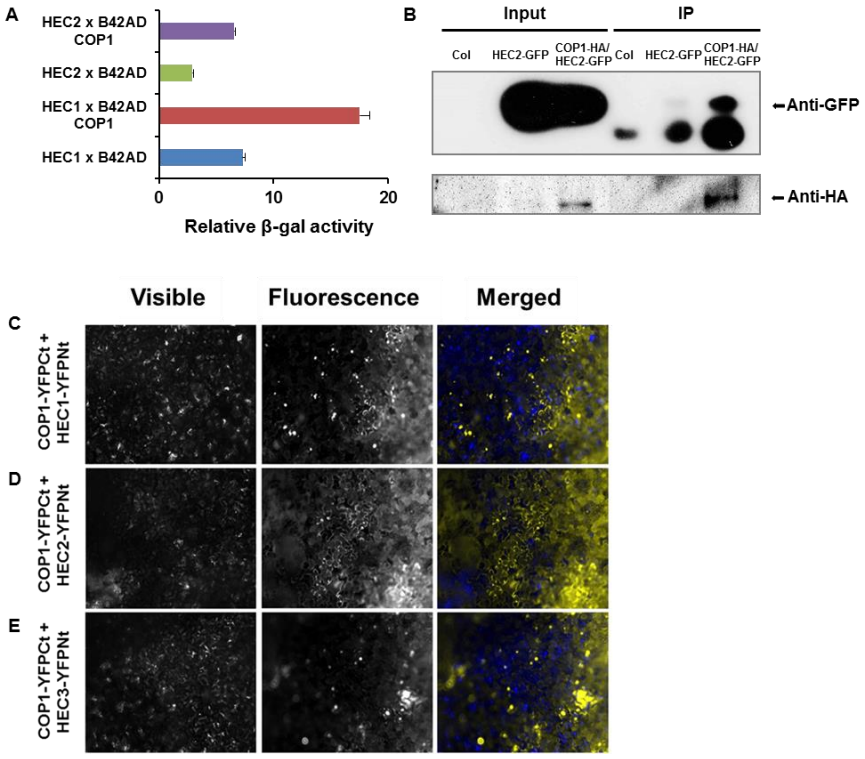

Figure 4.10: HEC1 and HEC2 physically interact with COP1 and PIF1.

(A) COP1 interacts with both HEC1 and HEC2 in yeast-two-hybrid assays. Full length HEC1 and HEC2 were cloned into LexA vector. Full length of COP1 was cloned into B42AD vector. Bar graph shows the average β-galactosidase activities from three independent experiments. The error bars represent standard deviation, (n=3). (B) HEC2 interacts with COP1 *in vivo*. HEC2-GFP and COP1-HA/HEC2-GFP double transgenic seeds were grown in the dark for 4 days, COP1-HA/HEC2-GFP seedlings were treated with proteasome inhibitor (40 μM Bortezomib) for 3hrs to block the HEC2 degradation before protein extraction. Co-IP was carried out using the anti-HA antibody and then probed with anti-GFP and anti-HA antibodies. (C-E) BiFC assays done by my collaborator

Dr. Juan Jose Ripoll from Dr. Martin F. Yanofsky lab showing interactions between COP1 and HEC1 (C), HEC2 (D), and HEC3 (E) in the nucleus and cytoplasm.

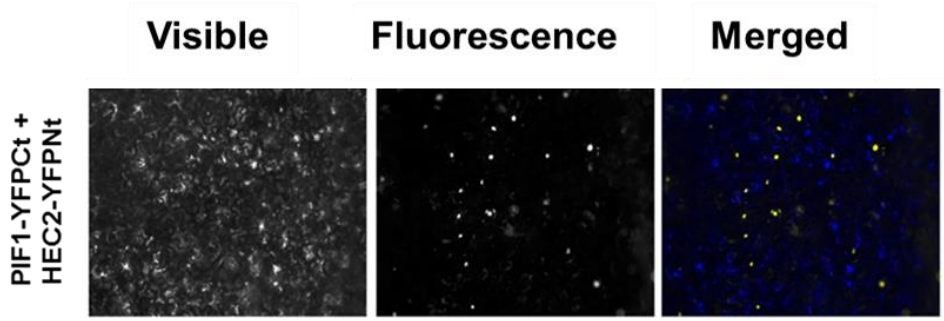

Figure 4.11: PIF1 interacts with HEC2 in bimolecular fluorescence (BiFC) assays.

BiFC experiments done by my collaborator Dr. Juan Jose Ripoll from Dr. Martin F. Yanofsky lab showing interactions between PIF1 and HEC2 in the nucleus.

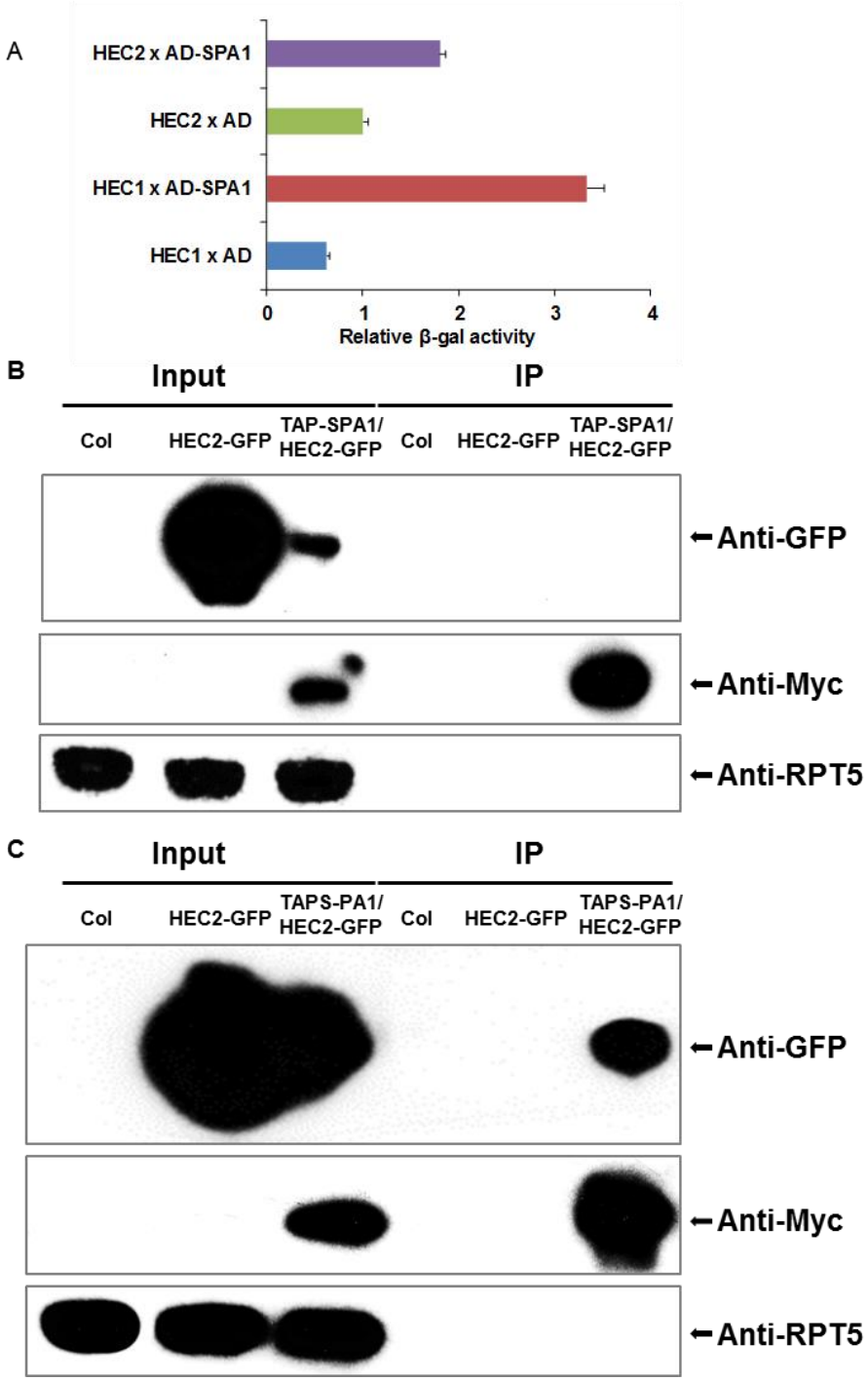

Figure 4.12: SPA1 physically interacts with HEC1 and HEC2.

(A) The full length SPA1 interacts with both HEC1 and HEC2 in yeast-two-hybrid assays. Full length HEC1 and HEC2 were cloned into LexA vector. Full length of SPA1 was cloned into B42AD vector. Bar graph shows the β-galactosidase activity in liquid ONPG assays. The error bars represent standard deviation, (n=3). (B) Overexpression of SPA1 triggers strong degradation of HEC2-GFP *in vivo*. HEC2-GFP and TAP-SPA1/HEC2-GFP double transgenic seeds were grown in the dark for 4 days. Co-IP assay was carried out using the anti-HA antibody and then probed with anti-GFP and anti-HA antibodies. (C) HEC2 interacts with SPA1 *in vivo*. TAP-SPA1/HEC2-GFP was treated with proteasome inhibitor (40 mM Bortezomib) for 4hrs to block the HEC2 degradation before Co-IP. Co-IP was carried out using the anti-Myc antibody and then probed with anti-GFP and anti-Myc antibodies.

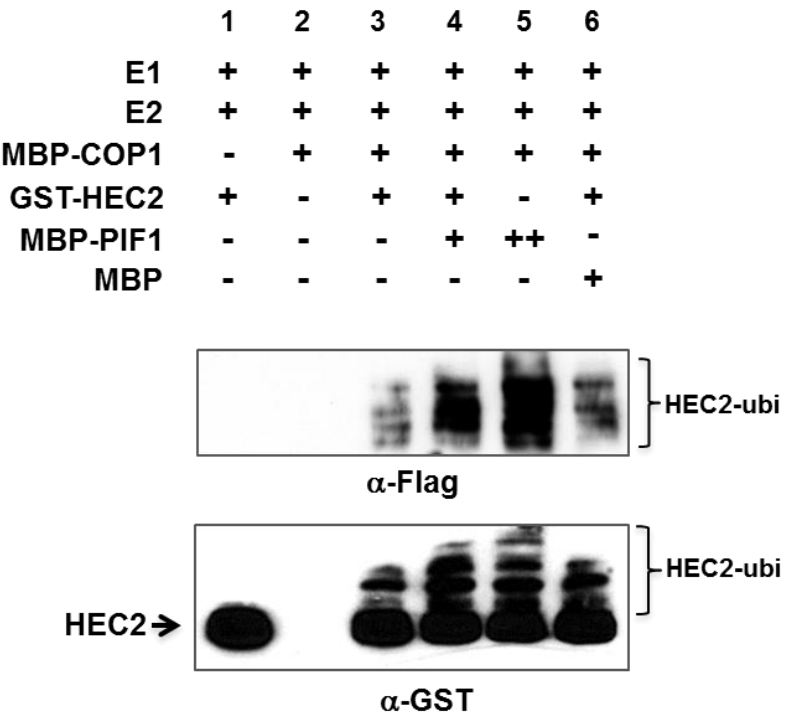

Figure 4.13: COP1 directly ubiquitinates HEC2 *in vitro* and PIF1 promotes the trans-ubiquitination activity of COP1.

Recombinant MBP-COP1, MBP-PIF1 and GST-HEC2 fusions proteins were purified from *E. coli*. *In vitro* Ubiquitination assay was performed using MBP-COP1 as E3, Flag-Ubiquitin, UBE1 (E1), UbcH5b (E2), GST-HEC2 and increasing concentrations of MBP-PIF1. MBP was used as a control. (Top panel) Ubiquitinated GST-HEC2 detected by anti-Flag antibody. (Bottom panel) Ubiquitinated GST-HEC2 detected by anti-GST antibody. Arrow indicates non-ubiquitinated GST-HEC2.

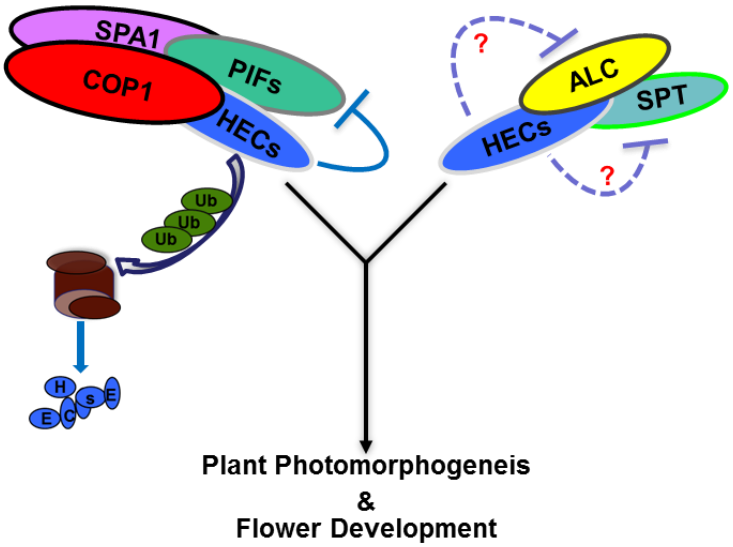

Figure 4.14: Schematic model shows how HECs regulate plant photomorphogenesis and reproductive development by interacting with light signaling and flower development factors.

PIF1, COP1, SPA1 and HEC2 directly interact with each other to form a complex. During photomorphogenesis, HECs are a group of positive regulators that are targeted by COP1 Ubiquitin E3 ligase for degradation in the dark. PIF1 promotes COP1-mediated ubiquitination and subsequent degradation of HEC2 through the 26S proteasome pathway. HECs also antagonize PIF activity to promote plant photomorphogenesis. During the reproductive development, PIFs display dual role in regulating flower development. On one hand, PIF1 promotes the degradation of HEC2 by COP1. On the other hand, PIFs directly bind and repress expression of flower pattern genes (e.g., *SEP1* and *SEP3*). HECs in turn negatively regulate the PIF function to activate the expression of flower pattern genes to regulate the flower development. HECs might also negatively regulate other bHLH transcription factors involved in reproductive development (e.g., ALC and SPT) through their direct interactions.

Table 4.1: Primer sequences used in experiments described in the Chapter IV.

Gene	Forward	Reverse
For qRT-PCR		
GFP	AAGCTGACCCTGAAGTTCATCTGC	CTTGTAGTTGCCGTCGTCCTTGAA
SEP1	GACCAGCTCTCGGATCTTC	ATCCAGCTTCATTGCCAAAG
SEP3	GAGCTCTCAGGACACAGTTTATGCT	GCATGCGTTCCTTACTCTGAAGAT
PP2A	TATCGGATGACGATTCTTCGTGCAG	GCTTGGTCGACTATCGGAATGAGAG
For ChIP-qPCR		
SEP1-a	CACAAGAGCCAATTATTTGGTGA	TTCTTTACTTTCATTCCCACGCTC
SEP1-b	AAGCTTAAGGGTAGATATGAGAACC	CAACAAAAGCCACACACACCT
SEP3-a	CAGGTGGATTTATCAGACCCTAC	TGAGTGATTGCAACCCTAAACAG
SEP3-b	GGATATTGTTTCCACGACAATCC	AGATGAATTTGACATTAGCGTCA

Chapter V: Summary

Since 2011, many studies have illuminated the hotspot mechanistic questions of the phytochrome-mediated signaling pathways. These include the identification of E3 ligases that degrade PIFs, key negative regulators, in response to light, a better view of how phytochromes inhibit another key negative regulator, COP1, and an understanding of why plants evolved multiple negative regulators to repress photomorphogenesis in darkness, which is the key question that I addressed in my dissertation. These advances will surely fuel future research on many unanswered questions that have intrigued plant photobiologists for decades.

E3 LIGASES FOR PIFS

Two recent reports described the identification of E3 ligases for PIF degradation (Ni et al., 2014; Zhu et al., 2015). These studies highlight the complex mechanism of how PIFs are regulated to fine tune photomorphogenesis.

One of those two studies described a CULLIN 3 (CUL3) based E3 ligase for PIF3 degradation (Figure 5.1, right). The substrate adaptor component for this ligase is LRB (Light-Response BTB) proteins (Ni et al., 2014). LRBs belong to the BTB family (Bric-a-Brack/Tramtrack/Broad) and display strong affinity for the phosphorylated form of PIF3, which is consistent with the light-induced phosphorylation and subsequent degradation of PIFs. In addition, $CUL3^{LRB}$ can catalyze ubiquitylation of a phosphomimic form of PIF3 *in vitro*. Interestingly, LRBs recruit both PIF3 and phyB in the $CUL3^{LRB}$ complex for polyubiquitylation and subsequent co-degradation by the 26S proteasome pathway. Because LRBs interact with each other to dimerize, it is possible that the PIF3-phyB bimolecular tetramer is recognized by two $CUL3^{LRB}$ complexes for light-induced ubiquitylation (Zhu and Huq, 2014; Christians, et al., 2012). This study also highlights the

importance of receptor desensitization in many eukaryotic systems, where the receptor is activated to transmit the incoming signal and then the receptor is either degraded or endocytosed to inactivate it. This prevents over-activation of the signaling pathways under prolonged incoming signals (Avraham and Yarden, et al., 2011). However, the drawback of this study is the lack of any biological significance of PIF3 degradation. *lrb* double and triple mutants do display photomorphogenic phenotypes; however, these phenotypes are not consistent with PIF3 degradation, but are consistent with phyB degradation. Thus, it is likely that additional E3 ligase(s) are necessary for PIF3 and other PIFs degradation in response to light. In line with this prediction, the other recent study described a well-established CUL4 based E3 ligase for PIF1 degradation in response to light (Zhu et al., 2015). In this case, COP1 and SPA proteins act as substrate adaptor components in recruiting preferentially the phosphorylated form of PIF1 in the $CUL4^{COP1\text{-}SPA}$ complex for light-induced ubiquitylation and subsequent degradation. The light-induced ubiquitylation followed by degradation of PIF1, but not the light-induced phosphorylation of PIF1 is defective in *cop1*, *spaQ* and *cul4cs* backgrounds compared to wild type. This rapid degradation of PIF1 is mostly regulated by phyA, and phyA is not degraded under these conditions, suggesting that PIF1 and phyA may not be co-degraded as previously shown for PIF3-phyB co-degradation (Ni, et al., 2014). In addition, *cop1* and *spaQ* mutants display a strong hyposensitive phenotype in seed germination assays consistent with the major role of PIF1 in this process. However, PIF1 is still degraded under prolonged light conditions in all the above mutants, suggesting additional E3 ligases are necessary for the degradation of PIF1 and other PIFs. In addition, because PIF3 is unstable in *cop1* and *spa* mutants (Leivar et al., 2008; Bauer et al., 2004), it is not clear if CUL4 based E3 ligase also plays a role in other PIF degradation.

KINASES FOR PIFS

Very recently, a targeted candidate gene approach has identified two kinases that phosphorylate PIFs directly. These include Casein Kinase II (CK2) and BRASSINOSTEROID INSENSITIVE 2 (BIN2) (Figure 5.1, right) (Bu et al, 2011a; Bernardo-García et al., 2014). CK2 has been shown to phosphorylate seven serine/threonine (S/T) residues present in PIF1 *in vitro* (Bu et al., 2011a). Serine to Alanine substitution mutations in six of these sites especially the three consecutive S residues at the carboxyl (C)-terminal end drastically reduced the degradation of PIF1 in response to light *in vivo*. However, PIF1 was still phosphorylated in response to light, suggesting that CK2 is not the light-regulated kinase that phosphorylates PIF1 in response to light. BIN2 has been shown to phosphorylate PIF4 *in vitro* and this phosphorylation alters the degradation kinetics of PIF4 in response to light and Brassinosteroid (BR) (Bernardo-García et al., 2014). However, it is still not clear whether CK2 and BIN2 phosphorylate PIFs in a light-dependent manner *in vivo*. Therefore, the light-regulated kinase that phosphorylates PIFs in response to light is still unknown (Bu et al., 2011b).

PHYTOCHROME-MEDIATED INHIBITION OF COP1 ACTIVITY

Two recent studies showed that phytochromes also directly interact with SPA1 and reorganize the COP1-SPA complex in a light-dependent manner (Lu et al., 2015; Sheerin et al., 2015). This reorganization leads to the separation of the physical contact between COP1 and SPA1, thereby reducing the COP1 activity to degrade the positively acting transcription factors (e.g., HY5/HFR1/LAF1 and others) (Figure 5.2, right). The increased abundance of the positively acting factors promotes photomorphogenesis in response to light. However, it is still not clear whether this separation only affects the SPA1-mediated

enhancement of COP1 activity and/or directly inhibits the COP1 activity to degrade the positively acting transcription factors.

NONTRANSCRIPTIONAL ROLES OF PIFS AS COFACTORS OF E3 LIGASE

Photomorphogenesis is repressed by two distinct classes of proteins: one (COP/DET/FUS) complex involves ubiquitin-mediated degradation of the positively acting factors (Figures 1.1, 5.2, left) and the other encodes bHLH transcription factors (PIFs) (Figures 1.1, 5.1 left) (Leivar and Quail, 2011; Lau and Deng, 2012). However, the relationship between these two groups of repressors was not clear until recently. Why are plants evolved with two classes of repressors? Do they function additively or synergistically? These are the key questions I asked in my dissertation.

In my dissertation, the three projects demonstrated that these two groups of proteins function synergistically to both repress photomorphogenesis and regulate reproductive development (flower development) (Xu et al., 2014; Xu et al., 2016ab). Genetic analysis showed that *cop1pif* or *spa1pif* combination mutants were more hypersensitive compared to the respective parents (Figure 5.3A). Biochemical analyses showed that positive regulators HY5, HFR1 and HEC2, the key target of COP1/SPA complex are much more abundant in the *cop1pif* or *spa1pif* combination mutants compared to the parental genotypes (Figure 5.3A) (Xu et al., 2014; Xu et al., 2016ab). PIF1 physically interacted with COP1, SPA1 and HY5, HFR1, HEC2 both *in vitro* and *in vivo*. Moreover, PIF1 enhanced the substrate recruitment, auto- and trans-ubiquitylation activity of COP1 toward HY5, HFR1, HEC2 (Figure 5.3B). PIFs have been shown to function as transcriptional regulators controlling gene expression in various signaling pathways including light (Leivar and Monte, 2014). However, the data from chapter II to IV suggest that PIFs have a pivotal non-transcriptional role in modulating signaling pathways in addition to

transcriptional regulation. In fact, the results suggest that PIF1 is functioning as a cofactor for COP1 in this process.

These results are consistent with previous reports that PIFs promote COP1 mediated ubiquitylation of type II phytochromes (phyB-E) *in vitro* (Jang et al., 2010), in line with the increased level of phyB in higher order *pif* mutants *in vivo* (Leivar and Quail, 2011). In addition, A B box containing protein, BBX19 interacts with COP1 and ELF3 and promotes COP1-mediated degradation of ELF3 (Wang et al., 2015). Very recently, DET1 has been shown to interact with PIFs and HFR1, and regulates HFR1 abundance posttranslationally through $CUL4^{DET1\text{-}COP10}$ E3 ligase (Shi et al, 2015; Dong et al., 2014). Apart from phytochromes, a host of diverse classes of factors directly interact with PIFs and regulate PIF functions. These include DELLA proteins (RGA/GAI), HLH proteins (HFR1/PAR/KIDARI), bZIP protein (HY5), transcriptional co-regulators (BZR1/FHY1), histone modifying enzyme (HDA15), circadian clock regulators (PRR1/ELF3) (Leivar and Monte, 2014; de Lucas, et al., 2008; Bu et al., 2011c, Hornitschek et al., 2009; Chen et al., 2013; Oh et al., 2012; Feng et al, 2008; Hyun et al., 2006; Roig-Villanova et al., 2007; Hao et al., 2012; Bai et al., 2012; Toledo-Ortiz et al., 2014; Luo et al., 2014; Chen et al., 2012; Yamashino et al., 2003). In addition, COP1 and DET1 directly interact with multiple proteins to regulate various signaling pathways (Figure 5.3B) (Lau and Deng, 2012). If PIFs interact with any of the COP1/DET1 substrates, PIFs might also regulate their abundance posttranslationally, increasing the potential of synergistic regulation of multiple signaling and developmental pathways (Figure. 5.3B). Thus it appears that the nontranscriptional roles of PIFs are playing an increasingly important if not equal role as transcriptional regulation by PIFs.

THE NEGATIVE REGULATION OF HLH TRANSCRIPTION FACTORS ON PIFS

Conventional wisdom holds that negative regulators of plant photomorphogenesis, PIFs, are stabilized in the dark and degraded in the light. However, in the project of chapter III, I showed that PIF1 suicidally co-degrades together with HFR1 by the COP1 E3 ligase mediated 26S proteasome pathway in the dark, which explains the lower seed germination phenotype of *hfr1* and *cop1-4hfr1* mutants compared with wild type and single mutant. This is consistent with the co-degradation mechanism of PIF3 and phyB by $CUL3^{LRB}$ E3 ligase that negative regulators, PIFs, are degraded at the same time when they are promoting the degradation of positive regulators or photoreceptors (Ni et al., 2014). Besides, the other group of repressors (COP1/SPA) also targets PIFs for ubiquitination and degradation to promote their rapid degradation under a small amount of light as reviewed above (Zhu et al., 2015). All these mechanisms allow plants to prevent over repression of photomorphogenesis in the dark and gradually transition to photomorphogenic development.

COP1/SPA complex and PIFs have been shown to play different roles in plant developmental processes. However, all previous studies mainly focused on the vegetative stage of plant growth and developments. In project III, I found that the *cop1 and pifs* mutant combinations and *spaQ* mutant showed stigmatic flower tissue overgrowth phenotype in reproductive stage. Further genetic and biochemical studies illustrated that this phenotype is caused by high abundance of HEC2, which is one of major female reproductive regulators, in those mutant backgrounds. Moreover, I showed that HEC2 is a substrate target of the COP1/SPA complex. HEC2 is targeted by COP1 for degradation via the ubi/26S proteasome pathway, and PIF1 promotes the poly-ubiquitination of HEC2 by COP1. More strikingly, we found that PIF1, PIF3, PIF4, PIF5 directly bind to the G-box regions of the promoters of class E MADS-box genes *SEPALLATA1* and *3* (*SEP1* and *3*).

HEC1 and HEC2 negatively regulate the function of PIFs to activate the expression of all these genes. All these data show new functions of light signaling factors, the COP1/SPA complex and PIFs, in regulating flower pattern formation and reveal the crosstalk between the light signaling pathway and reproductive development (flower development).

FUTURE PERSPECTIVES

The discovery of multiple repressors functioning synergistically to suppress photomorphogenesis suggests that photomorphogenesis is the default pathway for plant development. Skotomorphogenesis is a repressed state of photomorphogenesis. In my dissertation, I mainly discovered that plants employ the multiple layers of negative regulators, COP1/SPA complex and PIFs, to achieve sufficiently repressed state in the dark. This synergy is achieved by the conserved modulation of the COP1/SPA E3 ligase activity by PIFs to ubiquitinate and degrade positive regulators, HY5, HFR1, HEC2 (Xu et al., 2014). Moreover, the suicidal co-degradation of HFR1 and PIF1, together with PIF3 and phyB co-degradation reported recently, uncovers a new regulatory mechanism in plant photomorphogenesis (Ni et al., 2014). Finally, the novel discovery of the regulation of COP1/SPA1 complex and PIFs on reproductive development (flower development) expand the repertoire of developmental programs under the control of light signaling factors.

Other recent studies showed that light-activated phytochromes interact with PIFs to induce their phosphorylation by a yet unknown kinase, and the phosphorylated form is ubiquitylated by various E3 ligases and degraded through the 26S proteasome pathway to initiate photomorphogenesis (Ni et al., 2014; Zhu et al., 2015). Although we have a much better understanding of how light controls plant development, several key questions still

remain unanswered (Outstanding Questions as listed below). The answer to these questions awaits future research.

Outstanding Questions

1. What is the light-regulated kinase that phosphorylates PIFs in response to light?
2. HY5, the key positive regulator, is much more abundant in the *pifq* mutant in the dark, potentially contributing to the *pifq* phenotype in the dark. Because HY5 and PIFs bind to similar DNA sequence elements, are the PIF target genes also direct targets of HY5?
3. What is the biochemical function of phytochromes? Is phytochrome merely a scaffold protein to bring PIFs and the light-regulated kinase together? Alternatively, is phytochrome the light-regulated kinase as previously suggested?
4. What are the additional roles of light signaling factors on reproductive development? Does COP1/SPA target any other reproductive development factors for ubiquitination and degradation? How PIFs contribute to the regulation of these factors?

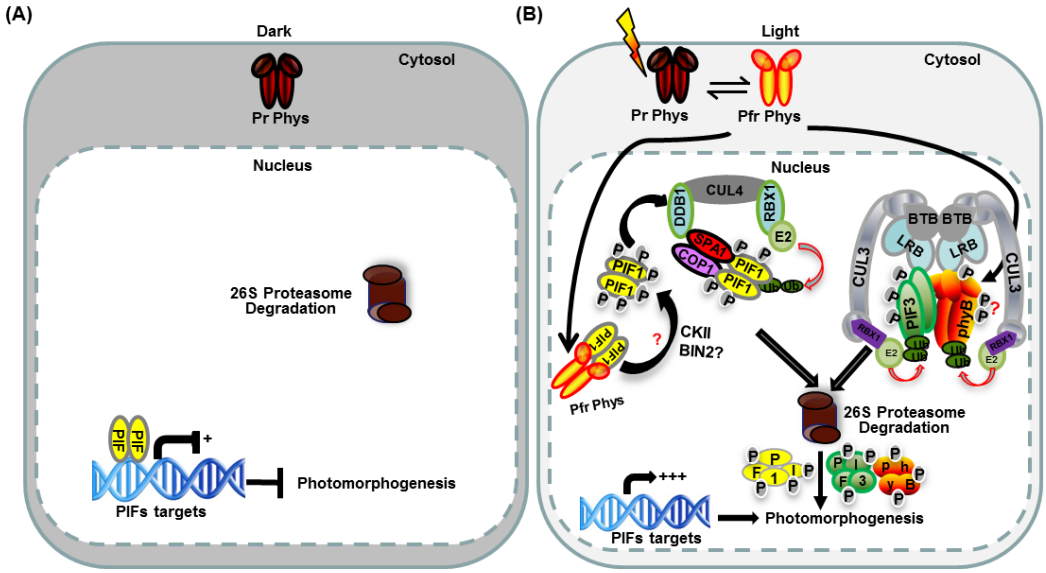

Figure 5.1: A model showing how light signals induces degradation of PIFs.

Left, in the dark, the biologically inactive Pr form of phytochrome is localized in the cytosol. The nuclear localized PIFs homo- and hetero-dimers bind to the promoter region of light-regulated target genes and repress their expression to prevent photomorphogenesis. Right, upon light exposure, the biologically active Pfr form of phytochrome translocates into nucleus. For PIF1, the interaction between the Pfr form of phytochromes and PIF1 triggers the rapid phosphorylation of PIF1 through unknown kinase. The phoshorylated form of PIF1 is recruited to the $CUL4^{COP1\text{-}SPA1}$ complex for rapid ubiquitylation and subsequent degradation through the 26S proteasome pathway. For PIF3, phyB and PIF3 homodimers interact with each other to form a quaternary complex, which is phosphorylated by an unknown kinase. The phosphorylated PIF3 and phyB bimolecular tetramer is ubiquitylated by CRL3 (CUL3–RBX1–LRB) E3 Ubiquitin Ligase Complex. Subsequently, phyB and PIF3 are concurrently degraded by the 26S proteasome pathway. The destruction of the PIFs derepresses the light-regulated gene expression and promotion of photomorphogenesis in response to light.

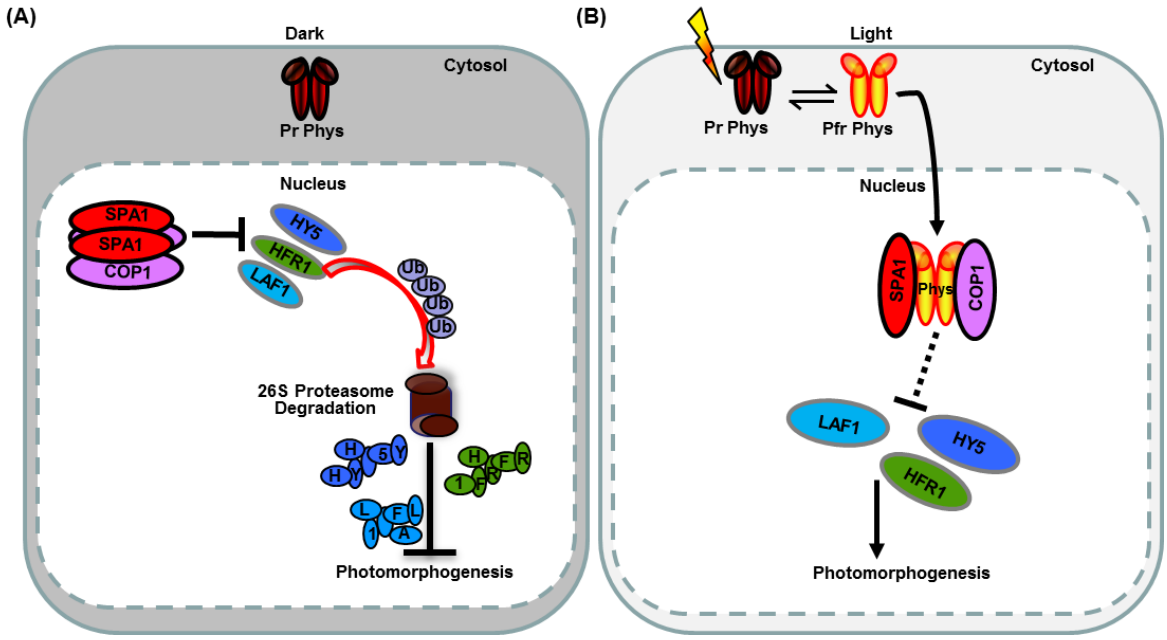

Figure 5.2: A model showing the mechanisms of inhibition of COP1 activity by phytochromes in response to light.

Left, in darkness, COP1-SPA complexes repress photomorphogeneis by their E3 ligase activity. COP1 and SPA homodimers interact with each other to form a tetrameric complex. SPAs activate the COP1's E3 ligase activity to trigger the poly-ubiquitylation and proteasome-mediated degradation of the positively acting transcription factors (such as HY5, HFR1 and LAF1) that promote photomorphogenesis. Right, upon light irradiation, the active Pfr form of phytochromes translocate into nucleus to interact with SPAs and disrupt the direct interaction between SPA1 and COP1. Without the activation of SPA, the positively acting transcription factors (HY5, HFR1 and LAF1) accumulate in response to light. Increased abundance of the positively acting transcription factors activates photomorphogenesis.

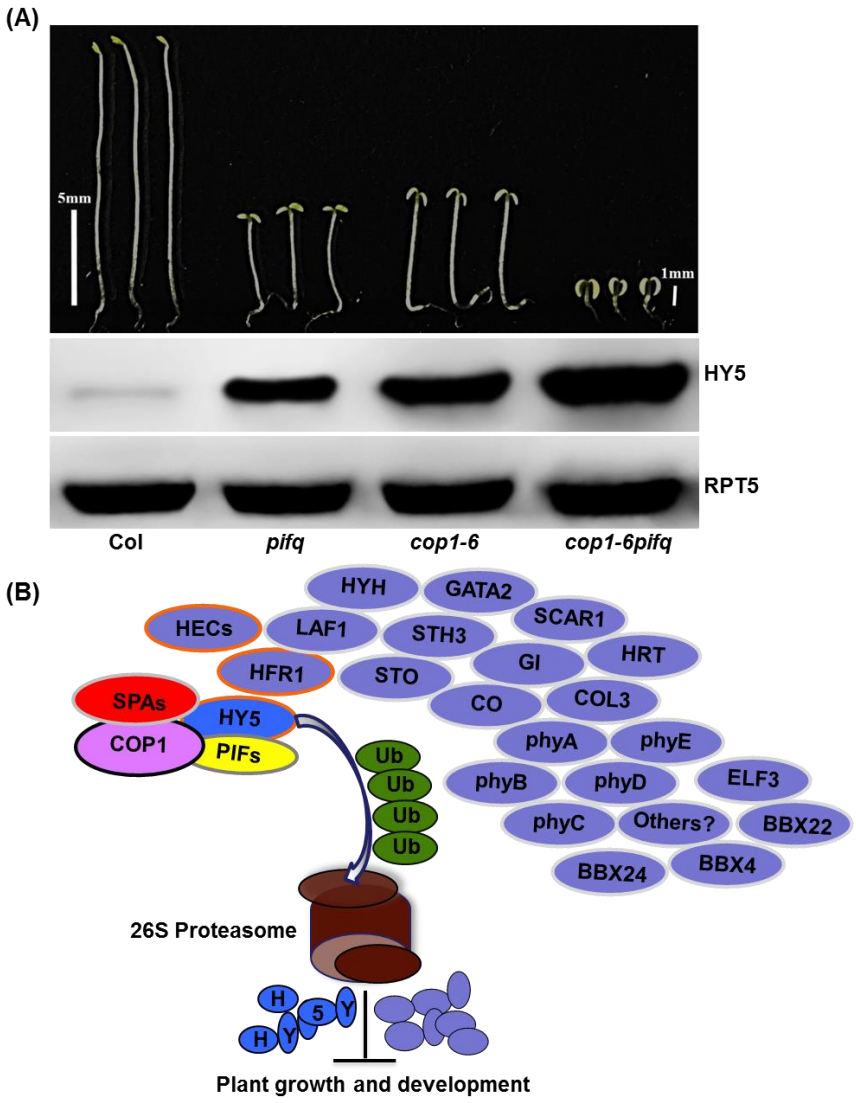

Figure 5.3: A model of how COP1 and PIF repressors function synergistically to regulate plant growth and development.

(A) Top, Visible phenotypes of the wild type, *pifq*, *cop1-6* and *cop1-6pifq* seedlings. Seeds of various genotypes were grown on MS medium without sucrose for 5 days in the dark. Bottom, Western blot shows the level of the key positively acting transcription factor HY5 in the 4 day-old dark-grown seedlings in wild type, *pifq*, *cop1-6* and *cop1-6pifq*

backgrounds. An RPT5 blot is shown as a loading control. (B) PIFs directly interact with COP1 and SPA1 as well as HY5. In one hand, these interactions promote the recruitment of HY5 to the COP1-SPA complex. On the other hand, PIFs also promote the auto- and trans-ubiquitylation of COP1's E3 ligase activity to enhance the degradation of HY5 to promote photomorphogenesis. A number of COP1 substrates are shown above. If PIFs interact with any of these substrates, PIFs might enhance their degradation through the COP1-SPA complex to regulate plant growth and development**.**

Reference

Alonso-Cantabrana, H., Ripoll, J.J., Ochando, I., Vera, A., Ferrándiz, C., and Martínez-Laborda, A. (2007). Common regulatory networks in leaf and fruit patterning revealed by mutations in the Arabidopsis ASYMMETRIC LEAVES1 gene. Development 134, 2663-2671.

Al-Sady, B., Kikis, E.A., Monte, E., and Quail, P.H. (2008). Mechanistic duality of transcription factor function in phytochrome signaling. Proc Natl Acad Sci U S A 105, 2232-2237.

Al-Sady, B., Ni, W., Kircher, S., Schafer, E., and Quail, P.H. (2006). Photoactivated Phytochrome Induces Rapid PIF3 Phosphorylation Prior to Proteasome-Mediated Degradation. Mol Cell 23, 439-446.

Ang, L.-H., Chattoadhyay, S., Wei, N., Oyama, T., Okada, K., Batshauer, A., and Deng, X.-W. (1998). Molecular interaction between COP1 and HY5 defines a regulatory switch for light control of seedling development. Mol Cell 1, 213–222.

Ausubel, F.M., Brent, R., Kingston, R.E., Moore, D.D., Seidman, J.G., Smith, J.A., and Struhl, K. (1994). Saccharomyces cerevisiae. In Current Protocols in Molecular Biology (Suppl.) (New York:: John Wiley and Sons)), pp. 13.16.12–13.16.14.

Avraham, R., and Yarden, Y. (2011). Feedback regulation of EGFR signalling: decision making by early and delayed loops. Nat Rev Mol Cell Biol. 12, 104-117.

Bae, G., and Choi, G. (2008). Decoding of light signals by plant phytochromes and their interacting proteins Annu Rev Plant Biol 59, 281-311.

Ballesteros, M.L., Bolle, C., Lois, L.M., Moore, J.M., Vielle-Calzada, J.P., Grossniklaus, U., and Chua, N.H. (2001). LAF1, a MYB transcription activator for phytochrome A signaling. Genes Dev 15, 2613-2625.

Bauer, D., Viczian, A., Kircher, S., Nobis, T., Nitschke, R., Kunkel, T., Panigrahi, K.C., Adam, E., Fejes, E., Schafer, E., and Nagy, F. (2004). Constitutive photomorphogenesis 1 and multiple photoreceptors control degradation of phytochrome interacting factor 3, a transcription factor required for light signaling in Arabidopsis. Plant Cell 16, 1433-1445.

Bernardo-García, S., de Lucas, M., Martínez, C., Espinosa-Ruiz, A., Davi ere, J.-M., and Prat, S. (2014). BR-dependent phosphorylation modulates PIF4 transcriptional activity and shapes diurnal hypocotyl growth. Genes & Development 28, 1681-1694

Bhoo, S.-H., Davis, S.J., Walker, J., Karniol, B., and Vierstra, R.D. (2001). Bacteriophytochromes are photochromic histidine kinases using a biliverdin chromophore. Nature 414, 776-779.

Bianchi, E., Denti, S., Catena, R., Rossetti, G., Polo, S., Gasparian, S., Putignano, S., Rogge, L., and Pardi, R. (2003). Characterization of human constitutive photomorphogenesis protein 1, a RING finger ubiquitin ligase that interacts with Jun transcription factors and modulates their transcriptional activity. Journal of Biological Chemistry 278, 19682-19690.

Boccalandro, H.E., Mazza, C.A., Mazzella, M.A., Casal, J.J., and Ballaré, C.L. (2001). Ultraviolet B radiation enhances a phytochrome-B-mediated photomorphogenic response in Arabidopsis. Plant Physiology 126, 780-788.

Boylan, M.T., and Quail, P.H. (1996). Are the phytochromes protein kinases? Protoplasma 195, 12-17.

Brady, S.M., and McCourt, P. (2003). Hormone cross-talk in seed dormancy. Journal of plant growth regulation 22, 25-31.

Briggs, W., Beck, C., Cashmore, A., Christie, J., Hughes, J., Jarillo, J., Kagawa, T., Kanegae, H., Liscum, E., and Nagatani, A. (2001). The phototropin family of photoreceptors. The Plant Cell 13, 993-997.

Briggs, W.R., and Christie, J.M. (2002). Phototropins 1 and 2: versatile plant blue-light receptors. Trends in plant science 7, 204-210.

Bu, Q., Castillon, A., Chen, F., Zhu, L., and Huq, E. (2011). Dimerization and blue light regulation of PIF1 interacting bHLH proteins in Arabidopsis. Plant Mol Biol 77, 501-511.

Bu, Q., Zhu, L., and Huq, E. (2011). Multiple kinases promote light-induced degradation of PIF1. Plant Sig. Behav. 6, 1119-1121.

Bu, Q., Zhu, L., Yu, L., Dennis, M., Lu, X., Person, M., Tobin, E., Browning, K., and Huq, E. (2011). Phosphorylation by CK2 enhances the rapid light-induced degradation of PIF1. J Biol Chem 286, 12066-12074.

Casal, J.J. (2013). Photoreceptor signaling networks in plant responses to shade. Annu Rev Plant Biol 64, 403-427.

Casal, J.J., and Sánchez, R.A. (1998). Phytochromes and seed germination. Seed Science Research 8, 317-329.

Castillon, A., Shen, H., and Huq, E. (2007). Phytochrome Interacting Factors: central players in phytochrome-mediated light signaling networks. Trends Plant Sci 12, 514-521.

Castillon, A., Shen, H., and Huq, E. (2009). Blue light induces degradation of the negative regulator Phytochrome Interacting Factor 1 to promote photomorphogenic development of Arabidopsis seedlings. Genetics 182, 161-171.

Chang, C.-S.J., Maloof, J.N., and Wu, S.-H. (2011). COP1-mediated degradation of BBX22/LZF1 optimizes seedling development in Arabidopsis. Plant physiology 156, 228-239.

Chaves, I., Pokorny, R., Byrdin, M., Hoang, N., Ritz, T., Brettel, K., Essen, L.-O., van der Horst, G.T., Batschauer, A., and Ahmad, M. (2011). The cryptochromes: blue light photoreceptors in plants and animals. Annual review of plant biology 62, 335-364.

Chen, A., Li, C., Hu, W., Lau, M.Y., Lin, H., Rockwell, N.C., Martin, S.S., Jernstedt, J.A., Lagarias, J.C., and Dubcovsky, J. (2014). PHYTOCHROME C plays a major role in the acceleration of wheat flowering under long-day photoperiod. Proceedings of the National Academy of Sciences 111, 10037-10044.

Chen, D., Xu, G., Tang, W., Jing, Y., Ji, Q., Fei, Z., and Lin, R. (2013). Antagonistic Basic Helix-Loop-Helix/bZIP Transcription Factors Form Transcriptional Modules That Integrate Light and Reactive Oxygen Species Signaling in Arabidopsis. Plant Cell 25, 1657-1673.

Chen, H.D., Huang, X., Gusmaroli, G., Terzaghi, W., Lau, O.S., Yanagawa, Y., Zhang, Y., Li, J.G., Lee, J.H., Zhu, D.M., and Deng, X.W. (2010). Arabidopsis CULLIN4-Damaged DNA Binding Protein 1 Interacts with CONSTITUTIVELY PHOTOMORPHOGENIC1-SUPPRESSOR OF PHYA Complexes to Regulate Photomorphogenesis and Flowering Time. Plant Cell 22, 108-123.

Chen, M., and Chory, J. (2011). Phytochrome signaling mechanisms and the control of plant development. Trends Cell Biol 21, 664-671.

Chen, M., Galvão, R.M., Li, M., Burger, B., Bugea, J., Bolado, J., and Chory, J. (2010). Arabidopsis HEMERA/pTAC12 initiates photomorphogenesis by phytochromes. Cell 141, 1230-1240.

Chory, J., Chatterjee, M., Cook, R., Elich, T., Fankhauser, C., Li, J., Nagpal, P., Neff, M., Pepper, A., and Poole, D. (1996). From seed germination to flowering, light controls plant development via the pigment phytochrome. Proceedings of the National Academy of Sciences 93, 12066-12071.

Christians, M.J., Gingerich, D.J., Hua, Z., Lauer, T.D., and Vierstra, R.D. (2012). The Light-Response BTB1 and BTB2 Proteins Assemble Nuclear Ubiquitin Ligases That Modify Phytochrome B and D Signaling in Arabidopsis. Plant Physiol 160, 118-134.

Christie, J.M., Yang, H., Richter, G.L., Sullivan, S., Thomson, C.E., Lin, J., Titapiwatanakun, B., Ennis, M., Kaiserli, E., and Lee, O.R. (2011). phot1 inhibition of ABCB19 primes lateral auxin fluxes in the shoot apex required for phototropism. PLoS Biol 9, e1001076.

Clack, T., Shokry, A., Moffet, M., Liu, P., Faul, M., and Sharrock, R.A. (2009). Obligate heterodimerization of Arabidopsis phytochromes C and E and interaction with the PIF3 basic helix-loop-helix transcription factor. Plant Cell 21, 786-799.

Colón-Carmona, A., Chen, D.L., Yeh, K.-C., and Abel, S. (2000). Aux/IAA proteins are phosphorylated by phytochrome in vitro. Plant Physiology 124, 1728-1738.

Crawford, B.C.W., and Yanofsky, M.F. (2011). HALF FILLED promotes reproductive tract development and fertilization efficiency in Arabidopsis thaliana. Development 138, 2999-3009.

de Lucas, M., Davière, J.M., Rodríguez-Falcón, M., Pontin, M., Iglesias-Pedraz, J.M., Lorrain, S., Fankhauser, C., Blaezquez, M.A., Titarenko, E., and Prat, S. (2008). A molecular framework for light and gibberellin control of cell elongation Nature 451, 480-484.

Demarsy, E., Schepens, I., Okajima, K., Hersch, M., Bergmann, S., Christie, J., Shimazaki, K.i., Tokutomi, S., and Fankhauser, C. (2012). Phytochrome Kinase Substrate 4 is phosphorylated by the phototropin 1 photoreceptor. The EMBO journal 31, 3457-3467.

Deng, X.-W., Matsui, M., Wei, N., Wagner, D., Chu, A.M., Feldmann, K.A., and Quail, P.H. (1992). COP1, an Arabidopsis regulatory gene, encodes a protein with both a zinc-binding motif and a Gβ homologous domain. Cell 71, 791-801.

Dong, J., Tang, D., Gao, Z., Yu, R., Li, K., He, H., Terzaghi, W., Deng, X.W., and Chen, H. (2014). Arabidopsis DE-ETIOLATED1 Represses Photomorphogenesis by Positively Regulating Phytochrome-Interacting Factors in the Dark. Plant Cell 26, 3630-3645.

Dornan, D., Wertz, I., Shimizu, H., Arnott, D., Frantz, G.D., Dowd, P., O' Rourke, K., Koeppen, H., and Dixit, V.M. (2004). The ubiquitin ligase COP1 is a critical negative regulator of p53. Nature 429, 86-92.

Duek, P.D., and Fankhauser, C. (2003). HFR1, a putative bHLH-transcription factor, mediates both phytochrome A and cryptochrome signaling. Plant J. 34, 827-836.

Duek, P.D., and Fankhauser, C. (2005). bHLH class transcription factors take centre stage in phytochrome signalling. Trends in plant science 10, 51-54.

Fairchild, C.D., Schumaker, M.A., and Quail, P.H. (2000). HFR1 encodes an atypical bHLH protein that acts in phytochrome A signal transduction. Genes Dev 14, 2377-2391.

Fankhauser, C., and Chen, M. (2008). Transposing phytochrome into the nucleus. Trends Plant Sci 13, 596-601.

Fankhauser, C., and Chory, J. (2000). RSF1, an Arabidopsis locus implicated in phytochrome A signaling. Plant Physiol 124, 39-45.

Fankhauser, C., and Christie, J.M. (2015). Plant phototropic growth. Current Biology 25, R384-R389.

Fankhauser, C., Yeh, K.-C., Clark, J., Zhang, H., Elich, T.D., and Chory, J. (1999). PKS1, a substrate phosphorylated by phytochrome that modulates light signaling in Arabidopsis. Science 284, 1539-1541.

Favory, J.J., Stec, A., Gruber, H., Rizzini, L., Oravecz, A., Funk, M., Albert, A., Cloix, C., Jenkins, G.I., and Oakeley, E.J. (2009). Interaction of COP1 and UVR8 regulates UV-B-induced photomorphogenesis and stress acclimation in Arabidopsis. The EMBO Journal 28, 591-601.

Finkelstein, R.R., Gampala, S.S., and Rock, C.D. (2002). Abscisic acid signaling in seeds and seedlings. The Plant Cell 14, S15-S45.

Fishbain, S., Inobe, T., Israeli, E., Chavali, S., Yu, H., Kago, G., Babu, M., and Matouschek, A. (2015). Sequence composition of disordered regions fine-tunes protein half-life. Nature Struct. Molec. Biol.

Fornara, F., Panigrahi, K.C., Gissot, L., Sauerbrunn, N., Rühl, M., Jarillo, J.A., and Coupland, G. (2009). Arabidopsis DOF transcription factors act redundantly to reduce CONSTANS expression and are essential for a photoperiodic flowering response. Developmental cell 17, 75-86.

Franklin, K.A., and Quail, P.H. (2010). Phytochrome functions in Arabidopsis development. J Exp Bot 61, 11-24.

Galvao, R.M., Li, M., Kothadia, S.M., Haskel, J.D., Decker, P.V., Van Buskirk, E.K., and Chen, M. (2012). Photoactivated phytochromes interact with HEMERA and promote its accumulation to establish photomorphogenesis in Arabidopsis. Genes & Development 26, 1851-1863.

Galvão, V.C., and Fankhauser, C. (2015). Sensing the light environment in plants: photoreceptors and early signaling steps. Current Opinion in Neurobiology 34, 46-53.

Galvão, V.C., and Fankhauser, C. (2015). Sensing the light environment in plants: photoreceptors and early signaling steps. Current Opinion in Neurobiology 34, 46-53.

Genoud, T., Schweizer, F., Tscheuschler, A., Debrieux, D., Casal, J.J., Schafer, E., Hiltbrunner, A., and Fankhauser, C. (2008). FHY1 Mediates Nuclear Import of the Light-Activated Phytochrome A Photoreceptor. Plos Genetics 4.

Girin, T., Paicu, T., Stephenson, P., Fuentes, S., Körner, E., O'Brien, M., Sorefan, K., Wood, T.A., Balanzá, V., and Ferrándiz, C. (2011). INDEHISCENT and SPATULA interact to specify carpel and valve margin tissue and thus promote seed dispersal in Arabidopsis. The Plant Cell 23, 3641-3653.

Gómez-Mena, C., de Folter, S., Costa, M.M.R., Angenent, G.C., and Sablowski, R. (2005). Transcriptional program controlled by the floral homeotic gene AGAMOUS during early organogenesis. Development 132, 429-438.

Gremski, K., Ditta, G., and Yanofsky, M.F. (2007). The HECATE genes regulate female reproductive tract development in Arabidopsis thaliana. Development 134, 3593-3601.

Groszmann, M., Paicu, T., Alvarez, J.P., Swain, S.M., and Smyth, D.R. (2011). SPATULA and ALCATRAZ, are partially redundant, functionally diverging bHLH genes required for Arabidopsis gynoecium and fruit development. Plant J 68, 816-829.

Guo, H., Yang, H., Mockler, T.C., and Lin, C. (1998). Regulation of flowering time by Arabidopsis photoreceptors. Science 279, 1360-1363.

Hardtke, C.S., Gohda, K., Osterlund, M.T., Oyama, T., Okada, K., and Deng, X.W. (2000). HY5 stability and activity in arabidopsis is regulated by phosphorylation in its COP1 binding domain. Embo J 19, 4997-5006.

Heisler, M.G., Atkinson, A., Bylstra, Y.H., Walsh, R., and Smyth, D.R. (2001). SPATULA, a gene that controls development of carpel margin tissues in Arabidopsis, encodes a bHLH protein. Development 128, 1089-1098.

Hennig, L., Stoddart, W.M., Dieterle, M., Whitelam, G.C., and Schäfer, E. (2002). Phytochrome E controls light-induced germination of Arabidopsis. Plant Physiology 128, 194-200.

Henriques, R., Jang, I.-C., and Chua, N.-H. (2009). Regulated proteolysis in light-related signaling pathways. Curr Opin Plant Biol 12, 49-56.

Hoecker, U. (2005). Regulated proteolysis in light signaling. Curr Op Plant Biol. 8, 469-476.

Hoecker, U., Tepperman, J.M., and Quail, P.H. (1999). SPA1, a WD-repeat protein specific to phytochrome A signal transduction. Science 284, 496-499.

Holm, M., Ma, L., Qu, L.J., and Deng, X.W. (2002). Two interacting bZIP proteins are direct targets of COP1-mediated control of light-dependent gene expression in Arabidopsis. Genes Dev. 16, 1247-1259.

Hornitschek, P., Kohnen, M.V., Lorrain, S., Rougemont, J., Ljung, K., López-Vidriero, I., Franco-Zorrilla, J.M., Solano, R., Trevisan, M., Pradervand, S., Xenarios, I., and Fankhauser, C. (2012). Phytochrome interacting factors 4 and 5 control seedling growth in changing light conditions by directly controlling auxin signaling. Plant J 71, 699-711.

Hornitschek, P., Lorrain, S., Zoete, V., Michielin, O., and Fankhauser, C. (2009). Inhibition of the shade avoidance response by formation of non-DNA binding bHLH heterodimers. Embo J 28, 3893-3902.

Huq, E., Al-Sady, B., and Quail, P.H. (2003). Nuclear translocation of the photoreceptor phytochrome B is necessary for its biological function in seedling photomorphogenesis. Plant J 35, 660-664.

Huq, E., Al-Sady, B., Hudson, M., Kim, C., Apel, K., and Quail, P.H. (2004). Phytochrome-interacting factor 1 is a critical bHLH regulator of chlorophyll biosynthesis. Science 305, 1937-1941.

Huq, E., Al-Sady, B., Hudson, M., Kim, C., Apel, K., and Quail, P.H. (2004). Phytochrome-interacting factor 1 is a critical bHLH regulator of chlorophyll biosynthesis. Science 305, 1937-1941.

Huq, E., and Quail, P.H. (2002). PIF4, a phytochrome-interacting bHLH factor, functions as a negative regulator of phytochrome B signaling in Arabidopsis. Embo J 21, 2441-2450.

Huq, E., and Quail, P.H. (2005). Phytochrome signaling. In Handbook of Photosensory Receptors, W.R. Briggs and J.L. Spudich, eds (Weinheim, Germany: Wiley-VCH), pp. 151-170.

Inoue, S.-i., Kinoshita, T., Matsumoto, M., Nakayama, K.I., Doi, M., and Shimazaki, K.-i. (2008). Blue light-induced autophosphorylation of phototropin is a primary step for signaling. Proceedings of the National Academy of Sciences 105, 5626-5631.

Ito, S., Song, Y.H., and Imaizumi, T. (2012). LOV domain-containing F-box proteins: light-dependent protein degradation modules in Arabidopsis. Molecular plant 5, 573-582.

Jang, I.-C., Henriques, R., Seo, H.S., Nagatani, A., and Chua, N.-H. (2010). Arabidopsis PHYTOCHROME INTERACTING FACTOR Proteins Promote Phytochrome B Polyubiquitination by COP1 E3 Ligase in the Nucleus. Plant Cell 22, 2370-2383.

Jang, I.C., Yang, J.Y., Seo, H.S., and Chua, N.H. (2005). HFR1 is targeted by COP1 E3 ligase for post-translational proteolysis during phytochrome A signaling. Genes Dev 19, 593-602.

Jenkins, G.I. (2014). The UV-B photoreceptor UVR8: from structure to physiology. The Plant Cell 26, 21-37.

Jeon, W., Aceti, D., Bingman, C., Vojtik, F., Olson, A., Ellefson, J., McCombs, J., Sreenath, H., Blommel, P., Seder, K., Burns, B., Geetha, H., Harms, A., Sabat, G., Sussman, M., Fox, B., and Phillips, G., Jr. (2005). High-throughput Purification and Quality Assurance of Arabidopsis thaliana Proteins for Eukaryotic Structural Genomics. J Struct Funct Genomics 6, 143-147.

Jiao, Y., Lau, O.S., and Deng, X.W. (2007). Light-regulated transcriptional networks in higher plants. Nature Reviews Genetics 8, 217-230.

José Ripoll, J., Bailey, L.J., Mai, Q.-A., Wu, S.L., Hon, C.T., Chapman, E.J., Ditta, G.S., Estelle, M., and Yanofsky, M.F. (2015). microRNA regulation of fruit growth. Nature Plants 1, 15036.

Kami, C., Lorrain, S., Hornitschek, P., and Fankhauser, C. (2010). Chapter two-light-regulated plant growth and development. Current topics in developmental biology 91, 29-66.

KeÇpczyński, J., and KeÇpczyńska, E. (1997). Ethylene in seed dormancy and germination. Physiologia Plantarum 101, 720-726.

Kim, B.C., Tennessen, D.J., and Last, R.L. (1998). UV-B-induced photomorphogenesis in Arabidopsis thaliana. The Plant Journal 15, 667-674.

Kim, W.-Y., Fujiwara, S., Suh, S.-S., Kim, J., Kim, Y., Han, L., David, K., Putterill, J., Nam, H.G., and Somers, D.E. (2007). ZEITLUPE is a circadian photoreceptor stabilized by GIGANTEA in blue light. Nature 449, 356-360.

Kong, S.-G., Arai, Y., Suetsugu, N., Yanagida, T., and Wada, M. (2013). Rapid severing and motility of chloroplast-actin filaments are required for the chloroplast avoidance response in Arabidopsis. The Plant Cell 25, 572-590.

Krall, L., and Reed, J.W. (2000). The histidine kinase-related domain participates in phytochrome B function but is dispensable. Proc Natl Acad Sci U S A 97, 8169-8174.

Krizek, B.A. (2015). Arabidopsis: flower development and patterning. In eLS, pp. 1-11.

Lau, O.S., and Deng, X.W. (2012). The photomorphogenic repressors COP1 and DET1: 20 years later. Trends Plant Sci 17, 584-593.

Laubinger, S., Fittinghoff, K., and Hoecker, U. (2004). The SPA Quartet: A Family of WD-Repeat Proteins with a Central Role in Suppression of Photomorphogenesis in Arabidopsis. Plant Cell 16, 2293-2306.

Lee, H.K., Cho, S.K., Son, O., Xu, Z., Hwang, I., and Kim, W.T. (2009). Drought Stress-Induced Rma1H1, a RING Membrane-Anchor E3 Ubiquitin Ligase Homolog, Regulates Aquaporin Levels via Ubiquitination in Transgenic Arabidopsis Plants. Plant Cell 21, 622-641.

Lee, K.P., Piskurewicz, U., Turečková, V., Carat, S., Chappuis, R., Strnad, M., Fankhauser, C., and Lopez-Molina, L. (2012). Spatially and genetically distinct control of seed germination by phytochromes A and B. Genes & development 26, 1984-1996.

Leivar, P., and Monte, E. (2014). PIFs: Systems Integrators in Plant Development Plant Cell 26, 56-78.

Leivar, P., and Quail, P.H. (2011). PIFs: pivotal components in a cellular signaling hub. Trends Plant Sci 16, 19-28.

Leivar, P., Monte, E., Al-Sady, B., Carle, C., Storer, A., Alonso, J.M., Ecker, J.R., and Quail, P.H. (2008a). The Arabidopsis Phytochrome-Interacting Factor PIF7, together with PIF3 and PIF4, regulates responses to prolonged red light by modulating phyB levels. Plant Cell 20, 337-352.

Leivar, P., Monte, E., Oka, Y., Liu, T., Carle, C., Castillon, A., Huq, E., and Quail, P.H. (2008b). Multiple phytochrome-interacting bHLH transcription factors

repress premature seedling photomorphogenesis in darkness. Curr Biol 18, 1815-1823.

Leivar, P., Tepperman, J.M., Monte, E., Calderon, R.H., Liu, T.L., and Quail, P.H. (2009). Definition of Early Transcriptional Circuitry Involved in Light-Induced Reversal of PIF-Imposed Repression of Photomorphogenesis in Young Arabidopsis Seedlings. Plant Cell 21, 3535-3553.

Lian, H.-L., He, S.-B., Zhang, Y.-C., Zhu, D.-M., Zhang, J.-Y., Jia, K.-P., Sun, S.-X., Li, L., and Yang, H.-Q. (2011). Blue-light-dependent interaction of cryptochrome 1 with SPA1 defines a dynamic signaling mechanism. Genes & development 25, 1023-1028.

Liljegren, S.J., Roeder, A.H., Kempin, S.A., Gremski, K., Ostergaard, L., Guimil, S., Reyes, D.K., and Yanofsky, M.F. (2004). Control of fruit patterning in Arabidopsis by INDEHISCENT. Cell 116, 843-853.

Lin, C. (2002). Blue light receptors and signal transduction. The Plant Cell 14, S207-S225.

Lin, Z., Zhong, S., and Grierson, D. (2009). Recent advances in ethylene research. Journal of experimental botany, erp204.

Liscum, E., and Briggs, W.R. (1995). Mutations in the NPH1 locus of Arabidopsis disrupt the perception of phototropic stimuli. The Plant Cell 7, 473-485.

Liscum, E., Hodgson, D.W., and Campbell, T.J. (2003). Blue light signaling through the cryptochromes and phototropins. So that's what the blues is all about. Plant physiology 133, 1429-1436.

Littlewood, T., Evans, G.I. (1998). Helix-Loop-Helix Transcription Factors. (New York: Oxford University Press).

Liu, B., Zuo, Z., Liu, H., Liu, X., and Lin, C. (2011). Arabidopsis cryptochrome 1 interacts with SPA1 to suppress COP1 activity in response to blue light. Genes & development 25, 1029-1034.

Liu, L.-J., Zhang, Y.-C., Li, Q.-H., Sang, Y., Mao, J., Lian, H.-L., Wang, L., and Yang, H.-Q. (2008). COP1-mediated ubiquitination of CONSTANS is implicated in cryptochrome regulation of flowering in Arabidopsis. The Plant Cell 20, 292-306.

Liu, Y., Li, X., Li, K., Liu, H., and Lin, C. (2013). Multiple bHLH proteins form heterodimers to mediate CRY2-dependent regulation of flowering-time in Arabidopsis. PLoS Genet 9, e1003861.

Lorrain, S., Allen, T., Duek, P.D., Whitelam, G.C., and Fankhauser, C. (2008). Phytochrome-mediated inhibition of shade avoidance involves degradation of growth-promoting bHLH transcription factors. Plant J 53, 312-323.

Lu, X.-D., Zhou, C.-M., Xu, P.-B., Luo, Q., Lian, H.-L., and Yang, H.-Q. (2015). Red-Light-Dependent Interaction of phyB with SPA1 Promotes COP1–SPA1

Dissociation and Photomorphogenic Development in Arabidopsis. Molecular Plant 8, 467-478.

Mara, C.D., Huang, T., and Irish, V.F. (2010). The Arabidopsis floral homeotic proteins APETALA3 and PISTILLATA negatively regulate the BANQUO genes implicated in light signaling. The Plant Cell 22, 690-702.

Martinez-Garcia, J.F., Huq, E., and Quail, P.H. (2000). Direct targeting of light signals to a promoter element-bound transcription factor. Science 288, 859-863.

Mathews, S., and Sharrock, R. (1997). Phytochrome gene diversity. Plant, Cell & Environment 20, 666-671.

Matsushita, T., Mochizuki, N., and Nagatani, A. (2003). Dimers of the N-terminal domain of phytochrome B are functional in the nucleus. Nature 424, 571-574.

McNellis, T.W., von Arnim, A.G., Araki, T., Komeda, Y., Misera, S., and Deng, X.W. (1994). Genetic and molecular analysis of an allelic series of cop1 mutants suggests functional roles for the multiple protein domains. Plant Cell 6, 487–500.

Medzihradszky, M., Bindics, J., Ádám, É., Viczián, A., Klement, É., Lorrain, S., Gyula, P., Mérai, Z., Fankhauser, C., and Medzihradszky, K.F. (2013). Phosphorylation of phytochrome B inhibits light-induced signaling via accelerated dark reversion in Arabidopsis. Plant Cell 25, 535-544.

Moon, J., Zhu, L., Shen, H., and Huq, E. (2008). PIF1 directly and indirectly regulates chlorophyll biosynthesis to optimize the greening process in Arabidopsis. Proc Natl Acad Sci U S A 105, 9433-9438.

Nagatani, A. (2004). Light-regulated nuclear localization of phytochromes. Curr. Opin. Plant Biol. 7, 708-711.

Nakagawa, T., Kurose, T., Hino, T., Tanaka, K., Kawamukai, M., Niwa, Y., Toyooka, K., Matsuoka, K., Jinbo, T., and Kimura, T. (2007). Development of series of gateway binary vectors, pGWBs, for realizing efficient construction of fusion genes for plant transformation. J. Biosci. Bioeng. 104, 34-41.

Neff, M.M., Fankhauser, C., and Chory, J. (2000). Light: an indicator of time and place. Genes & Development 14, 257-271.

Ni, W., Xu, S.-L., Chalkley, R.J., Pham, T.N.D., Guan, S., Maltby, D.A., Burlingame, A.L., Wang, Z.-Y., and Quail, P.H. (2013). Multisite light-induced phosphorylation of the transcription factor PIF3 is necessary for both its rapid degradation and concomitant negative feedback modulation of photoreceptor phyB levels in Arabidopsis. The Plant Cell 25, 2679-2698.

Ni, W., Xu, S.-L., Tepperman, J.M., Stanley, D.J., Maltby, D.A., Gross, J.D., Burlingame, A.L., Wang, Z.-Y., and Quail, P.H. (2014). A mutually assured destruction mechanism attenuates light signaling in Arabidopsis. Science 344, 1160-1164.

Oh, E., Kang, H., Yamaguchi, S., Park, J., Lee, D., Kamiya, Y., and Choi, G. (2009). Genome-Wide Analysis of Genes Targeted by PHYTOCHROME INTERACTING FACTOR 3-LIKE5 during Seed Germination in Arabidopsis. Plant Cell 21, 403-419.

Oh, E., Kim, J., Park, E., Kim, J.-I., Kang, C., and Choi, G. (2004). PIL5, a phytochrome-interacting basic helix-loop-helix protein, is a key negative regulator of seed germination in Arabidopsis thaliana. The Plant Cell 16, 3045-3058.

Osterlund, M.T., and Deng, X.W. (1998). Multiple photoreceptors mediate the light-induced reduction of GUS-COP1 from Arabidopsis hypocotyl nuclei. Plant J. 16, 201-202-208.

Osterlund, M.T., Hardtke, C.S., Wei, N., and Deng, X.W. (2000). Targeted destabilization of HY5 during light-regulated development of Arabidopsis. Nature 405, 462 - 466.

Oyama, T., Shimura, Y., and Okada, K. (1997). The Arabidopsis HY5 gene encodes a bZIP protein that regulates stimulus-induced development of root and hypocotyl. . Genes & Development 11, 2983–2995.

Pacín, M., Legris, M., and Casal, J.J. (2013). COP1 re-accumulates in the nucleus under shade. Plant J. 75(4):631-41.

Pacín, M., Legris, M., and Casal, J.J. (2014). Rapid Decline in Nuclear COSTITUTIVE PHOTOMORPHOGENESIS1 Abundance Anticipates the Stabilization of Its Target ELONGATED HYPOCOTYL5 in the Light. Plant Physiol 164, 1134-1138.

Paik, I., Yang, S., and Choi, G. (2012). Phytochrome regulates translation of mRNA in the cytosol. Proceedings of the National Academy of Sciences 109, 1335-1340.

Park, E., Park, J., Kim, J., Nagatani, A., Lagarias, J.C., and Choi, G. (2012). Phytochrome B inhibits binding of phytochrome-interacting factors to their target promoters. Plant J 72, 537-546.

Pelaz, S., Ditta, G.S., Baumann, E., Wisman, E., and Yanofsky, M.F. (2000). B and C floral organ identity functions require SEPALLATA MADS-box genes. Nature 405, 200-203.

Penfield, S., Josse, E.-M., Kannangara, R., Gilday, A.D., Halliday, K.J., and Graham, I.A. (2005). Cold and light control seed germination through the bHLH transcription factor SPATULA. Current Biology 15, 1998-2006.

Quail, P.H. (2000). Phytochrome-interacting factors. Semin Cell Dev Biol 11, 457-466.

Rajani, S., and Sundaresan, V. (2001). The Arabidopsis myc/bHLH gene ALCATRAZ enables cell separation in fruit dehiscence. Curr Biol 11, 1914-1922.

Ripoll, J.J., Ferrándiz, C., Martínez-Laborda, A., and Vera, A. (2006). PEPPER, a novel K-homology domain gene, regulates vegetative and gynoecium development in Arabidopsis. Developmental biology 289, 346-359.

Rizzini, L., Favory, J.-J., Cloix, C., Faggionato, D., O'Hara, A., Kaiserli, E., Baumeister, R., Schäfer, E., Nagy, F., and Jenkins, G.I. (2011). Perception of UV-B by the Arabidopsis UVR8 protein. Science 332, 103-106.

Rodríguez-Cazorla, E., Ripoll, J.J., Andújar, A., Bailey, L.J., Martínez-Laborda, A., Yanofsky, M.F., and Vera, A. (2015). K-homology nuclear ribonucleoproteins regulate floral organ identity and determinacy in Arabidopsis. PLoS Genet 11, e1004983.

Rösler, J., Klein, I., and Zeidler, M. (2007). Arabidopsis fhl/fhy1 double mutant reveals a distinct cytoplasmic action of phytochrome A. Proc Natl Acad Sci U S A 104, 10737-10742.

Ryan, P.E., Kales, S.C., Yadavalli, R., Nau, M.M., Zhang, H., and Lipkowitz, S. (2012). Cbl-c ubiquitin ligase activity is increased via the interaction of its RING finger domain with a LIM domain of the paxillin homolog, Hic 5. PLos One 7, e49428.

Saijo, Y., Sullivan, J.A., Wang, H., Yang, J., Shen, Y., Rubio, V., Ma, L., Hoecker, U., and Deng, X.W. (2003). The COP1-SPA1 interaction defines a critical step in phytochrome A-mediated regulation of HY5 activity. Genes Dev 17, 2642-2647.

Sawa, M., Nusinow, D.A., Kay, S.A., and Imaizumi, T. (2007). FKF1 and GIGANTEA complex formation is required for day-length measurement in Arabidopsis. Science 318, 261-265.

Schaefer, E., and Nagy, F. (2006). Photomorphogenesis in plants and bacteria. (Dordrecht, The Netherlands: Springer).

Schmidt, R., and Mohr, H. (1981). Time-dependent chnages in the responsiveness to light of phytochrome-mediated anthocyanin synthesis. Plant Cell Environ 4, 433-437.

Schuster, C., Gaillochet, C., and Lohmann, J.U. (2015). Arabidopsis HECATE genes function in phytohormone control during gynoecium development. Development 142, 3343-3350.

Schuster, C., Gaillochet, C., Medzihradszky, A., Busch, W., Daum, G., Krebs, M., Kehle, A., and Lohmann, J.U. (2014). A Regulatory Framework for Shoot Stem Cell Control Integrating Metabolic, Transcriptional, and Phytohormone Signals. Developmental Cell 28, 438-449.

Schwechheimer, C. (2008). Understanding gibberellic acid signaling—are we there yet? Current opinion in plant biology 11, 9-15.

Schwechheimer, C., and Deng, X.-W. (2000). The COP/DET/FUS proteins—regulators of eukaryotic growth and development. In Seminars in cell & developmental biology, Volume 11. (Elsevier), pp. 495-503.

Seo, H.S., Watanabe, E., Tokutomi, S., Nagatani, A., and Chua, N.-H. (2004). Photoreceptor ubiquitination by COP1 E3 ligase desensitizes phytochrome A signaling. Genes Dev 18, 617-622.

Seo, H.S., Yang, J.Y., Ishikawa, M., Bolle, C., Ballesteros, M.L., and Chua, N.H. (2003). LAF1 ubiquitination by COP1 controls photomorphogenesis and is stimulated by SPA1. Nature 423, 995-999.

Sharrock, R.A. (2008). The phytochrome red/far-red photoreceptor superfamily. Genome Biol 9, 230.

Sharrock, R.A., and Clack, T. (2004). Heterodimerization of type II phytochromes in Arabidopsis. Proc Natl Acad Sci U S A 101, 11500-11505.

Sheerin, D.J., Menon, C., zur Oven-Krockhaus, S., Enderle, B., Zhu, L., Johnen, P., Schleifenbaum, F., Stierhof, Y.-D., Huq, E., and Hiltbrunner, A. (2015). Light-activated phytochrome A and B interact with members of the SPA family to promote photomorphogenesis in Arabidopsis by reorganizing the COP1/SPA complex. Plant Cell 27, 189-201.

Shen, H., Ling, Z., Castillon, A., Majee, M., Downie, B., and Huq, E. (2008). Light-induced phosphorylation and degradation of the negative regulator PHYTOCHROME INTERACTING FACTOR 1 depends upon its direct physical interactions with photoactivated phytochromes. Plant Cell 20, 1586-1602.

Shen, H., Moon, J., and Huq, E. (2005). PIF1 is regulated by light-mediated degradation through the ubiquitin-26S proteasome pathway to optimize seedling photomorphogenesis in Arabidopsis. Plant J 44, 1023-1035.

Shen, H., Zhu, L., Castillon, A., Majee, M., Downie, B., and Huq, E. (2008). Light-induced phosphorylation and degradation of the negative regulator PHYTOCHROME-INTERACTING FACTOR1 from Arabidopsis depend upon its direct physical interactions with photoactivated phytochromes. The Plant Cell 20, 1586-1602.

Shen, Y., Khanna, R., Carle, C.M., and Quail, P.H. (2007). Phytochrome induces rapid PIF5 phosphorylation and degradation in response to red-light activation. Plant Physiol 145, 1043-1051.

Shen, Y., Zhou, Z., Feng, S., Li, J., Tan-Wilson, A., Qu, L.-J., Wang, H., and Deng, X.W. (2009). Phytochrome A mediates rapid red light–induced phosphorylation of Arabidopsis FAR-RED ELONGATED HYPOCOTYL1 in a low fluence response. The Plant Cell 21, 494-506.

Shi, H., Liu, R., Xue, C., Shen, X., Wei, N., Deng, X.W., and Zhong, S. (2016). Seedlings Transduce the Depth and Mechanical Pressure of Covering Soil Using COP1 and Ethylene to Regulate EBF1/EBF2 for Soil Emergence. Curr Biol doi.org/10.1016/j.cub.2015.11.053.

Shi, H., Wang, X., Mo, X., Tang, C., Zhong, S., and Deng, X.W. (2015). Arabidopsis DET1 degrades HFR1 but stabilizes PIF1 to precisely regulate seed germination. Proc Natl Acad Sci U S A 112, 3817-3822.

Shi, H., Zhong, S., Mo, X., Liu, N., Nezames, C.D., and Deng, X.W. (2013). HFR1 Sequesters PIF1 to Govern the Transcriptional Network Underlying Light-Initiated Seed Germination in Arabidopsis. The Plant Cell 25, 3770-3784.

Shin, J., Kim, K., Kang, H., Zulfugarov, I.S., Bae, G., Lee, C.-H., Lee, D., and Choi, G. (2009). Phytochromes promote seedling light responses by inhibiting four negatively-acting phytochrome-interacting factors. Proceedings of the National Academy of Sciences 106, 7660-7665.

Shinomura, T., Nagatani, A., Chory, J., and Furuya, M. (1994). The induction of seed germination in Arabidopsis thaliana is regulated principally by phytochrome B and secondarily by phytochrome A. Plant physiology 104, 363-371.

Song, Y.H., Smith, R.W., To, B.J., Millar, A.J., and Imaizumi, T. (2012). FKF1 conveys timing information for CONSTANS stabilization in photoperiodic flowering. Science 336, 1045-1049.

Srivastava, A.K., Senapati, D., Srivastava, A., Chakraborty, M., Gangappa, S.N., and Chattopadhyay, S. (2015). Short Hypocotyl in White Light1 Interacts with Elongated Hypocotyl5 (HY5) and Constitutive Photomorphogenic1 (COP1) and Promotes COP1-Mediated Degradation of HY5 during Arabidopsis Seedling Development. Plant physiology 169, 2922-2934.

Subramanian, C., Kim, B.H., Lyssenko, N.N., Xu, X., Johnson, C.H., and von Arnim, A.G. (2004). The Arabidopsis repressor of light signaling, COP1, is regulated by nuclear exclusion: mutational analysis by bioluminescence resonance energy transfer. Proc Natl Acad Sci USA. 101, 6798-6802.

Suesslin, C., and Frohnmeyer, H. (2003). An Arabidopsis mutant defective in UV-B light-mediated responses. The Plant Journal 33, 591-601.

Suetsugu, N., and Wada, M. (2013). Evolution of three LOV blue light receptor families in green plants and photosynthetic stramenopiles: phototropin, ZTL/FKF1/LKP2 and aureochrome. Plant and Cell Physiology 54, 8-23.

Sui, G., El Bachir, A., Shi, Y., Brignone, C., Wall, N.R., Yin, P., Donohoe, M., Luke, M.P., Calvo, D., Grossman, S.R., and Shi, Y. (2004). Yin Yang 1 Is a Negative Regulator of p53. Cell 117, 859-872.

Sullivan, J.A., and Deng, X.W. (2003). From seed to seed: the role of photoreceptors in Arabidopsis development. Developmental biology 260, 289-297.

Tepperman, J.M., Hwang, Y.S., and Quail, P.H. (2006). phyA Dominates in Transduction of Red-light Signals to Rapidly-responding Genes at the Initiation of Arabidopsis Seedling Deetiolation. Plant J. 48, doi: 10.1111/j.1365-1313X.2006.02914.x.

Toledo-Ortiz, G., Huq, E., and Quail, P.H. (2003). The Arabidopsis basic/helix-loop-helix transcription factor family. Plant Cell 15, 1749-1770.

Toledo-Ortíz, G., Huq, E., and Rodríguez-Concepción, M. (2010). Direct regulation of phytoene synthase gene expression and carotenoid biosynthesis by Phytochrome-Interacting Factors. Proc Natl Acad Sci U S A 107, 11626-11631.

Ulm, R., Baumann, A., Oravecz, A., Máté, Z., Ádám, É., Oakeley, E.J., Schäfer, E., and Nagy, F. (2004). Genome-wide analysis of gene expression reveals function of the bZIP transcription factor HY5 in the UV-B response of Arabidopsis. Proceedings of the National Academy of Sciences of the United States of America 101, 1397-1402.

van der Lee, R., Lang, B., Kruse, K., Gsponer, J., Sanchez de Groot, N., Huynen, M.A., Matouschek, A., Fuxreiter, M., and Babu, M.M. (2014). Intrinsically disordered segments affect protein half life in the cell and during evolution. Cell Rep 8, 1832-1844.

Varkonyi-Gasic, E., Moss, S.M., Voogd, C., Wu, R., Lough, R.H., Wang, Y.-Y., and Hellens, R.P. (2011). Identification and characterization of flowering genes in kiwifruit: sequence conservation and role in kiwifruit flower development. BMC Plant Biology 11, 1.

Vierstra, R.D., and Davis, S.J. (2000). Bacteriophytochromes: new tools for understanding phytochrome signal transduction. In Seminars in cell & developmental biology, Volume 11. (Elsevier), pp. 511-521.

Wada, M., Kagawa, T., and Sato, Y. (2003). Chloroplast movement. Annual Review of Plant Biology 54, 455-468.

Wang, C.-Q., Sarmast, M.K., Jiang, J., and Dehesh, K. (2015). The Transcriptional Regulator BBX19 Promotes Hypocotyl Growth by Facilitating COP1-Mediated EARLY FLOWERING3 Degradation in Arabidopsis. Plant Cell 27, 1128-1139.

Wang, H., Ma, L.-G., Li, J.-M., Zhao, H.-Y., and Deng, X.W. (2001). Direct interaction of Arabidopsis cryptochromes with COP1 in light control development. Science 294, 154-158.

Wei, N., and Deng, X.-W. (1996). The role of the COP/DET/FUS genes in light control of Arabidopsis seedling development. Plant Physiology 112, 871.

Weitbrecht, K., Müller, K., and Leubner-Metzger, G. (2011). First off the mark: early seed germination. Journal of experimental botany 62, 3289-3309.

Xia, Y., Pao, G.M., Chen, H.W., Verma, I.M., and Hunter, T. (2003). Enhancement of BRCA1 E3 ubiquitin ligase activity through direct interaction with the BARD1 protein. J Biol Chem 278, 5255-5263.

Xu, X., Paik, I., Zhu, L., and Huq, E. (2015). Illuminating Progress in Phytochrome-Mediated Light Signaling Pathways. Trends in plant science 20, 641-650.

Xu, X., Paik, I., Zhu, L., Bu, Q., Huang, X., Deng, X.W., and Huq, E. (2014). PHYTOCHROME INTERACTING FACTOR1 Enhances the E3 Ligase Activity of CONSTITUTIVE PHOTOMORPHOGENIC1 to Synergistically Repress Photomorphogenesis in Arabidopsis. Plant Cell 26, 1992-2006.

Xu, X., Bu, Q., Nguyen, A., and Huq, E. (2016a). Suicidal co-degradation of the positive and negatively acting transcription factors fine tunes photomorphogenesis in Arabidopsis. In preparation.

Xu, X., Ripoll, J.J., Nguyen, A., Yanofsky, M.F., and Huq, E. (2016b). PIF1 promotes HECATE2 degradation via COP1 to regulate photomorphogenesis and flower development. In preparation.

Yang, H.-Q., Tang, R.-H., and Cashmore, A.R. (2001). The signaling mechanism of Arabidopsis CRY1 involves direct interaction with COP1. The Plant Cell 13, 2573-2587.

Yang, H.-Q., Wu, Y.-J., Tang, R.-H., Liu, D., Liu, Y., and Cashmore, A.R. (2000). The C termini of Arabidopsis cryptochromes mediate a constitutive light response. Cell 103, 815-827.

Yang, J., Lin, R., Sullivan, J., Hoecker, U., Liu, B., Xu, L., Deng, X.W., and Wang, H. (2005). Light Regulates COP1-Mediated Degradation of HFR1, a Transcription Factor Essential for Light Signaling in Arabidopsis. Plant Cell 17, 804-821.

Yang, J.P., Lin, R.C., James, S., Hoecker, U., Liu, B.L., Xu, L., Deng, X.W., and Wang, H.Y. (2005). Light regulates COP1-mediated degradation of HFR1, a transcription factor essential for light signaling in arabidopsis. Plant Cell 17, 804-821.

Yeh, K.-C., and Lagarias, J.C. (1998). Eukaryotic phytochromes: light-regulated serine/threonine protein kinases with histidine kinase ancestry. Proceedings of the National Academy of Sciences 95, 13976-13981.

Yi, C., and Deng, X.W. (2005). COP1–from plant photomorphogenesis to mammalian tumorigenesis. Trends in cell biology 15, 618-625.

Yu, J.-W., Rubio, V., Lee, N.-Y., Bai, S., Lee, S.-Y., Kim, S.-S., Liu, L., Zhang, Y., Irigoyen, M.L., and Sullivan, J.A. (2008). COP1 and ELF3 control circadian function and photoperiodic flowering by regulating GI stability. Molecular cell 32, 617-630.

Zhang, H.Y., He, H., Wang, X.C., Wang, X.F., Yang, X.Z., Li, L., and Deng, X.W. (2011). Genome-wide mapping of the HY5-mediated genenetworks in Arabidopsis that involve both transcriptional and post-transcriptional regulation. Plant Journal 65, 346-358.

Zhang, Y., Mayba, O., Pfeiffer, A., Shi, H., Tepperman, J.M., Speed, T.P., and Quail, P.H. (2013). A Quartet of PIF bHLH Factors Provides a Transcriptionally Centered Signaling Hub That Regulates Seedling Morphogenesis through Differential

Expression-Patterning of Shared Target Genes in Arabidopsis. Plos Genetics 9, e1003244.

Zhao, Q., Tian, M., Li, Q., Cui, F., Liu, L., Yin, B., and Xie, Q. (2013). A plant-specific in vitro ubiquitination analysis system. The Plant Journal 74, 524-533.

Zhu, D.M., Maier, A., Lee, J.-H., Laubinger, S., Saijo, Y., Wang, H.Y., Qu, L.-J., Hoecker, U., and Deng, X.W. (2008). Biochemical Characterization of Arabidopsis Complexes Containing CONSTITUTIVELY PHOTOMORPHOGENIC1 and SUPPRESSOR OF PHYA Proteins in Light Control of Plant Development. Plant Cell 20, 2307-2323.

Zhu, L., and Huq, E. (2014). Suicidal co-degradation of the Phytochrome Interacting Factor 3 and phytochrome B in response to light. Mol Plant 7, 1709-1711.

Zhu, L., Bu, Q., Xu, X., Paik, I., Huang, X., Hoecker, U., Deng, X.W., and Huq, E. (2015). CUL4 forms an E3 ligase with COP1 and SPA to promote light-induced degradation of PIF1. Nature communications 6, 7245.

Zhu, L., Xin, R., Bu, Q., Shen, H., Dang, J., and Huq, E. (2016). A negative feedback loop between PHYTOCHROME INTERACTING FACTORs and HECATE proteins fine tunes photomorphogenesis in Arabidopsis. Plant Cell submitted.

Zhu, Y., Tepperman, J.M., Fairchild, C.D., and Quail, P.H. (2000). Phytochrome B binds with greater apparent affinity than phytochrome A to the basic helix–loop–helix factor PIF3 in a reaction requiring the PAS domain of PIF3. Proceedings of the National Academy of Sciences 97, 13419-13424.

Zuo, Z., Liu, H., Liu, B., Liu, X., and Lin, C. (2011). Blue light-dependent interaction of CRY2 with SPA1 regulates COP1 activity and floral initiation in Arabidopsis. Current Biology 21, 841-847.

Vita

Xiaosa Xu graduated from Wulian NO.1 High School, Rizhao city, Shandong Province, China, in 2007. In 2011, he obtained his Bachelor's degree in Top Students Program of Agriculture from Nanjing Agricultural University, Nanjing city, Jiangsu Province, China. From 2007-2011, Xiaosa Xu conducted an undergraduate Student Research Training project for detection and functional characterization of rice high yield QTLs in Dr. Jianmin Wan lab of the State Key Laboratory of Crop Genetics and Germplasm Enhancement in Nanjing Agricultural University.

In 2011, Xiaosa Xu joined the Plant Biology graduate program of Molecular Biosciences Department at the University of Texas at Austin to pursue a Ph.D. degree in Dr. Enamul Huq laboratory to study the conserved modulation of the CONSTITUTIVE PHOTOMORPHOGENIC1 E3 ubiquitin ligase activity by the bHLH transcription factors, PHYTOCHROME INTERACTING FACTORs.

Author email: jackxu@utexas.edu

This manuscript was typed by the author.